ISTANBUL TECHNICAL UNIVERSITY ★ GRADUATE SCHOOL

FABRICATION AND CHARACTERIZATION OF HYBRID NANOFILLER REINFORCED POLYURETHANE NANOCOMPOSITES

Ph.D. THESIS

Amir NAVIDFAR

Department of Mechanical Engineering

Mechanical Engineering Doctorate Programme

SEPTEMBER 2021

ISTANBUL TECHNICAL UNIVERSITY ★ GRADUATE SCHOOL

FABRICATION AND CHARACTERIZATION OF HYBRID NANOFILLER REINFORCED POLYURETHANE NANOCOMPOSITES

Ph.D. THESIS

Amir NAVIDFAR
(503142016)

Department of Mechanical Engineering

Mechanical Engineering Doctorate Programme

Thesis Advisor: Prof. Dr. Levent TRABZON

SEPTEMBER 2021

ISTANBUL TEKNİK ÜNİVERSİTESİ ★ LİSANSÜSTÜ EĞİTİM ENSTİTÜSÜ

HİBRİT NANODOLGU TAKVİYELİ POLİÜRETAN NANOKOMPOZİTLERİN ÜRETİMİ VE KARAKTERİZASYONU

DOKTORA TEZİ

Amir NAVIDFAR
(503142016)

Makina Mühendisliği Anabilim Dalı

Makina Mühendisliği Doktora Programı

Tez Danışmanı: Prof. Dr. Levent TRABZON

EYLÜL 2021

Amir NAVIDFAR, a Ph.D. student of ITU Graduate School student ID 503142016, successfully defended the thesis/dissertation entitled “Fabrication and Characterization of Hybrid Nanofiller Reinforced Polyurethane Nanocomposites”, which he prepared after fulfilling the requirements specified in the associated legislations, before the jury whose signatures are below.

Thesis Advisor :	**Prof. Dr. Levent TRABZON** İstanbul Technical University	.....
Jury Members :	**Prof. Dr. Mustafa BAKKAL** Istanbul Technical University	.....
	Prof. Dr. Haluk KÜÇÜK Marmara University	.....
	Assist. Prof. Dr. Alaeddin Burak İREZ Istanbul Technical University	.....
	Assist. Prof. Dr. Osman EKSİK Gebze Technical University	.....

Date of Submission : 08 September 2021
Date of Defense : 17 September 2021

To my parents and siblings,

FOREWORD

I would like to express my sincere gratitude and appreciation to my advisor Prof. Levent TRABZON for his significant, invaluable counsel and contributions throughout entire my Ph.D. study.

The author also would like to thanks Prof. Yakup Erhan BOKE, Prof. Ferid SALEHLI and Assoc. Prof. Osman BULUT for their support during my time at Istanbul Technical University.

Special thanks to Mr. Osman CELEBI for his continued support during my experimental works.

I would also like to extend my thanks to the friends I have who over the years have made my student life in Istanbul a very special time – Dr. Houman Bahmani Jalali, Araz Khakzadi, Armin Gharibi, Kaveh Rahimzadeh, Anali Azabdaftari, Delara Razzaghmanesh and anyone else I may have missed unintentionally.

Last but not the least; I sincerely thank my parents, Reza NAVIDFAR (RIP, I am sorry that he cannot see me graduate) and Aghdas LOTFALIZADEH, for their lifelong support and endless love. Without their economic support and effort, I would not have had a chance to study in Turkey and I hope that I have made them proud. I would like to dedicate my gratitude to my siblings, Ali and Reihaneh NAVIDFAR for their support.

September 2021

Amir NAVIDFAR
(Mechanical Engineer)

TABLE OF CONTENTS

Page

ABBREVIATIONS

1D	**:** One-dimensional
2D	**:** Two-dimensional
3D	**:** Three-dimensional
DC	**:** Dielectric Constant
DL	**:** Dielectric Loss
DMA	**:** Dynamic Mechanical Analysis
EC	**:** Electrical Conductivity
FTIR	**:** Fourier Transform Infrared
GNP	**:** Graphene Nanoplatelets
H_2O_2	**:** Hydrogen Peroxide
MWCNT	**:** Multi-walled Carbon Nanotubes
PI	**:** Performance Index
PU	**:** Polyurethane
QD	**:** Quantum Dots
SiO_2	**:** Silicon dioxide (Silica)
SEM	**:** Scanning Electron Microscopy
TEM	**:** Transmission Electron Microscopy
TC	**:** Thermal Conductivity
TGA	**:** Thermogravimetric Analysis
TL	**:** Transmission Loss
TS	**:** Tensile Strength
XRD	**:** X-ray Diffraction

SYMBOLS

C	: Shape Factor
D_G	: Diameter of GNPs
E	: Elastic Modulus
E'	: Storage Modulus
E''	: Loss Modulus
f_p	: Critical Volume Fraction for the Nonlinear Conductivity Variation
I_D/I_G	: D-band to G-band Intensity Ratio
l	: Length
H_G	: Distance Between Two Half GNPs
K_B	: Boltzmann constant
K, K_e, K_m	: Intrinsic, Equivalent and Matrix Thermal Conductivity
R_K	: Nanofiller-Matrix Interface Resistance
T	: Temperature
$\tan \delta$	: Damping Factor
T_g	: Glass Transition Temperatures
t_G	: Thickness of GNPs
V_f	: Volume Fraction
α	: Critical Conductivity Exponent
ρ	: Density
$\sigma_C, \sigma_L, \sigma_T$	: Composites, Longitudinal And Transverse Tensile Strength
σ_f, σ_{PU}	: Nanofillers And PU Tensile Strength
η	: Straightness Factor
θ	: Degree
ε	: Strain
ψ	: Exponential Shape Factor
λ	: Cross-link Density

LIST OF TABLES

Page

LIST OF FIGURES

Page

FABRICATION AND CHARACTERIZATION OF HYBRID NANOFILLER REINFORCED POLYURETHANE NANOCOMPOSITES

SUMMARY

Polyurethane (PU) foams, which are economic due to their low density, low cost and easy processability, are frequently used in a wider range of applications, such as insulation goals, automotive and electronic industries. However, their applications are limited because of some poor properties. Nanomaterials were generally used to enhance desired properties of polymeric matrices. Combining varied nanofillers with dissimilar dimensions can lead to synergy through effective dispersion. Carbon-nanofillers are known for improving the desired properties of polymers. The dispersion quality of nanofillers in the matrix is vital for the fabrication of high-performance nanocomposites. Hybrid nanocomposites possess better properties in comparison with conventional nanocomposites that lead to the formation of an effective network.

The thesis is composed of seven chapters and it is organized as follows: The first chapter will give a detailed literature survey and technical background for the research thesis and the last chapter is a concise but complementary conclusion with inspiring recommendations for future researches. The second, third and fourth chapters are a copy of published articles, where the following two chapters are complementary research findings as well as they are also articles in the press. In brief, the content of chapters related to research findings is to be given.

In the second chapter, the effects of nanofiller addition into polyurethane on mechanical properties and thermal stability by means of tensile, Charpy impact, hardness tests, and thermogravimetric analysis were studied. Nanofillers added to polyurethane are multi-walled carbon nanotubes (MWCNT), two types of silica nanoparticles, and MWCNT/silica as hybrid fillers. Hybrid polyurethane/silica/MWCNT nanocomposite with the constant overall content of 0.75 wt% showed higher tensile strength, hardness, and thermal stability than either of nanofillers at this content, which approves a synergistic effect between multi-walled carbon nanotubes and silica nanoparticles.

In the third chapter of the dissertation, micromechanical modeling and mechanical properties of PU hybrid nanocomposite foams with MWCNTs and graphene nanoplatelets (GNPs) were investigated through tensile strength, hardness, impact strength and modified Halpin–Tsai equation. Three types of GNPs, with varied flake sizes and specific surface areas (SSA), were utilized to study the effect of GNP types on the synergistic effect of MWCNT/GNP hybrid nanofillers. The results indicate a remarkable synergetic effect between MWCNTs and GNP-1.5 (1:1) with a flake size of 1.5 μm and a higher SSA (750 m^2/g), which tensile strength of PU was improved by 43% as compared to 19% for PU/MWCNTs and 17% for PU/GNP-1.5 at 0.25 wt% nanofiller loadings. The synergy was successfully predicted using a unit cell modeling, which the calculated values agree with the experimental results.

Combining various carbon nanofillers with different dimensions can lead to a synergistic effect through the formation of an efficient conductive network. In the

fourth chapter, hybrid PU nanocomposites containing MWCNTs and GNPs were fabricated to study experimental and theoretical aspects of thermal conductivity (TC) enhancement. The optimization of hybrid nanofillers combinations was done to synergically enhance the TC using various types of graphene, nanofillers concentrations and ratios. A synergistic thermal conductivity improvement with MWCNTs and GNPs was confirmed at low nanofillers contents. The TC of hybrid nanocomposite at 0.25 wt% is approximately equivalent to the TC of individual nanofillers at 0.75 wt%. An analytical model for the effective thermal conductivity of single and hybrid nanocomposites was considered with variables of volume fraction, interfacial thermal resistance, straightness of the nanofillers and the percolation effect, in which the predictions of the modified models agreed with the experimental results.

In the fifth chapter, an effective approach for improving dispersion states of MWCNTs and GNPs was employed via hybrid inclusion of the nanofillers in polyurethane matrix to further enhancing viscoelastic properties. Nanocomposites based on MWCNTs, two groups of graphene and hybrid MWCNT/graphene with varied weight fractions and ratios were fabricated via a simple, quick and scalable approach. Dynamic mechanical analysis results indicated an improvement of up to 86% in storage modulus at 25ºC for hybrid MWCNT/GNP-S750 at only 0.25 wt% loading, whereas solely MWCNTs and graphene nanocomposites showed 9% and 15% enhancement at the same content, respectively. The glass transition temperature value was enhanced by about 9.5 ˚C with 0.25 wt% inclusion of well-dispersed three-dimensional MWCNT/GNP-S750 structure, which disclosed a noticeable synergistic effect in thermomechanical properties.

In the sixth chapter of the study, the acoustic and dielectric properties of PU hybrid nanocomposites were investigated. PU containing MWCNT and GNPs were used to evaluate the effects of single and hybrid nanofillers on the final properties of nanocomposites. The results showed a synergistic effect between nanofillers, in which the hybrid nanocomposites exhibit better performance, relative to the single inclusion of the nanofillers. These hybrid nanofillers improved dispersion quality in the polymer matrix due to the formation of a GNPs/CNTs 3D architecture, in which acoustic transmission loss and dielectric constant of PU were enhanced by about 51% and 13% at 0.25 wt% loadings, respectively.

The overall properties of the hybrid nanocomposite revealed the superiority over the single nanofiller system in multifunctionality, evaluated by a performance index. Finally, to compare diverse nanocomposite systems, the performance index (PI) formula was introduced that is based on mechanical, thermal, acoustic and dielectric results of nanocomposites, in which PU with hybrid GNPs/CNTs showed higher PI compared to single GNPs and CNTs, approving its higher multifunctionality. The high multifunctionality of the hybrid nanocomposites in comparison with single nanofiller included nanocomposites reveals the superiority of the hybrid approach that is appropriate for a wide range of applications.

HİBRİT NANODOLGU TAKVİYELİ POLİÜRETAN NANOKOMPOZİITLERİN ÜRETİMİ VE KARAKTERIZASYONU

ÖZET

Düşük yoğunluk, düşük maliyet ve kolay üretimleri nedeniyle ekonomik olan poliüretan (PU) köpükler, yalıtım, otomotiv ve elektronik endüstrileri gibi çok geniş bir uygulama yelpazesinde sıklıkla kullanılmaktadırlar. Ancak, bazı zayıf özellikleri nedeniyle uygulamaları sınırlıdır. Nanomalzemeler genellikle polimerik matrislerin istenen özelliklerini geliştirmek için kullanılmıştır. Farklı boyutlara sahip çeşitli nanodolgu maddelerinin birleştirilmesi, etkili dağılım yoluyla sinerjik etkiye yol açabilir. Karbon nanodolguleın, polimerlerin istenen özelliklerini iyileştirdiği bilinmektedir. Nanodolgu maddelerinin matris içindeki dağılım kalitesi, yüksek performanslı nanokompozitlerin üretimi için hayati önem taşımaktadır. Hibrit nanokompozitler, etkili bir ağ oluşumuna yol açar ve geleneksel nanokompozitlere kıyasla daha iyi özelliklere sahiptir.

Tez yedi bölümden oluşmaktadır ve şu şekilde düzenlenmiştir: İlk bölüm, araştırma tezi için ayrıntılı bir literatür taraması ve teknik arka plan sunacaktır ve son bölüm, gelecekteki araştırmalar için ilham verici önerilerle birlikte kısa ama tamamlayıcı sonuçları göstermektedir. İkinci, üçüncü ve dördüncü bölümler yayınlanmış makalelerin bir kopyası olup, sonraki iki bölüm tamamlayıcı araştırma bulguları olup basılacak iki makalelerdendir. Kısaca araştırma bulguları ile ilgili bölümlerin içeriğine yer verilecektir.

İkinci bölümde çok duvarlı karbon nanotüpler (MWCNT'ler) ve silika nanodolgu maddeleri ile güçlendirilmiş çok işlevli poliüretan köpüklerin spesifik özellikleri geliştirilmiştir. Poliüretan içerisine nanodolgu ilavesinin mekanik özellikler ve termal stabilite üzerindeki etkileri çekme, Charpy darbe testi, sertlik testleri ve termogravimetrik analiz yöntemleriyle incelenmiştir. Poliüretana eklenen nanodolgu maddeleri, çok duvarlı karbon nanotüpler, iki tip silika nanoparçacık ve hibrit dolgu olarak çok duvarlı karbon nanotüp/küresel silikadır. Deney sonuçlarına göre, ağırlıkça %0,25 Silika-A, Silika-B ve MWCNT eklenmesi PU'nun çekme dayanımını sırasıyla yaklaşık %33, %27 ve %15 arttırmıştır, ancak daha fazla nanodolgu ilavesi mukavemeti azaltmıştır. Darbe testi sonuçları, saf PU ile karşılaştırıldığında yaklaşık %96 iyileşme ile ağırlıkça %0,5 MWCNT içeren nanokompozitte maksimum darbe dayanımının görülebildiğini ortaya koymaktadır. Ayrıca, ağırlıkça %0,75 Silika-B ve ağırlıkça %1 Silika-A ilavesi, PU'nun darbe mukavemetini sırasıyla yaklaşık %82 ve %75 artırmıştır. Shore-A sertliğinde, ağırlıkça %0,5 Silika-B içeren nanokompozit köpük en yüksek sertliğe sahiptir. Ağırlıkça %0,25 Silika-A ve %0,5 MWCNT içeren hibrit nanokompozit maksimum çekme mukavemeti, elastik modül ve sertlik gösterirken, MWCNT/PU nanokompozitte bu en yüksek sonuçlar ağırlıkça %0,25 MWCNT'de elde edilmiştir. Ağırlıkça %0,75 sabit toplam içeriğe sahip hibrit poliüretan/küresel silika/çok duvarlı karbon nanotüp nanokompoziti, bu içerikteki nanodolgulardan herhangi birine göre daha yüksek çekme mukavemeti, sertlik ve termal kararlılık göstermiştir, buda çok duvarlı karbon nanotüpler ve silika nanopartiküller arasındaki sinerjik bir etkiyi onaylamaktadır.

Tezin üçüncü bölümünde, MWCNT'ler ve grafen nanoplateletler (GNP'ler) içeren PU hibrit nanokompozit köpüklerin mikromekanik modellemesi ve mekanik özellikleri, çekme mukavemeti, sertlik, darbe mukavemeti ve modifiye Halpin-Tsai denklemi aracılığıyla incelenmiştir. Grafen türlerinin CNT/GNP hibrit nanodolgu maddelerinin sinerjistik etkisi üzerindeki etkisini incelemek için çeşitli boyutlarda ve spesifik yüzey alanlarına (SSA) sahip üç tip grafen kullanılmıştır. Sonuçlar, MWCNT'ler ile GNP-1.5 (1:1) arasında, 1,5 μm'lik bir pul boyutu ve daha yüksek bir SSA (750 m^2/g) ile kayda değer bir sinerjik etki göstermektedir; PU'nun çekme mukavemeti ağırlıkça %0,25 nanofiller yüklemelerinde PU/CNT için %19 ve PU/GNP-1.5 için %17'ye kıyasla %43 oranında iyileştirilmiştir. Sinerji, hesaplanan değerlerin deneysel sonuçlarla uyumlu olduğu bir birim hücre modellemesi kullanılarak başarıyla tahmin edilmiştir. Tek ve hibrit nanokompozitlerin çekme mukavemeti sonuçlarına uyması için üstel bir şekil faktörü ile modifiye Halpin-Tsai modellemesi kullanılmıştır. Modelleme sonuçlarının deneysel verilerle son derece uyumlu olduğu ve en yüksek sinerjiyi elde etmek ve hibrit nanokompozitlerdeki nanodolgu maddelerinin optimal oranı ve içeriğini tahmin etmek için grafenleri ve MWCNT'leri içeren bir birim hücre modeli geliştirilmiştir. Grafenler ve CNT'ler arasındaki bağlantılar, karbon nanotüplerin uzunluğu, birim hücredeki grafenler arasındaki boşluktan daha yüksek olduğunda daha olasıdır. Sunulan model, birçok deney olmadan farklı CNT'ler ve grafenler arasında sinerjik etki elde etmek için bir kılavuz olabilir.

Dördüncü bölümde, farklı boyutlarda çeşitli karbon nanodolgu maddelerinin birleştirilmesi, verimli bir iletken ağ oluşumu yoluyla sinerjik bir etkiye yol açabilir. Tezin dördücü bölümünde, termal iletkenlik (TC) geliştirmenin deneysel ve teorik yönlerini incelemek için CNT'ler ve grafenler içeren hibrit PU nanokompozitleri üretilmiştir. Termal iletkenliği sinerjik olarak geliştirmek için hibrit nanodolgu kombinasyonlarının optimizasyonu, çeşitli grafen türleri, nanodolgu konsantrasyonları ve oranları kullanılarak yapılmıştır. CNT'ler ve grafenler ile sinerjik bir termal iletkenlik gelişimi, düşük nanodolgu içeriklerinde doğrulanmıştır. Hibrit nanodoldurucular, termal iletkenliği etkili bir şekilde artırabilir, böylece tek boyutlu (1D) CNT'ler, daha verimli bir üç boyutlu (3D) termal iletken ağ oluşturmak için bitişik iki boyutlu (2D) grafeni birbirine bağlayabilirler. Sonuç olarak, ağırlıkça %0,25'teki hibrit nanokompozitin termal iletkenliği yaklaşık olarak ağırlıkça %0,75'teki tekli nanodolgu maddelerinin termal iletkenliğine eşdeğerdir. Buda, viskoziteyi azaltmak ve nanokompozitlerin işlenebilirliğini geliştirmek için hayati önem taşımaktadır. Bu nedenle, hibrit nanokompozitlerin imalatının, gerekli nanodolgu maddesi içeriğini azaltarak daha yüksek işlenebilirliğe sahip uygun maliyetli bir yöntem olduğu sonucuna varılabilir. Ek olarak, daha büyük olan GNP-L150 için daha yüksek nanodolgu içeriğinde (ağırlıkça %0,75) sinerjizm görülebilir. Ayrıca, düzlük faktörü ve süzülme etkisini fit parametreleri olarak dahil ederek tekli ve hibrit nanokompozitlerin termal iletkenliği üzerine analitik bir çalışma sunulmuştur ve burada modifiye edilmiş model tahminleri ile deneysel sonuçlar arasında olağanüstü bir uyum olduğu gösterilmiştir. Sonuçlar, nanodoldurucuların düzlüğünün nanokompozitlerin termal iletkenliğini derinden etkilediğini ve daha büyük grafenin polimer matrisinde daha dalgalı veya daha az düz olma eğiliminde olduğunu, böylece grafen pul boyutunun arttırılmasıyla hesaplanan düzlük oranının azaldığı görülmüştür.

Poliüretan matrisine eklenen CNT'lerin ve grafenlerin dağılımlarını iyileştirmek için etkili bir yaklaşım olan hibrit nanodolgular viskoelastik özellikleri daha da arttırmaya yardımcı olmuştur. Beşinci bölümde karbon nanotüplere ve farklı tip grafenlere dayalı nanokompozitler, çeşitli ağırlıklar ve oranlarda basit, hızlı ve ölçeklenebilir hibrit

yaklaşımla üretilmiştir. PU nanokompozitlerin viskoelastik özellikleri, depolama modülü, sönümleme aktörü (Tanδ) ve camsı geçiş sıcaklığının (T_g) incelendiği dinamik mekanik analiz (DMA) kullanılarak gerçekleştirilmiştir. PU'nun depolama modülü, tekli nanodolgular ile iyileştirilmiştir ve maksimum PU/GNP-S750 için ağırlıkça %0,75 içerikte %22 artmıştır. Fakat T_g değeri yüksek konsantrasyonlarda (%0,75) azalmıştır. DMA sonuçları, hibrit MWCNT/GNP-S750 için yalnızca ağırlıkça %0,25 yüklemede 25ºC'de depolama modülünde %86'ya kadar bir iyileşme gösterirken, tekli MWCNT ve grafenli nanokompozitler aynı içerikte sırasıyla %9 ve %15 geliştirme göstermişlerdir. Camsı geçiş sıcaklığı iyi dağılmış üç boyutlu MWCNT/GNP-S750 yapısının ağırlıkça %0,25 eklenmesiyle yaklaşık 9,5 ˚C artmıştır, buda termomekanik özelliklerde gözle görülür bir sinerjistik etki ortaya koymaktadır. CNT'lerin bitişik grafeni birbirine bağladığı hibrit nanokompozitlerde bir 3D hibrit ağ oluşturulmuştur. Grafen/CNTs hibrit nanokompozitleri gerildiğinde, nanodolguların mesafesi artar, ancak, gevşemeden sonra ilk durumuna tekrar geri dönerler, buda PU'nun depolama modülünün artmasına yol açar. Üretilen nanokompozitlerin C-faktörü (takviye katsayısı), dolaşıklık derecesi ve çapraz bağ yoğunluğu, tekli ve hibrit karbon nanodolgu maddelerinin PU matrisi ile etkileşimini değerlendirmek için depolama modülü değeri kullanılarak incelenmiştir. Tüm bu sonuçlar, daha küçük boyutta, daha yüksek bir özgün yüzey alanına ve daha fazla yüzeysel kusura sahip GNP-S750'nin daha etkili bir 3D mimarisi oluşturmak için daha yüksek bir potansiyele sahip olduğunu ve buda hibrit nanodolgu olarak CNT'ler ile birleştirildiğinde PU'nun depolama modülünü ve T_g'sini daha da iyileştirdiğini ortaya koymuştur. Bu hibrit grafen/CNT nanokompozitleri, ambalajlama ve yapısal sönümleme malzemeleri gibi termal stabilite ve termomekanik özelliklerin çok önemli ilkeler olduğu hafif köpük uygulamaları için uygundur.

Çalışmanın altıncı bölümünde PU hibrit nanokompozitlerin akustik ve dielektrik özellikleri incelenmiştir. PU içeren CNT ve grafenler, tekli ve hibrit nanodolguların nanokompozitlerin nihai özellikleri üzerindeki etkilerini değerlendirmek için kullanılmıştır. Sonuçlar, nanokompozitlerin hibrit nanodolguların tekli dahil edilmesine göre daha iyi performans sergilediği ve nanodoldurucular arasında sinerjik bir etki olduğunu göstermiştir. Hibrit GNPs/CNTs'lerin üç boyutlu mimarisinin oluşumundan dolayı polimer matrisinde dağılım kalitesi iyileşmiştir ve bu hibrit nanodoldurucular, PU'nun akustik iletim kaybının ve dielektrik sabitinin ağırlıkça %0,25 yüklemelerde sırasıyla yaklaşık %51 ve %13 artırmıştır. Hibrit grafen/CNT'ler, tekli CNT'lere ve GNP'lere göre daha yüksek dielektrik sabiti, elektriksel iletkenlik ve dielektrik kaybı göstermiştir. Bununla birlikte, hibrit sistemlerin yüksek dielektrik kaybı nanokompozitlerin pratik uygulamalarını kısıtlamaktadır ve gelecekte çözülmesi gereken bir problemdir.

Son olarak, hibrit nanokompozitin genel özellikleri, bir performans indeksi (PI) ile değerlendirilmiştir ve tekli nanodolgu sistemi üzerindeki üstünlüğünü ortaya koymuştur. Çeşitli nanokompozitleri karşılaştırmak için, nanokompozitlerin mekanik, termal, akustik ve dielektrik sonuçlarına dayanan performans indeksi formülü tanıtılmıştır. Burada PU, hibrit GNP/CNT'ler ile tek GNP'ler ve CNT'lere kıyasla daha yüksek PI göstermiştir, buda hibrit nanokompozitlerin çok işlevliliğini onaylamaktadır. Hibrit nanokompozitlerin tekli nanodolgu içeren nanokompozitlere kıyasla çok işlevliliği, geniş bir uygulama yelpazesi için uygun olan hibrit yaklaşımın üstünlüğünü ortaya koymaktadır.

1. INTRODUCTION

1.1 Research Background

The composites refer to materials that comprise two phases or more, where have a mixture of characteristics that varies from the properties of their components. The energy efficiency requirements increasingly demand lightweight structures such as polymeric foams. The simple fabrication of polyurethane (PU) structures and their composites in a single processing step is the main advantage of PU technology (Kausar, 2018). Due to their low density, PU foams have been used in versatile applications such as insulation, packaging, seating and sound-absorbing materials (Burgaz & Kendirlioglu, 2019; Hoseinabadi, Naderi, Najafi, Motahari, & Shokri, 2017). However, PU foams have some disadvantages, such as low mechanical properties and deficient structural stability in high temperatures, which hinder their widespread application in the automobile and aerospace industries (Engels et al., 2013).

Reinforcing polymers by incorporation of nanofillers can considerably improve the preferred properties of the polymeric nanocomposite, where there are abundant potential applications that can benefit from them (Coleman, Khan, Blau, & Gun'ko, 2006; Faraji, Yardim, Can, & Sarac, 2017; Mahmoodi, Arjmand, Sundararaj, & Park, 2012). Besides, constituents of PUs (polyol and isocyanate) are in a liquid form, which allows for the simple integration of solid nanofillers.

There are main challenges that have to be taken into consideration to fabricate nanocomposites with an effective nanofiller reinforcement, where a large aspect ratio, good dispersion, alignment, and interfacial stress transfer are required. Due to high surface area and surface tension and strong force between the nanofillers, they tend to agglomerate, whereas to improve their dispersion in polymer matrixes, their surface should be treated (Bandarian, Shojaei, & Rashidi, 2011; Faraji et al., 2017). Agglomerations are initiated by the stacked formation of nanofillers, which generate the development of many defects sites in the nanocomposites. These defects will

diminish the reinforcement effects whereby it will trigger deformations causing early failure (B. Li & Zhong, 2011).

Carbon nanofillers such as multi-walled carbon nanotubes (MWCNTs) and graphene nanoplatelets (GNPs) are one of the most promising nanomaterials. Their extraordinary mechanical strength, thermal and electrical properties make them highly demanding in reinforcing polymeric materials (Benzait & Trabzon, 2018; Ciecierska et al., 2016; Eda, Fanchini, & Chhowalla, 2008; Rashahmadi, Hasanzadeh, & Mosalman, 2017; D. Yuan, Pedrazzoli, Pircheraghi, & Manas-Zloczower, 2017). However, agglomerations and the restacking tendency of these nanofillers enhanced dispersion difficulty in the polymer matrix (Ayub Karimzad Ghavidel, Azdast, Shabgard, Navidfar, & Sadighikia, 2015; Amir Navidfar, 2014; Amir Navidfar, Azdast, & Karimzad Ghavidel, 2016a; A Navidfar, Azdast, Karimzad Ghavidel, Sadighikia, & Mamaghani Shishevan, 2014). Hybridization of the one-dimensional (1D) MWCNTs and two-dimensional (2D) graphene with different geometry can overcome this dispersion challenge. The synergistic effect between CNTs and graphene has been shown to enhance mechanical properties (Bagotia, Choudhary, & Sharma, 2019; Chatterjee et al., 2012; Amir Navidfar & Trabzon, 2019), thermal (min Kim, Lee, Song, & Lee, 2019; Amir Navidfar & Trabzon, 2021), electrical conductivity (Ayub Karimzad Ghavidel et al., 2015; Ayub Karimzad Ghavidel, Navidfar, Shabgard, & Azdast, 2016; Hongming Zhang et al., 2018) and dielectric properties (Ke, McMaster, Christopherson, Singer, & Manas-Zloczower, 2019).

Besides, silica (SiO_2) nanoparticles have been widely used with polymers to enhance heat resistance, radiation resistance, and mechanical properties (G. Chen, Zhou, Gu, & Wu, 2007). Recent studies have investigated beneficial outcomes for nanocomposites containing two or more geometrically different fillers (Sapkota et al., 2017; Szeluga, Kumanek, & Trzebicka, 2015). The improvements in nanofillers dispersion led to considerably better properties due to their synergistic effects. Studies demonstrate that the geometric shape, surface properties, and the ratio of nanofillers within the combination are significant factors governing the reinforcing effects in nanocomposites (Mansour & Tzetzis, 2013; Wu et al., 2017). Therefore, CNT and silica nanoparticle combinations can be an effective route to enhance their reinforcing performance (Cheni, Guo, & Wu, 2012).

Even though the number of scientific research published in the literature regarding the effect of processing conditions and contents of nanofillers on final properties of polymeric nanocomposites, the exact details remain inconsistent, especially about hybrid nanofiller included nanocomposites. Owing to the complexity of nanocomposites in the case of nanofiller dispersion, self-assembly, nanofiller-chain interactions and lack trustworthy experiments (Jancar et al., 2010). The state of the art of research regarding polymeric nanocomposites will be studied for creating pragmatic results. CNTs, GNPs and silica nanoparticles will be use exploited as nanofillers into PU matrix to fabricate polymeric nanocomposites.

1.2 Research Aims and Objectives

The main aim of this dissertation is to fabricate multifunctional nanocomposites containing single and hybrid incorporation of GNPs, CNTs, and silica nanoparticles with improved mechanical, thermal, viscoelastic and acoustic properties. To achieve these goals, various contents of functionalized MWCNTs, spherical silica (Silica-A), amorphous silica (Silica-B) nanoparticles and three types of GNPs were added to the PU matrix. A key question is which types of nanofillers are best suited to show a synergistic effect to reinforcing polymeric nanocomposites. To investigate this, we compared three commercially available varieties of GNPs with different flake sizes (24, 5 and 1.5 μm), aspect ratios and specific surface areas (150 and 750 m^2/g) to study the synergistic effect of GNPs with MWCNTs on the tensile test, hardness, dynamic mechanical analysis (DMA), impact test, thermal conductivity, acoustic properties, etc. of PU hybrid nanocomposites. Various nanofiller ratios were tested to find the optimal loading and the highest synergy. The tensile strength of the single and hybrid nanocomposites was also compared with the predictions of the well-established Halpin-Tsai model, which was modified by adding an exponential shape factor, and the results fitted the experimental data successfully (Montazeri, Javadpour, Khavandi, Tcharkhtchi, & Mohajeri, 2010; Yeh, Tai, & Liu, 2006). In addition, a unit cell comprising GNPs and MWCNTs was considered, which the synergistic effect was successfully predicted.

Structures and morphologies of nanocomposites were studied by scanning electron microscopy (SEM) and transmission scanning electron microscopy (TEM), X-ray diffraction (XRD), and Raman spectroscopy. A theoretical study on the effective

thermal conductivity of single and hybrid nanocomposites by incorporating the straightness factor and percolation effect as fitting parameters is presented. Our analytical results are found to be in reasonable agreement with experimental data, which well describe the thermal conductivity improvement of single and hybrid nanocomposites.

Successful dispersing of these hybrid carbon nanofillers in the polymeric matrix can pave the way toward low-cost and efficient composite fabrication. Successful dispersing of these hybrid carbon nanofillers in the polymeric matrix can pave the way toward low-cost and efficient composite fabrication.

The specific objectives are;

a) To fabricate multifunctional PU nanocomposites with the incorporation of single and hybrid nanofillers.

b) To investigate the effect of nanofiller types and contents on the final properties of PU nanocomposites.

c) To optimize hybrid nanofillers contents and ratios to maximize the synergistic effect between nanofillers, which was expected to surpass the performance of individual nanofiller systems in PU matrix.

d) To fabricate a multifunctional nanocomposite, which reveals improved overall properties.

e) Theoretical modeling of nanocomposites to be in reasonable agreement with experimental data.

1.3 Thesis Outline

This dissertation is divided into seven chapters based on three published and two in press academic papers regarding experimental and analytical research of mechanical, thermal and dynamic mechanical analysis of multifunctional PU nanocomposites, as well as their acoustic and dielectric studies in the last section. Chapter 1 describes briefly about research background, aims and objectives of the study and an overview of the literature that relates to the used nanofillers and their polymeric nanocomposites. Widespread reviews of former works were considered and documented in all sections for a better understanding of each study. Chapter 2 studied the effect of MWCNTs and

silica nanoparticles additions into PU foams on mechanical properties and thermal stability using tensile, Charpy impact, hardness tests and thermogravimetric analysis (TGA). Chapter 3 presents micromechanical modeling and mechanical properties of hybrid nanocomposite foams with MWCNTs and GNPs, which were investigated through tensile strength, hardness, impact strength and modified Halpin–Tsai equation. Three types of GNPs, with varied flake sizes and specific surface areas (SSA), were utilized to study the effect of GNP types on the synergistic effect of MWCNT/GNP hybrid nanofillers. Chapter 4 explains the results and discussions containing experimental and theoretical aspects of thermal conductivity (TC) enhancement of PU with MWCNTs/GNPs. The optimization of hybrid nanofillers combinations was done to synergically enhance the TC using various types of graphene, nanofillers concentrations and ratios. Chapter 5 focused on the viscoelastic behavior of PU foam nanocomposites reinforced with graphene/MWCNTs hybrid nanofillers, in which storage modulus, damping factor (Tan δ) and the glass transition temperature (T_g) were studied. Chapter 6 summarized other characteristics of fabricated nanocomposites e.g. acoustic and dielectric properties. At the end (Chapter 7), results and discussion of this work were summarized and recommendations for future works were suggested to additional progress about the polymeric nanocomposites.

1.4 Literature Review

1.4.1 Materials

1.4.1.1 Polyurethane

Polyurethane foams, which are economic due to their low density, are frequently used in a wider range of applications, such as insulation goals, automotive and electronic industries. Its components (polyol and isocyanate) are in a liquid form, which allows its manufacturers to simply integrate solid nanofillers. PU foams were considered due to their lightweight and cellular structure, high global volume production, low cost, and solid nanofillers inclusion facility. It is known as a desirable sound absorber, low thermal conductivity and low water absorption material. PU is one of the most useful plastic materials, in which the nature of the chemistry permits PU to solve challenging difficulties, to be molded into unusual forms and to improve industrial and customer

products via adding comfort, warmth and convenience to our lives. PU is constructed by reacting a polyol (an alcohol with more than two reactive hydroxyl groups per molecule) with a diisocyanate with proper catalysts and additives. A broad range of PU can be prepared to meet the needs of particular applications due to a diversity of diisocyanates and polyols. Mostly PU foams are used in two types of rigid and flexible, where rigid ones are commonly used for thermal insulation and flexible ones are utilized for cushioning transportation and packaging applications. One of the most significant properties of PU foam is its thermal conductivity that is between 0.02 and 0.03 W/mK (Hu Zhang, Fang, Li, & Tao, 2017). However, PU can be found as coatings, adhesives, sealants, binders and elastomers in the forms of thermoplastic polyurethane (TPU) and waterborne polyurethane (WPU). Appropriation of its reactant and manufacturing process allows a wide range of applications (Klempner & Frisch, 1991).

Rigid PU applications demand about 30% of global polyisocyanate and polyols. It is intensely cross-linked, closed-pore foams fabricated through treating polyether and/or polyester polyols with polymer MDI grades. The density of rigid PU foams can be controlled with the addition of physical blowing agents or the construction of carbon dioxide, which is formed by the reaction of water and isocyanates. The synthesized resins are fabricated by a chemical reaction between an isocyanate and a hydroxyl group, where a compound comprising two or more isocyanate groups per molecule reacts with a polyol, displayed in Figure 1.1 (Trovati, Sanches, Neto, Mascarenhas, & Chierice, 2010). The insulating properties of a rigid PU foam are dependent on its cell size. It could be concluded that the smaller cells deliver the lower the thermal conductivity and the better the insulating performance. Lightweight PU foams have been confirmed to be crucial, mostly in motor vehicle acoustics as a result of the need to minimize weight, where is using as an insulator for an average of 14 m^2 of a vehicle's interior (Engels et al., 2013).

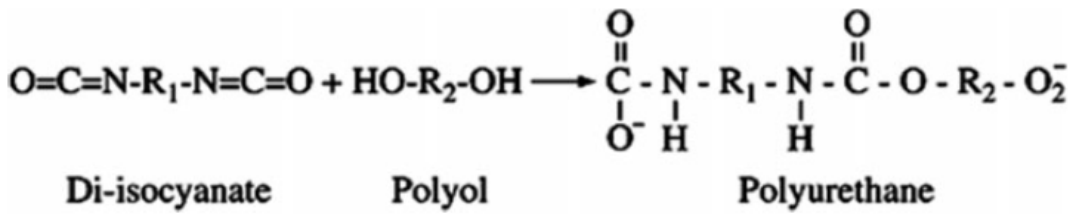

Figure 1.1 : Urethane polymerization (Trovati et al., 2010).

1.4.1.2 Carbon nanotubes

Since their discovery, CNTs as one-dimensional nanofillers, have seized a significant role in polymeric nanocomposites fields owing to their exceptional electrical current carrying capacity (10^3–10^5 S/m), superior thermal stability (>600 ˚C) and conductivity (2000 W/mK), stiffness (modulus ~1 TPa, strength ~100 GPa) and high aspect ratio (Mittal, Dhand, Rhee, Park, & Lee, 2015). CNTs properties mainly depend on their morphology, size and diameter, which can be metallic or semiconducting, depends on their atomic arrangement. Several techniques such as arc evaporation, chemical vapor deposition (CVD), laser ablation, flame synthesis, electrolysis, etc. are broadly used for the fabrication of CNTs (Mubarak, Abdullah, Jayakumar, & Sahu, 2014). CNTs can be categorized into two types of single-walled carbon nanotubes (SWCNT) and MWCNTs, which their properties extremely depend on their morphology, size and diameter. Several papers summarized the mechanical (Lourie & Wagner, 1998; Yakobson, Brabec, & Bernholc, 1996; M.-F. Yu, Files, Arepalli, & Ruoff, 2000), electrical (Dai, Wong, & Lieber, 1996; Ebbesen et al., 1996) and thermal (Berber, Kwon, & Tománek, 2000; Hone, Whitney, Piskoti, & Zettl, 1999) properties of CNTs in the literature (A. Kumar, Sharma, & Dixit, 2020a, 2020b). CNTs have exceptionally high elastic modulus and strength, relative to carbon fibers (CFs) (Higgins & Brittain, 2005), while their density is lower than that of CFs (J. P. Lu, 1997). The properties of used MWCNTs is summarized in Table 1.1.

High surface area, as a result of their high aspect ratio and nanostructure, helps in the better interaction with polymers, therefore nanocomposites with lower CNTs loadings can be fabricated with efficiently improved mechanical strength. CNTs/polymer nanocomposites are employed in numerous fields to potentially use their extraordinary properties.

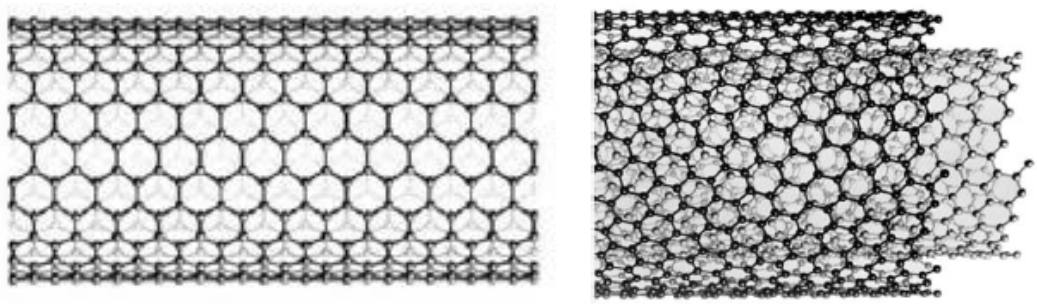

Figure 1.2 : Structure of SWCNT (left) and MWCNT (right) (Iijima, 2002).

Table 1.1 : Typical properties of used MWCNTs.

Property	Value
Diameter (nm)	8 - 10
Average Length (µm)	1 - 3
Aspect ratio	100 - 375
Density (g/cm^3)	~2.1
Carbon Purity (%)	92
Electrical Conductivity (S/cm)	98
Specific surface area (m^2/g)	290
Elastic modulus (GPa)	1000 [1]
Tensile strength (GPa)	10 – 60 [1]
Electron mobility (cm^2/Vs)	10^4 - 10^5 [1]
Thermal conductivity (W/mK)	3000 [1]
Coefficient of thermal expansion (K^{-1})	Negligible [1]
Thermal stability (ºC)	>600 (in air), 2800 (in vacuum)[1]

1.4.1.3 Graphene and graphene-based materials

Graphene, a single-layer carbon atom sheet with thickness around 0.4 - 1.7 nm, has become popular since the 2010 Nobel Prize in physics. Graphene, a two-dimensional (2D) single layer of carbon atoms, is the strongest and stiffest nanomaterial ever reported (Hu, Kulkarni, Choi, & Tsukruk, 2014). The slight diminishing of Young's modulus and the strength with the increase of sheet number is attributed to the weak van der Waals between layers (Y. Y. Zhang & Gu, 2013). Graphene has been broadly used in polymeric composites as reinforcement owing to its exceptional properties, e.g., high surface area (2630 m^2/g), superior thermal conductivity (~5000 W/mK), high electrical conductivity (~10^4 S cm^{-1}), high mechanical properties (tensile strength 130 GPa, Young's modulus 1 TPa and fracture toughness 4-5 MPa m$^{1/2}$), excellent intrinsic carrier mobility (2×10^5 cm^2 V^{-1} s^{-1}) and barrier properties (A. Kumar et al., 2020a, 2020b). Its planar construction and high aspect ratio are very appropriate for stress transferring in nanocomposites, however, the high agglomeration tendency restricts its applications that could reason stress concentration and initiate cracks (Moosaei, Sharif, & Ramezannezhad, 2017). Besides, the properties of 2D materials

[1] References data

can significantly differ due to the existence of vacancy and Stone-Wales defects (M. Li et al., 2019). Many scientists have used molecular modeling, simulation and experimental methods to discover the different properties of graphene, which are summarized in various reviews (Akinwande et al., 2017; Geim, 2009; A. Kumar et al., 2020a, 2020b; Naumis, Barraza-Lopez, Oliva-Leyva, & Terrones, 2017). The presence of the sheets number, surface modifications, size, orientation and total oxygen content categorized graphene-based nanostructured materials, which their properties depend on these factors (Qin, Yan, Guo, & Gao, 2018; Y. J. Sun, Ma, & Xu, 2013; Zandiatashbar et al., 2014; Y. Y. Zhang & Gu, 2013). Graphene nanoplatelets (GNP), graphene oxides (GO), reduced GO (rGO) and recently graphene nanoribbons (GNR) are much more commonly studied due to their accessibility. Various published review papers can be found on the synthesis, processing and application of graphene (W.-W. Liu, Chai, Mohamed, & Hashim, 2014; Papageorgiou, Kinloch, & Young, 2017; Singh et al., 2011; Terrones et al., 2010), in which various conventional synthesis methods of graphene can be outlined as, mechanical exfoliation, CVD, CNT unzipping (for obtaining nanoribbons), liquid-phase exfoliation, electrochemical exfoliation, epitaxial growth, and reduction of GO. Each method has advantages and drawbacks that have been outlined by Raccichini et al. in terms of graphene quality, scalability, purity and fabrication cost (Raccichini, Varzi, Passerini, & Scrosati, 2015). Scientists are making sensational efforts to use graphene and its composites in applications such as super capacitors, batteries, fuel cells, sensors, solar cells, optoelectronics, energy storage, electronics, biomedical applications, etc. (Lawal, 2019).

GO is intrinsically hydrophilic due to functionalities such as carboxyl, hydroxyls, and epoxy groups on its basal plane (D. Zhang et al., 2016). GO showed higher dispersion rates in matrixes, but the existence of functional groups and defects deteriorated their electrical and thermal conductivity. Therefore, as a cost-effective approach to prepare graphene, chemically and physically rGO was obtained with good electrical properties. On the other hand, GNRs are elongated strips of graphene, which can be prepared using three main approaches of longitudinal unzipping of CNTs (most scalable), bottom-up synthesis and lithographic cutting of graphene (Habibpour et al.). The composites including graphene, as an outstanding candidate nanofiller, exhibited huge improvement, relative to unfilled materials (Arif et al., 2020; X. Sun et al., 2020; Raquel Verdejo, Bernal, Romasanta, & Lopez-Manchado, 2011).

1.4.2 Functionalization of Graphene and CNTs

As previously mentioned, the dispersibility of graphene/CNTs is a crucial factor in nanocomposites fabrication. Functionalization of graphene and CNTs is necessitated to avoid their agglomeration, which makes them more effective in the polymer matrix and improved the properties of nanocomposites. Functionalization techniques can be divided into two types of covalent functionalization and non-covalent functionalization that have been previously reviewed (Boukhvalov & Katsnelson, 2009; Ji, Xu, Zhang, Cui, & Liu, 2016; Layek & Nandi, 2013; G.-h. Yang et al., 2017). Both methods modify the surface of carbon-based nanofillers, along with improving their interaction with the polymer chains due to their high surface area and roughness (Bagotia, Choudhary, & Sharma, 2018). Covalent modification is much more appropriate when stronger interaction is needed. Covalent linkage between carbon and other functional groups such as oxidation, carboxyl, nitration, ketone, fluorination, etc. takes place in covalent functionalization, where strong acids and other oxidizing agents such as HNO_3, H_2O_2, $H_2SO_4 + HNO_3$, $H_2SO_4 + KMnO_4$ have been used (Ferreira et al., 2016; Mittal et al., 2015). The covalent functionalization of graphene has been generally achieved before the GO reduction process (Uyor, Popoola, Popoola, & Aigbodion, 2018). Covalent functionalization methods have a drawback of distortion in the structure of carbon-based nanofillers, which leads to compromise their electrical and thermal properties. Non-covalent functionalization helps in linking molecules without forming chemical bonds, which can be attained by π–π interactions, van der Waals forces, hydrophobic forces, ionic bonding, hydrogen bonding and electrostatic effects that work by supramolecular chemistry (Ji et al., 2016). Suspension of nanofillers occurred in the existence of polymers such as poly(sodium 4-styrenesulfonate), Polyvinylpyrrolidone, etc. (Karim et al., 2017; Steuerman et al., 2002). In addition to polymers, surfactants can be used for functionalization, such as sodium dodecyle sulfonate (SDS), sodium deoxycholate (DOC), sodium cholate (SC), sodium dodecyle benzene sulfonate (SDBS) (Simmons, Hashim, Vajtai, & Ajayan, 2007; Zeng et al., 2018), etc. which declines the surface tension, thus inhibiting the nanofillers agglomerations. Generally, functionalization processes have the drawback that the structure of nanofillers may be destroyed during ultrasonication and surface treatment (Monthioux et al., 2001). Preventing the structure of nanofillers is required so that high aspect ratio nanofillers (like graphene and CNTs) cannot transfer their

strength or stiffness to the polymer matrix below a critical dimension (K. Song et al., 2013). Therefore, interfacial progress is essential to improve nanofillers dispersion and their interaction with the polymer matrix, along with maintaining their structure (Schadler, 2007).

Decoration of graphene with other nanofillers can be employed to mitigate its agglomerates. This hybridization approach provides ease in the fabrication of nanocomposites relative to the functionalization of graphene, which has been outlined in the present review. Hybrid nanofillers have become very fascinating and favorable materials for compensating the unpleasant properties of functionalized graphene in the nanocomposites (A. Kumar, Sharma, & Dixit, 2019). Min et al. (Min et al., 2018) reported that tensile strength of polyimide (PI) nanocomposites with GO nanosheets and carboxyl-functionalized MWCNTs (GO/MWCNTs) enhanced about 25.1% at a ratio of 3:1, as compared with the pure PI owing to strong interfacial covalent bonds between GO/MWCNTs and the PI matrix. Navidfar and Trabzon (Amir Navidfar & Trabzon, 2019) introduced a 3D hybrid nanofiller by combining GNPs and functionalized MWCNTs (using H_2O_2). They observed a 43% improvement in tensile strength of PU nanocomposites, relative to a 19% and 17% increase for PU/MWCNTs and PU/GNPs, respectively.

1.4.3 Fabrication of CNTs and Graphene Nanocomposites

To adequately disperse nanofillers into the polymer matrix with strong adhesion and interaction, several conventional and developed fabrication techniques have been presented in the literature. The interface between the nanofillers and the matrix along with a homogeneous dispersion and the aspect ratio of nanofillers are key parameters for preparing polymeric nanocomposites, which are the ultimate properties of nanocomposites critically depend on them. In general, the fabrication systems of polymeric nanocomposites with single carbon nanofillers can also be applied to hybrid nanocomposites. This section briefly summarizes the mainly used traditional methods with commercial feasibility such as melt compounding, solution mixing, in-situ polymerization and layer by layer (LbL) assembly (Mohamadi & Sharifi-Sanjani, 2016). These methods are partially applicable for additive manufacturing techniques, which allow the fabrication of hybrid nanocomposites with 3D networks and tailored morphologies.

1.4.3.1 Solution blending

Solution blending is the most broadly used method for the fabrication of graphene/CNTs based polymeric nanocomposites, which involves the compounding of nanofillers with a polymer in an adequate solvent using a mechanical or magnetic stirrer or ultrasonication. The suspension is evaporated in an organized condition after casting into a mold or on the surface of a substrate. Generally, solution mixing delivers favorable dispersion of the nanofillers that has been extensively used owing to its low energy consumption, facility and versatility (Elashmawi, Alatawi, & Elsayed, 2017; Guan, Xing, Wang, Li, & Li, 2017; Shang et al., 2015; Shen, Zhai, Tao, Lu, & Zheng, 2013; C. Yang, Hao, Dai, & Zhang, 2017). However, re-aggregation of nanofillers may take place after solvent evaporation. To overcome this drawback, the researchers introduced some developed techniques, such as the co-solvent method (Liao, Park, Abdala, & Macosko, 2013), spin casting (Du, Fischer, & Winey, 2003) and surfactant addition (Sen et al., 2004).

1.4.3.2 Melt compounding

Melt compounding mainly deals with thermoplastic polymers, which involves melting polymers at high temperatures to form viscous liquid along with shear mixing of nanofillers using extrusion and injection molding techniques, etc. Although melt mixing generally causes a less efficient nanofillers distribution than solution mixing and in situ polymerization (Mahmoud, 2011), nanocomposites with favorable properties can be prepared. This method is popular due to its simplicity and adaptability with large-scale industrial fabrication and it can be used for polymers that are not appropriate for solution mixing and in situ polymerization. However, breakage, wrinkling, folding and bending of nanofillers with a high aspect ratio may result during the melt mixing due to the high shear force needed for effective mixing in this approach (Dasari, Yu, & Mai, 2009). The melt compounding method is recently modified by research groups to develop dispersion of nanofillers and the subsequent improvement of the desired properties of nanocomposites. For instance, the orientation of nanofillers in the polymer matrix provides homogeneity in which a substantial enhancement was reported for the final properties of nanocomposites (Gaska, Kádár, Rybak, Siwek, & Gubanski, 2017; Pandit et al., 2020). The hybrid nanofiller strategy can also improve both the dispersion and consequently the properties of nanocomposites prepared by

melt mixing (Ning et al., 2013; P. a. Song et al., 2013), which will be discussed in the next section.

1.4.3.3 In-situ polymerization

In-situ polymerization has also been used to disperse graphene/CNTs into a polymer matrix in which monomers are the starting materials instead of polymers. This approach leads to better distribution and better interaction between nanofillers and can be used for the polymer matrixes that are thermally unstable and insoluble (Ding et al., 2014). Nevertheless, in-situ polymerization is not an economically appealing and scalable approach, relative to solution or melt mixing techniques (H. Kim, Abdala, & Macosko, 2010). The challenge of high viscosity during polymerization at higher nanofiller loadings is another limitation of this approach (Raquel Verdejo et al., 2011).

1.4.3.4 Layer by layer (LbL) assembly

To prepare multilayer thin films with hierarchical nanostructures, layer by layer (LbL) assembly has been exploited over the past few years. The morphology of multilayer nanocomposites films with desired nano-architectures can be excellently controlled for a multitude of applications including electric devices, membranes, energy storage and biological usages. Lee et al. (T. Lee et al., 2015) reviewed the recent development in the LbL assembly of hybridized graphene nanocomposites, where their desired performance improved over the individual components.

1.4.3.5 Combining methods

Moreover, some nanocomposites can be fabricated by merging solution mixing or in-situ polymerization, with additional techniques such as melt compounding and shear blending (Mohamadi & Sharifi-Sanjani, 2016; Scaffaro & Maio, 2019; Xiao et al., 2016). Combining diverse methods can be a favorable approach due to the improved dispersion of nanofillers in the polymer matrix, which can alleviate the drawbacks of each method (Mohamadi & Sharifi-Sanjani, 2016).

1.4.4 Graphene and CNTs based hybrid nanocomposites

The main goal of polymeric nanocomposites fabrication with graphene and CNTs is to improve the properties of polymers to using them for various applications. As previously mentioned, graphene and CNTs have outstanding properties, where the

mechanical, electrical, thermal, EMI shielding, acoustic and viscoelastic properties of a nanocomposite can be enhanced manifolds by the addition of these nanofillers. In recent years, several works have been done to investigate potential ways to develop these nanocomposites (X. Sun et al., 2020). A limiting aspect in the fabrication of nanocomposites is the challenge of homogeneous and uniform distribution of the nanofillers within the polymer matrix. Graphene restacks and wrinkles because of the Vander Waals forces and strong π-π stacking effects and CNTs showed entangled and crooked phenomena that diminish their reinforcement effect in polymers. In addition, the interfacial interaction between nanofillers and the polymer matrix is another factor in the load transfer between the matrix and nanofillers. The hybridization technique of graphene and CNTs possess a better dispersion, leading to the formation of an effective nanofillers network within the host matrix, which can overcome the dispersion challenge of individually loaded nanocomposites. Therefore, the desired properties of nanocomposites can be synergically improved for practical applications, which have been studied in this dissertation.

1.4.5 Experimental Methods

1.4.5.1 Tensile test

As a simple and relatively inexpensive method to study the mechanical properties of a material, tensile test is a destructive test process that delivers information about the ultimate tensile strength, yield strength, elongation and Young's modulus (Czichos, Saito, & Smith, 2006). A tensile sample is usually a standardized sample cross-section, including two shoulders and a gauge section between them so that the deformation and failure generally take place in this area (Figure 1.3).

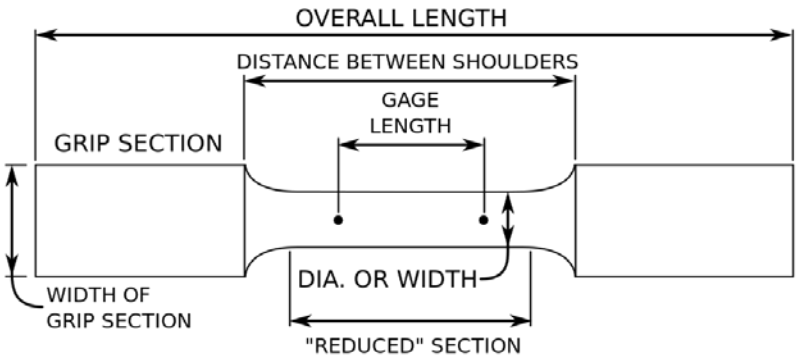

Figure 1.3 : Dumbbell-shaped tensile specimen (Czichos et al., 2006).

The test specimen slowly extends until its fracture, where the elongation of the gauge section and the applied force is measured. The elongation result is used to calculate the engineering strain (ε) using the following equation (Czichos et al., 2006)

$$\varepsilon = \frac{\Delta L}{L_o} = \frac{L - L_o}{L_o} \tag{1.1}$$

where ΔL is the difference in gauge length, L_o is the initial gauge length, and L is the final length. To calculate the engineering stress (σ), the force measurement is used according to the following equation (Czichos et al., 2006):

$$\sigma = \frac{F}{A} \tag{1.2}$$

where F is the tensile force and A is the cross-section area of the specimen. The result points could be graphed into a stress-strain curve.

Tensile specimens of fabricated nanocomposites were prepared according to ISO 1926 to evaluate their mechanical properties. The strain measurement was done using a video extensometer by tracking two opposing tape marks on the surface of samples. Tensile properties were performed on at least five samples of each nanocomposite using Shimadzu, a UTS machine equipped with a 1 kN load cell under a strain rate of 5 mm/min at room temperature.

1.4.5.2 Thermal conductivity

Thermal conductivity defines how efficiently a material can conduct heat. Thermal conductivity tests were performed to evaluate the ability of nanofillers to enhance the thermal conductivity of polyurethane. The guarded comparative longitudinal heat flow technique (ASTM Standard E1225) is a steady-state comparative method that determines the thermal conductivity of a solid sample using a reference part with known thermal conductivity (Stand, 1987). The permitted thermal conductivity recognition range of this method covers 0.2 to 200 W/mK, and measurements can be done between 90K and 1300K. Figure 1.4 depicts the needed setup for accurate thermal conductivity measurement for this method. An upper stack heater creates a heat flow through the specimens. Excess heat is removed through a liquid-cooled heat sink at the bottom of the stack that controls the average temperature. To ensure excellent thermal contact between the reference and test specimens a force is applied

to the top of the stack. An insulation material surrounded either side of the stack for reducing radial heat flow. The measurement was conducted in a cylinder specimen with a diameter of 113 mm and a thickness of 10 mm and the thermal conductivity was given by:

$$Q_r = Q_n \tag{1.3}$$

$$Q_r = \frac{k_r}{l_r} A(T_2 - T_3) \tag{1.4}$$

$$Q_t = \frac{k_t}{l_t} A(T_1 - T_2) \tag{1.5}$$

Where Q_r and Q_t are amounts of heat flow through reference and target specimens, respectively. K_r and K_t represent the thermal conductivity of reference and target specimens. T is the temperature of thermocouples. A and l are heat transfer area and thickness of samples, respectively.

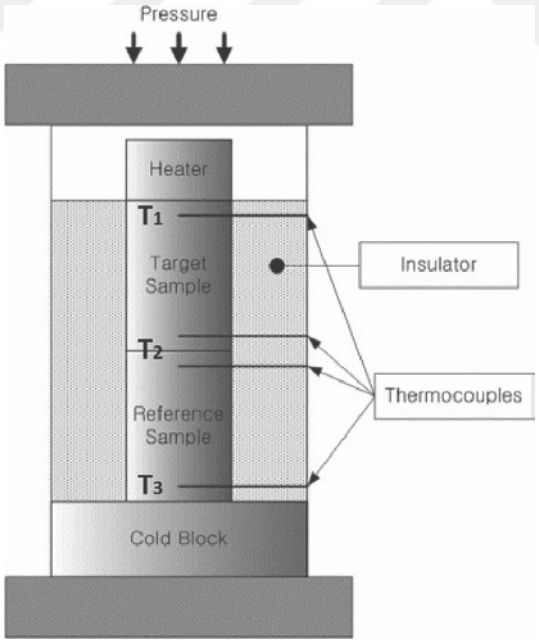

Figure 1.4 : Schematic of the apparatus for thermal conductivity measurement (Kang, Shin, Jung, & Park, 2006).

1.4.5.3 Dynamic mechanical analysis (DMA)

DMA is designed to determine the viscoelastic properties of polymeric materials. It measures dynamic moduli, dissipation energy, damping (Tan(δ)) and glass transition

(T_g). The responses of samples to the mechanical deformation with multi-frequency strain are controlled by applying oscillated stress as a function of temperature.

Storage modulus (E') is a measure of the capability of materials to store energy, whereas loss modulus (E'') or viscous modulus is a measure of the ability of materials to dissipate energy. In addition, a phase lag (δ) between stress and strain is the complex modulus (E^*) considering both storage and loss modulus in viscoelastic materials. The glass transition temperature can be originated from the E' onset, E'' peak or the material damping curve, the peak value of tan(δ).

$$E' = \frac{\sigma_o}{\varepsilon_o} Cos\delta \tag{1.6}$$

$$E'' = \frac{\sigma_o}{\varepsilon_o} Sin\delta \tag{1.7}$$

$$E^* = E' + i\,E'' \tag{1.8}$$

$$Tan\delta = \frac{E''}{E'} \tag{1.9}$$

where i represents a complex factor that equals $\sqrt{-1}$, where σ_o/ε_o is stress versus strain.

DMA technique was used to measure the viscoelastic properties of fabricated nanocomposites using TA Instruments Q800 DMA at a loading frequency of 1 Hz from 25 °C to 180 °C with a heating rate of 3 °C/min in single cantilever mode. In the single cantilever mode, the specimen is attached to a stationary clamp and the movable clamp is vibrated at the required frequency and stress (Figure 1.5).

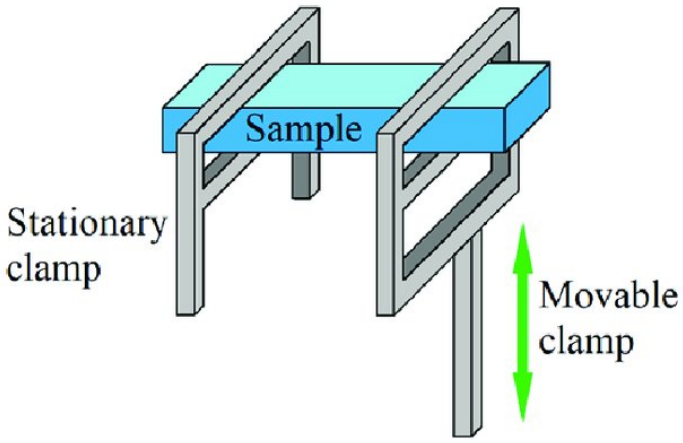

Figure 1.5 : Schematic of typical DMA single cantilever setup (Menard & Menard, 2020).

The values obtained from DMA through their transition behaviors can be used to analyze polymers molecular properties.

1.4.5.4 Acoustic properties

Sound is a vibration that is expressed as an oscillation in pressure, stress, particle velocity, particle displacement, etc., transmitted through a medium such as a gas, liquid, or solid as an acoustic wave. The sound waves are propagated by a sound source that generates vibrations in the nearby medium. Waves can be reflected, refracted, or attenuated by the medium during propagation [5]. Acoustic absorption refers to the property of any material that diminishes the sound intensity through the change of the energy into heat when sound waves strike. Materials have acoustic properties such as absorption, reflection, or transmittance. Generally, soft and porous materials are used as acoustic insulators that absorbing most sound, while hard and dense materials reflect most. The incident sound that encounters a material that is not reflected is defined as sound absorption. There is some loss caused by absorption when sound travels through any medium. The acoustic tests were performed according to a Bruuel & Kjaer 4206 acoustic test system comprising an impedance tube, speaker, three microphones and a digital frequency analyzer to measure the sound transmission loss. The understanding the full range of acoustical response in measurements, the small and large tubes of impedance setup were used for the frequency range of 20 Hz–6300 Hz. Samples were cut in small and large sizes with 29mm and 100mm in diameter for acoustical measurements.

1.4.5.5 Thermogravimetric analysis (TGA)

TGA is the simplest method for thermal characterization, in which the mass variations of specimens are measured as a function of temperature in a controlled atmosphere. The thermal stability of pure PU and carbon nanofiller nanocomposites can be studied by TGA. The specimen mass change is measured during the heating. If degradation happens and releases a volatile constituent, mass loss is identified. TGA is usually demonstrated as a plot of measured mass loss to temperature (Figure 1.7 (a)). The normal form of mass loss is sigmoidal, with most mass loss happening at the chief reaction temperature, however, some residual mass loss takes place afterward (Gaisford, Kett, & Haines, 2019).

Derivative plot is another data demonstration, regularly named derivative thermogravimetry (DTG), where the X-axis is the temperature and Y-axis is the rate of mass loss against temperature (dm/dT) (Gaisford et al., 2019). The derivative plot looks like a board peak over a range of temperatures.

2. POLYURETHANE HYBRID NANOCOMPOSITE FOAMS REINFORCED WITH MULTI-WALLED CARBON NANOTUBES AND SILICA NANOPARTICLES [2]

2.1 Abstract

Multifunctional polyurethane foams reinforced with multi-walled carbon nanotubes and silica nanoparticles enhanced specific properties. We studied the effects of nanoparticle addition into polyurethane on mechanical properties and thermal stability by means of tensile, Charpy impact, hardness tests and Thermogravimetric analysis. Nanoparticles added to polyurethane are multi-walled carbon nanotubes, two types of silica nanoparticles, and multi-walled carbon nanotubes/spherical silica as a hybrid filler. Hybrid polyurethane/spherical silica/multi-walled carbon nanotubes nanocomposite with the constant overall content of 0.75 wt% showed higher tensile strength, hardness and thermal stability than either of nanoparticles at this content, which approves a synergistic effect between multi-walled carbon nanotubes and Silica nanoparticles.

2.2 Introduction

Reinforcing of polymers by incorporation of nanoparticles can considerably improve the preferred properties of the polymeric nanocomposite (Coleman et al., 2006; Faraji et al., 2017; Mahmoodi et al., 2012). Carbon nanotubes (CNT) as an interesting additive due to their superior properties such as low density, high aspect ratio, high electrical conductivity, and strength make them favorable additives for reinforcement. To fabricate CNT nanocomposites with effective reinforcement, a large aspect ratio, good dispersion, alignment and interfacial stress transfer are required (Coleman et al., 2006) (Abbasi, 2009). Since CNTs tend to agglomerate, in order to improve the dispersion of carbon nanotubes in polymer matrixes, their surface is firstly treated

[2] **A.Navidfar**, A. Sancak, K. B. Yildirim, L. Trabzon, "*A study on polyurethane hybrıd nanocomposıte foams reınforced wıth multı-walled carbon nanotubes and sılıca nanopartıcles*" Polymer-plastıcs technology and engıneerıng", 57(14), 2018, 1463-1473"

(Bandarian et al., 2011). The appropriate treatment of nanoparticles, not only leads to better dispersion and compatibility in a polymer matrix but also can form physical and chemical interactions with polymers, which lead to improved mechanical properties (X. Gao et al., 2011). The nanotubes modified with carboxyl and hydroxyl groups have much more influence on mechanical and acoustic enhancement of polyurethane (PU) foams, compared to other functional groups (Bandarian et al., 2011). This phenomenon can be explained by the better dispersion and interfacial interaction of modified CNTs with the polymer matrix (Bandarian et al., 2011). Besides, silica (SiO_2) nanoparticles have been widely used with polymers to enhance heat resistance, radiation resistance, and mechanical properties (G. Chen et al., 2007). Polymeric foams such as PU are a group of lightweight materials, which are appropriate for a broad range of applications such as thermal and electrical insulation, shock and sound absorbents, composite foam cores, and panels (Bandarian et al., 2011). Since the mechanical properties of PU foams are not appropriate in many applications, reinforcement of them by nanoparticles has been studied intensely in the last decade (Bandarian et al., 2011; G. Chen et al., 2007; X. Gao et al., 2011).

In recent years, there have been numerous reports on how adding nanoparticles to polymeric nanocomposites with enhanced properties in mechanical (Amir Navidfar, Azdast, & Karimzad Ghavidel, 2016b), electrical (Ayub Karimzad Ghavidel et al., 2015) (Ayub Karimzad Ghavidel et al., 2016), and other characteristics (Ayob Karimzad Ghavidel, Azdast, Shabgard, Navidfar, & Mamaghani Shishavan, 2015). However, a review of the literature reveals that a few studies have focused on the reinforcing of polymeric foams such as PU with CNTs or silica nanoparticles for improving the properties of nanocomposites. A number of researchers have studied various PU types reinforced with Silica nanoparticles (J. Lee, Kim, & Ha, 2012), MWCNTs (L. Zhang, Yilmaz, Schjødt-Thomsen, Rauhe, & Pyrz, 2011) (Kausar, 2017), and nano clay (Xu, Tang, Gu, & Fang, 2007). Among them, carbon nanotubes are most widely used, not only for improving mechanical properties but also for enhancing electrical (Athanasopoulos, Baltopoulos, Matzakou, Vavouliotis, & Kostopoulos, 2012), thermal and electromagnetic interference (EMI) shielding properties (L. Zhang et al., 2011). Jiawen et al. (Xiong et al., 2006) studied thermal and mechanical properties of PU elastomer reinforced with functionalized MWCNTs. They showed that treated CNTs were successfully connected with the PU chain and

they can be dispersed into the polymer matrix in lower CNT concentration. Results of thermogravimetric analysis (TGA) and tensile analysis approve improving thermal stability and mechanical strength of the elastomer nanocomposites. The study by Lingfei Zhang et al. (L. Zhang et al., 2011) demonstrated that the reinforcing effect of pristine and functionalized MWCNTs depends on mixing time. In this work, the highest mechanical improvement belongs to the nanocomposites containing 0.5 wt% in both pristine and treated MWCNTs. McClory et al. (McClory, McNally, Brennan, & Erskine, 2007) investigated mechanical properties of uniformly dispersed MWCNT in a thermosetting polyurethane. Reinforcement effect was obtained in this study by adding 0.1 wt% MWCNT into PU matrix so that Young's modulus, ultimate tensile strength and strain at break increased by 561, 397 and 302%, respectively. In the case of silica nanoparticles, Joonmo Lee et al. (J. Lee et al., 2012) reported that tensile strength and Young's modulus of PU slightly enhanced by increasing silica nanoparticles up to 1 parts by weight (pbw).

On the other hand, recent studies have investigated beneficial outcomes for nanocomposites containing two or more geometrically different fillers (Sapkota et al., 2017) (Szeluga et al., 2015). The improvements in nanoparticle dispersion led to considerably better properties due to synergistic effects. Studies demonstrate that the geometric shape, surface properties and the ratio of nanoparticles within the combination are significant factors governing the reinforcing effects in nanocomposites (Mansour & Tzetzis, 2013; Sapkota et al., 2017; Szeluga et al., 2015; Wu et al., 2017). Therefore, carbon nanotubes and silica nanoparticles combinations can be an effective route to enhance their reinforcing performance (Cheni et al., 2012). Rahmanian et al. (Rahmanian et al., 2015) attempted to identify the reinforcement effect of multiscale (hybrid) fillers of CNT–silica within an epoxy resin to fabricate a multiscale composite. Their results showed significant improvements in the elastic modulus, tensile strength, and Izod impact strength with the incorporation of multiscale fillers. Epoxy resin nanocomposites with carbon nanotubes and graphene platelets revealed a higher strength, modulus, and thermal conductivity than nanocomposites comprising a similar weight fraction of either of the fillers, due to a reduction of agglomerations in the hybrid composites (S.-Y. Yang et al., 2011). Moreover, the study by Kia Yang et al. (K. Yang & Gu, 2010) revealed that the hybrid filler system could offer synergistic effects and cost reduction simultaneously. Higher

nanoparticle loadings may lead to a decrease in the mechanical properties of the nanocomposites due to the formation of large agglomerates. In large nanoparticle contents, the viscosity of pre-curing nanocomposites is higher and the mixing process is a challenge. In the consolidation of the PU nanocomposites, voids or air pockets can be formed in these large agglomerates, which lead to lower mechanical properties (K. Yang & Gu, 2010). The formation of a hybrid structure can alter the state of dispersion not only in the uncured foam but also in the cured nanocomposite foam (K. Yang & Gu, 2010). Experimental and theoretical studies were combined to examine the electrical percolation of carbon nanotubes in a polymer matrix and exhibited that the percolation threshold can be considerably lowered by adding small amounts of spherical latex particles (Kyrylyuk et al., 2011). These examples show that combining two different nanoparticle geometries can lead to synergistic effects, mainly by improving the dispersion.

This paper aims to investigate the reinforcement influences of functionalized multi-walled carbon nanotubes, spherical silica (Silica-A), amorphous silica (Silica-B) nanoparticles and the synergistic properties arising when using their combinations as a hybrid additive on the mechanical properties and thermal stability of polyurethane foams. To achieve these goals, various contents of MWCNTs and/or silica nanoparticles are mixed with a polyol. Then, the isocyanate is added to the mixture and subsequently poured into a two-part wooden mold. After cutting and preparing desired samples, tensile test, Charpy impact test, hardness, TGA and Fourier transform infrared (FTIR) analysis of the nanocomposite foams are carried out and discussed.

2.3 Materials and Experimental setup

2.3.1 Materials

For polymerization of PU, diisocyanate and polyol are mixed with a ratio of 1:1 at room temperature, which is supplied by Ravago Petrochemical, according to Table 2.1. Used MWCNTs were purchased from Nanografi Co. Ltd, which were grown by chemical vapor deposition (CVD) with a specific diameter of 10-15 nm, a length of 3μm and purity of more than 90%. Silica nanoparticles (Nanografi Co. Ltd) with two different diameters are plotted in Table 2.2 Spherical silica (Silica-A) and amorphous silica (Silica-B) nanoparticles are used to determine the mechanical properties of

nanocomposites. Silica-A is also amorphous, but it has a particular geometry of a sphere.

Table 2.1 : Properties of H 1710/06 polyol and isocyanate components.

Physical properties	Unit	Polyol	Isocyanate	Standards
Density (20°C)	g/cm^3	1.1	1.230	DIN 51 757
Viscosity (20°C)	MPa.s	-	210	DIN 53 018
NCO content	H_2O	-	31,5	ASTM D
Storage life	Month		6	5155-96 A

Table 2.2 : Properties of Silica Nano-Particles.

Symbol	Materials	Characteristics
Silica-A	S-Type Spherical Silica	(99.5+%, S-type, Spherical, Nanoporous and Amorphous, 15-20 nm)
Silica-B	Amorphous Silica	(98%, Amorphous, 60 - 70 nm)

2.3.2 Carbon nanotubes functionalization

Prior to the synthesis of PU foam, used MWCNTs were functionalized with hydrogen peroxide (H_2O_2). 1.5 g of MWCNTs were mixed with 500 mL of 35% H_2O_2 at room temperature for 90 min. Subsequently, the solution was filtered and washed twice with distilled water to remove any H_2O_2 and then dried in an oven at 80 °C for 12 hours.

2.3.3 Nanocomposite preparation

For the preparation of PU foam reinforced with MWCNTs, the various percentages of carbon nanotubes (up to 1 wt%) were first mixed with the polyol for about 10 minutes using overhead stirrer equipment at speed of 200 to 2000 rpm. No surfactant, catalyst nor distilled water were added to the MWCNT/polyol mixture at this stage. For polymerization of PU reinforced with carbon nanotubes, isocyanate was added to the MWCNT/Polyol composition, which was mixed for a minute and then poured into a two-part wooden mold with a diameter of 180 mm and height of 80 mm to form free-rise PU foam. The same procedures were carried out for PU reinforced with silica nanoparticles and MWCNT/silica combinations according to Figure 2.1. Table 2.3 indicates levels of produced PU reinforced with carbon nanotubes, silica nanoparticles and their mixtures in this work.

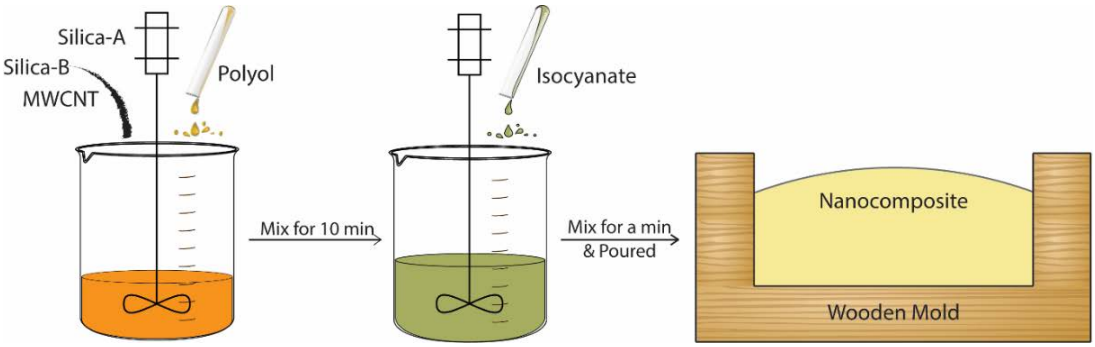

Figure 2.1 : Scheme of nanocomposites producing steps.

Table 2.3 : Levels of produced nanocomposites.

Nanoparticles	Levels (wt %)			
Silica-A	0.25	0.50	0.75	1.00
Silica-B	0.25	0.50	0.75	1.00
MWCNT	0.25	0.50	0.75	-
0.25% Silica-A	0.25[3]	0.50[2]	0.75[2]	-
0.50% Silica-A	0.25[2]	0.50[2]	0.75[2]	-
Silica-A + Silica-B + MWCNT	0.25[3]	0.50[4]	-	-

2.3.4 Specimen preparation

After molding the nanocomposites in a cylindrical mold, a turning machine was used for cutting slices of foams with a thickness of 10 mm. Produced slices were cut in CNC machine according to ISO 1926 for tensile tests of rigid cellular plastics and ASTM 6111 for Charpy impact tests. Figure 2.2 shows fabricated nanocomposite specimens for the tensile and impact tests.

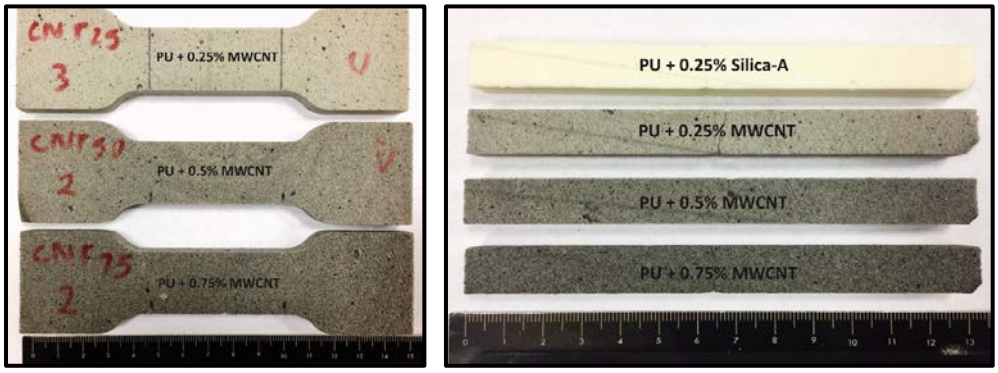

Figure 2.2 : Tensile and impact specimens in various loadings.

[3] Content of MWCNT.
[4] Content of each nanoparticle.

2.3.5 Characterizations

Tensile properties of the nanocomposite foams were carried out using Shimadzu, UTS machine under strain rate of 5 mm/min at room temperature. Devotrans Charpy impact machine was used for investigating the impact strength of unnotched samples. Zwick hardness tester is employed in order to investigate Shore-A hardness tests and at least five points of a sample in perpendicular to blowing direction were examined. More than 20 types of PU foams were reinforced with MWCNTs, silica nanoparticles, and their combinations were studied. The presented results are the mean values and the standard deviation of at least five measurements. Fabricating nanocomposites and investigating mechanical tests were carried out at various times and circumstances. Therefore, due to the aging factor of used polyol and isocyanate and also various weather and humidity conditions, all test results were normalized to results of pure polyurethane. Thermogravimetric analysis was carried out under nitrogen atmosphere on a Q600, TA Instruments using 2-3 mg specimens at a temperature range from 30 to 600 oC and heating rate of 10 ^{o}C/min. Fourier transform infrared spectroscopy of the samples was examined in the wave number range from 4000 to 650 cm^{-1} at a resolution of 4 cm^{-1} using a Thermo Scientific iS10 FTIR at room temperature.

2.4 Results and discussion

2.4.1 Morphological characterization

The microstructure of polymer foams plays a significant role in the properties of fabricated nanocomposites. Therefore, we have first characterized the microstructure of PU nanocomposites using FEI Nova NanoSEM 450. Figure 2.3 shows SEM images of cryo-fractured neat PU cross-sections and PU reinforced with various nanoparticles, which provide evidence of the foam cellular microstructure with values for the average cell size. The observation reveals that the addition of MWCNTs and silica nanoparticles has an obvious effect on the cell size of polyurethane foam. As can be seen, polyurethane within nanoparticles has a smaller cell size, compared to neat PU. The decrease in cell size at nanoparticle loadings can also be attributed to the higher viscosity, which affects the mechanical properties of foams (R Verdejo et al., 2009). The cell size deviation and the number of open cells seemed to increase with adding of nanoparticles (Baltopoulos, Athanasopoulos, Fotiou, Vavouliotis, & Kostopoulos, 2013). In other words, the cell structure of neat PU is more uniform (L. Zhang et al.,

2011). The increase in the number of open cells may be due to nanoparticle-induced defects in the cell walls, which leads to more open cells (L. Zhang et al., 2011). The reduction in cell size at nanoparticle loading can be attributed to the higher viscosity, which will bound the expansion of the entire foam and consequently increase the density of fabricated foams (R Verdejo et al., 2009). The hybrid nanocomposite containing 0.50 wt% MWCNT and 0.25 wt% Silica-A exhibits the lowest cell size, which declares better dispersion of added nanoparticles. Likewise, the cell size of the nanocomposite with triple fillers is higher than other nanocomposites (Figure 2.3(f)), which can be attributed to poor dispersion (Baltopoulos et al., 2013).

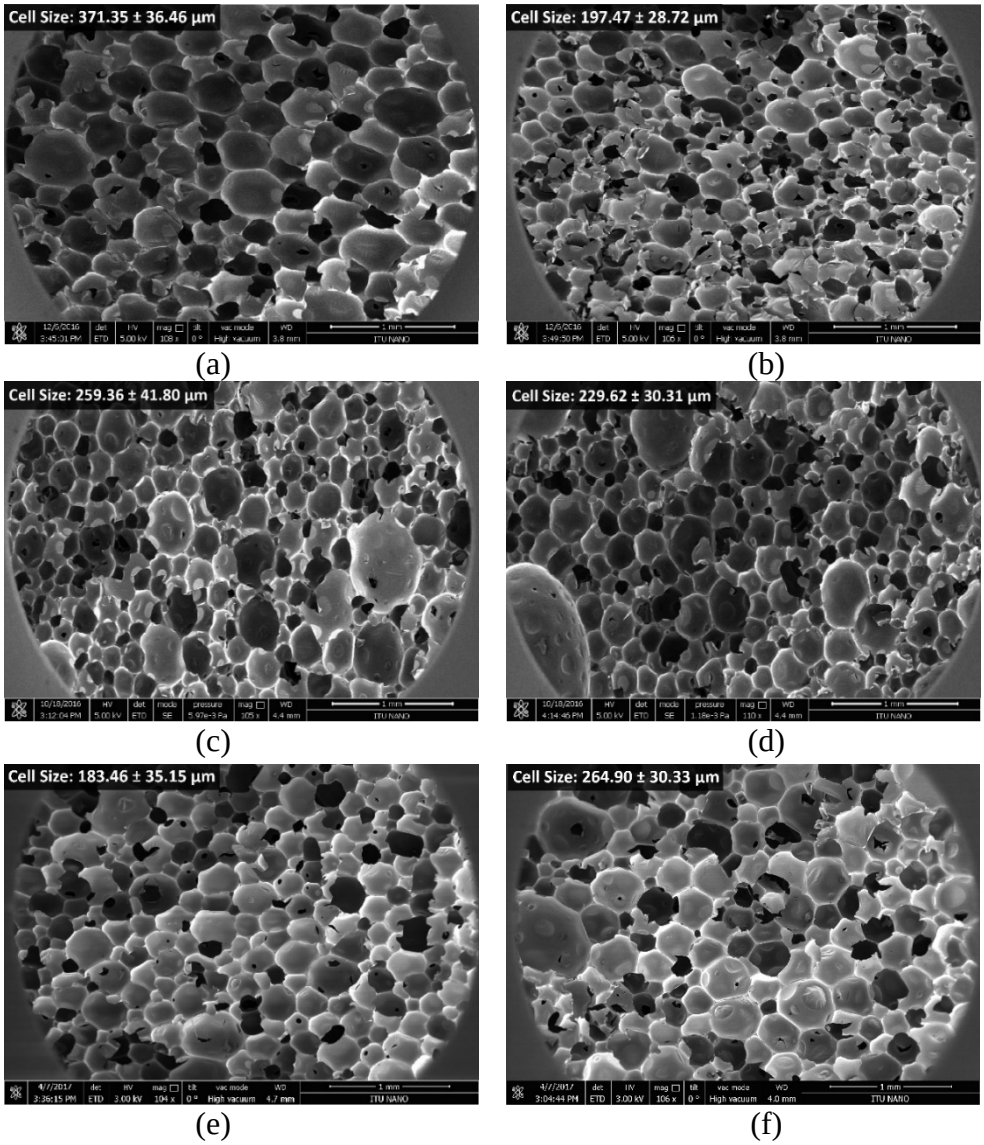

Figure 2.3 : SEM images of the nanocomposites (Scale bars represent 1 mm), (a) Polyurethane (b) PU with 0.5 wt% Silica-A, (c) PU with 0.5 wt% MWCNT, (d) PU with 0.5 wt% Silica-B, (e) PU with 0.5 wt% MWCNT + 0.25 wt% Silica-A, (f) PU with 0.5 wt% Silica-B + 0.5 wt% Silica-A + 0.5 wt% MWCNT.

2.4.2 Tensile Test

The main effects of MWCNTs and silica nanoparticles on normalized yield tensile strength of PU are plotted in Figure 2.4(a). According to this figure, the existence of MWCNTs and Silica nanoparticles has a noticeable effect on the tensile strength of nanocomposite foams. The neat PU presented the lower mechanical properties in the term of the tensile strength (1.22 MPa), whereas the highest strength can be seen in the nanocomposites comprising 0.25 wt% Silica-A with 33% improvement (1.62 MPa). After attaining an optimum level, further Silica-A addition decreased the strength of the PU/Silica-A foams. This phenomenon can be seen in adding Silica-B and MWCNT into the polymer matrix, in which the tensile strength increases from 1.22 MPa for neat PU to 1.54 MPa for 0.25 wt% Silica-B and to 1.4 MPa for 0.25 wt% MWCNT. However, further nanoparticle adding reduced the strength. This result can be clarified by the fact that agglomerations can easily form in higher nanoparticle concentrations and the consolidation process, voids and air pockets would exist in these agglomerated bundles, which act as points of stress concentration and sites for crack initiation and therefore reduced the yield strength of the nanocomposite foams (Amir Navidfar et al., 2016b) (S.-Y. Yang et al., 2011). When nanoparticles content is large, the viscosity of pre-cured nanocomposite is higher and mixing is difficult and consequently, nanoparticles were not well dispersed within the polyurethane matrix (S.-Y. Yang et al., 2011). This outcome demonstrated that nanoparticles were well dispersed in the foam matrix in lower concentration (0.25 wt%) and subsequently higher strength can be achieved. In addition, the elastic modulus of fabricated nanocomposites is investigated and demonstrated in Figure 2.5(a), which is similar to the tensile strength trends. Elastic modulus increases from 16.35 MPa for PU to 21.38 MPa for polyurethane reinforced with 0.25 wt% Silica-A. Tensile strength and elastic modulus of rigid PU foams published in the literature can be also seen in the same range (0.9-1.7 MPa and 22-29 MPa) (Xu et al., 2007; L. Zhang et al., 2011). However, because of differences in PU types, used constituents and producing methods, the mechanical properties of polyurethanes can be varied.

Silica-A with a smaller diameter has a higher tensile strength in comparison to Silica-B with a larger diameter. This result is similar to the work by Yongchun Chen et al. (Y. Chen, Zhou, Yang, & Wu, 2005), which studied the influence of silica nanoparticle size on the tensile strength of PU/nanosilica. According to this study, nanocomposites

with a silica size of 28 nm, have the highest strength, especially in comparison with that of 68nm, which is similar to Figure 2.4(a) outcomes.

In order to produce nanocomposites with higher MWCNT content and prevent the appearance of large agglomerations, hybrid nanocomposites are produced, which can lessen large agglomerations (Sapkota et al., 2017) (Rahmanian et al., 2015). The formation of a hybrid structure can alter the state of dispersion (K. Yang & Gu, 2010). The synergistic effect of nanoparticles within polyurethane matrix, as a hybrid nanocomposite is demonstrated in Figure 2.4(b). In this figure, MWCNT content is changed with a fixed amount of Silica-A and/or Silica-B. In this part, tensile strength and elastic modulus of neat polyurethane measured 1.12 MPa and 14.63 MPa, respectively. As a noticeable consequence, in the hybrid nanocomposite with fixed 0.25 wt% Silica-A (black line), maximum strength can be seen in 0.5 wt% MWCNT, whereas in the nanocomposite with carbon nanotubes (single filler), maximum tensile strength was at 0.25 wt% (Figure 2.4(a)). It means that nanocomposites with 0.75 wt% single fillers (S.1, S.2, and S.3 in Figure 2.4(a)) have lower strength than that of 0.5 wt%, whereas hybrid nanocomposites with the overall content of 0.75 wt% (H.2 and H.3 in Figure 2.4(b)) have higher strength than 0.5 wt% (H.1).

Nanocomposites with the constant overall content of 0.75 wt% also display synergistic effects of multi-fillers according to Figure 2.4(c). Normalized tensile strength enhanced from 1.16 for 0.75 wt% Silica-A (S.1), 1.17 for 0.75 wt% Silica-B (S.2) and 0.92 for 0.75 wt% MWCNT (S.3) to 1.36 for H.3 and 1.25 for H.2. These results demonstrate the synergetic effect of MWCNT and Silica-A so that spherical Silica-A nanoparticles are filled in the fibrous CNT networks, which the space of the CNT-CNT network can be entirely used (K. Yang & Gu, 2010). The synergistic effect of a hybrid filler system within epoxy nanocomposite was also mentioned by Rahmanian et al. (Rahmanian et al., 2015), Kia Yang et al (K. Yang & Gu, 2010) and Sapkota et al. (Sapkota et al., 2017). As a comprehensive result, fabricating a hybrid nanocomposite with geometrically different fillers enhances dispersion of nanoparticles and mitigates large agglomerations with relatively low cost, which can improve desired properties of nanocomposites (Sapkota et al., 2017) (Rahmanian et al., 2015) (K. Yang & Gu, 2010).

The combination of Silica-A and Silica-B with carbon nanotubes showed lower tensile strength. It can be concluded that higher loading of nanoparticles within the PU matrix

has a negative effect on the strength and the lowest strength can be seen in the highest nanoparticle loading. Furthermore, Figure 2.5(b) reveals the elastic modulus of hybrid nanocomposites, which the synergistic effect is obvious. The highest modulus can be seen in PU containing 0.25 wt% Silica-A and 0.5 wt% MWCNT.

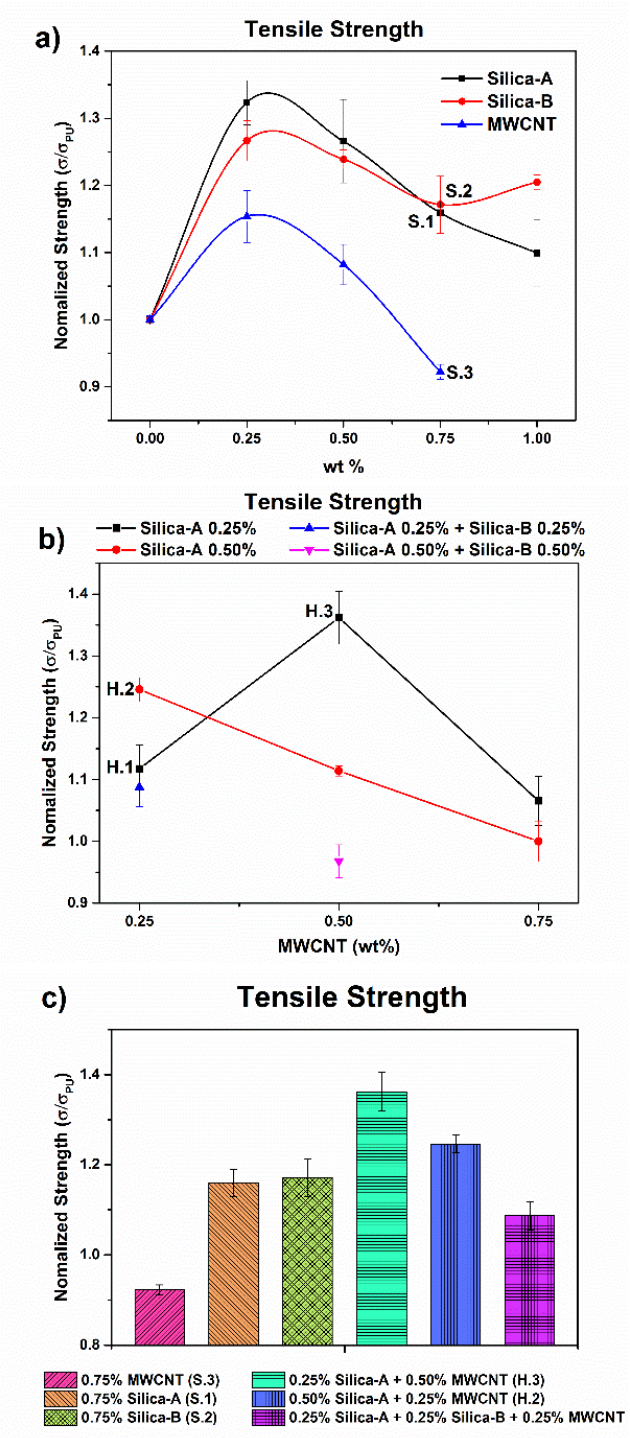

Figure 2.4 : Normalized yield tensile strength of (a) PU with various nanoparticles, (b) hybrid nanocomposite foams and (c) PU with 0.75 wt% nanoparticles.

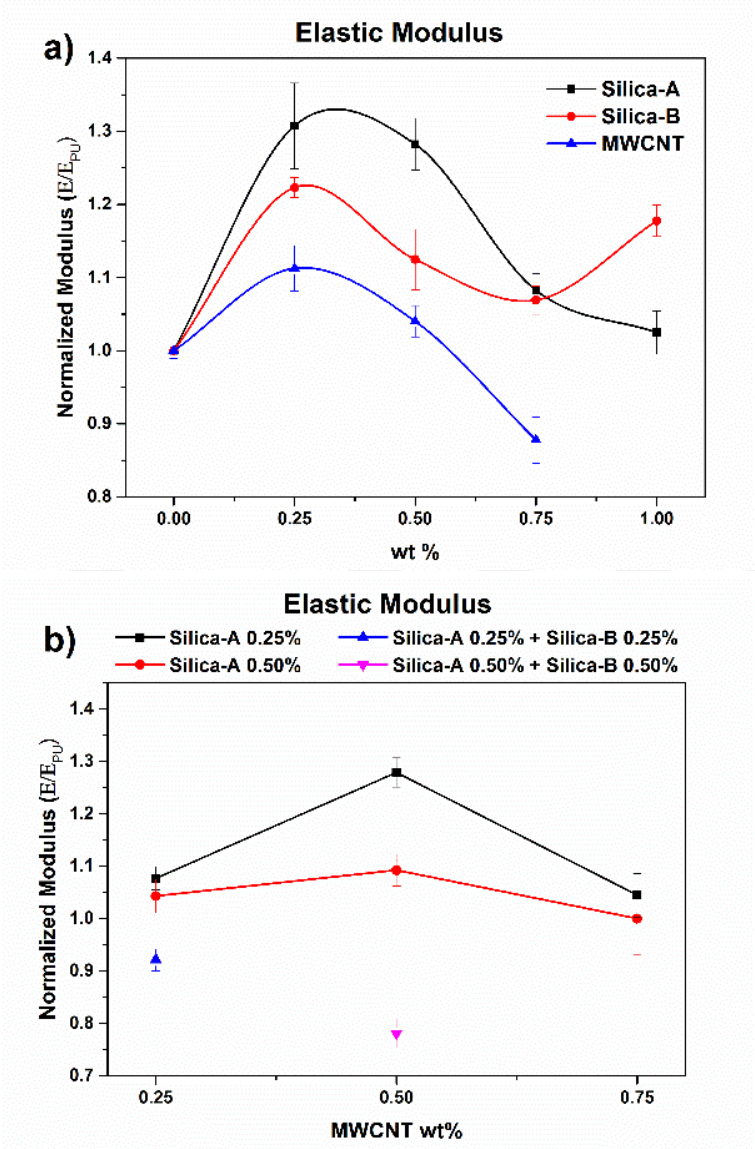

Figure 2.5 : Normalized elastic Modulus of (a) PU with various nanoparticles and (b) hybrid nanocomposite foams.

2.4.3 Impact Test

Apart from tensile strength, impact properties are important in foam application, which is related to fracture toughness (Amir Navidfar et al., 2016b). Figure 2.6(a) depicts the impact strength of unnotched samples in different levels of nanoparticles. The nanocomposite containing 0.5 wt% MWCNT has the highest impact strength among other nanocomposites with approximately 96% improvement in comparison to neat PU with an impact strength of 4.53 kJ/m^2. The folding property of carbon nanotube makes it a shock damper (Reich, Thomsen, & Maultzsch, 2008), which absorbs the

part of shocks. As Fig 2.6 (a) demonstrates, adding this reinforcer to the polymer matrix in nanometer size improved the impact strength. On the other hand, dispersion and agglomeration have a key role in impact strength so that when the MWCNT content is increased from 0.5 wt% up to 0.75 wt%, due to probably the presence of nanotube agglomerations in polyurethane matrix the impact strength reduced consequently. In the case of Silica-B nanocomposites, the strength of specimens enhanced up to 0.75 wt%, while further increasing reduced the impact strength. Adding Silica-A to PU first decreased the impact strength, but further increasing of Silica-A up to 1 wt% improved impact properties.

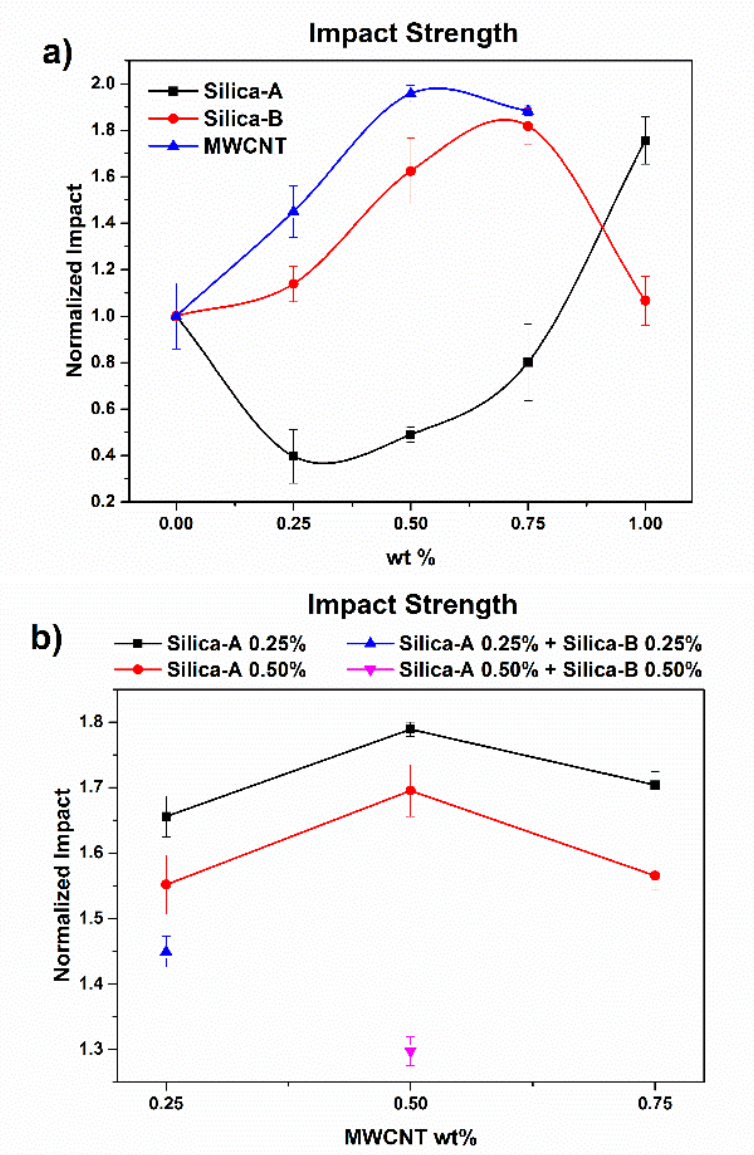

Figure 2.6 : The normalized impact strength of (a) PU with various nanoparticles and (b) hybrid nanocomposite foams.

The effect of nanoparticle combinations with various contents on the impact strength of hybrid nanocomposites is represented in Figure 2.6(b). Unlike tensile strength, synergistic effects cannot be seen in the impact test results, so the highest impact strength can be seen in the nanocomposite with 0.5 wt% MWCNT. This phenomenon reveals the dominant reinforcement effect of carbon nanotubes on impact strength. It is evident that, due to the presence of higher nanoparticle content and agglomerations in the polymer matrix, combinations of Silica-A and Silica-B with MWCNT have lower impact properties similar to tensile strength results. In other words, the nanocomposite with Silica-A, Silica-B, and MWCNT each 0.5 wt% approves that the foam with the highest nanoparticle loading has the lowest impact strength.

2.4.4 Hardness

Figure 2.7(a) depicts the main effect of nanoparticles and their concentrations on the hardness of the nanocomposite foams, which normalized to the hardness of neat PU (54.5 Shore-A). Among nanoparticles, the highest hardness can be seen in the nanocomposite comprising 0.5 wt% Silica-B, but further Silica-B loading reduced the hardness. Also, adding Silica-A up to 0.5 wt% improved the hardness of samples, but in higher loadings, hardness decreased strongly, due to uneven dispersion of Silica-A. Regarding carbon nanotubes, adding 0.25 wt% of MWCNT enhanced hardness, but when CNT content exceeds 0.25 wt%, the foam hardness is reduced. As described in the tensile results, agglomerations occurred in higher nanoparticle loadings, which have a negative impact on the hardness of foams.

Figure 2.7(b) reveals the hardness of hybrid nanocomposites that the synergistic effect of MWCNT and Silica-A is clear. Hardness results normalized to 43.6, which is Shore-A hardness of PU. The highest hardness can be seen in the foam containing 0.5 wt% MWCNT with 0.25 wt% Silica-A (H.1), whereas the foam with 0.25 wt% MWCNT had the highest hardness among carbon nanotube composites, according to Figure 2.7(a). In other words, adding 0.25 t% of Silica-A to the nanocomposite with 0.5 wt% MWCNT improved the hardness. Figure 2.7(c) also demonstrates the synergistic effect in the nanocomposites with constant overall content at the level of 0.75 wt%. Normalized hardness improved from 0.97 for 0.75 wt% Silica-A (S.1) and 0.95 for 0.75 wt% MWCNT (S.2) to 1.1 for PU with 0.25 wt% Silica-A and 0.5 wt% MWCNT

(H.1) and also to 1.04 for 0.5 wt% Silica-A and 0.25 wt% MWCNT nanocomposites (H.2).

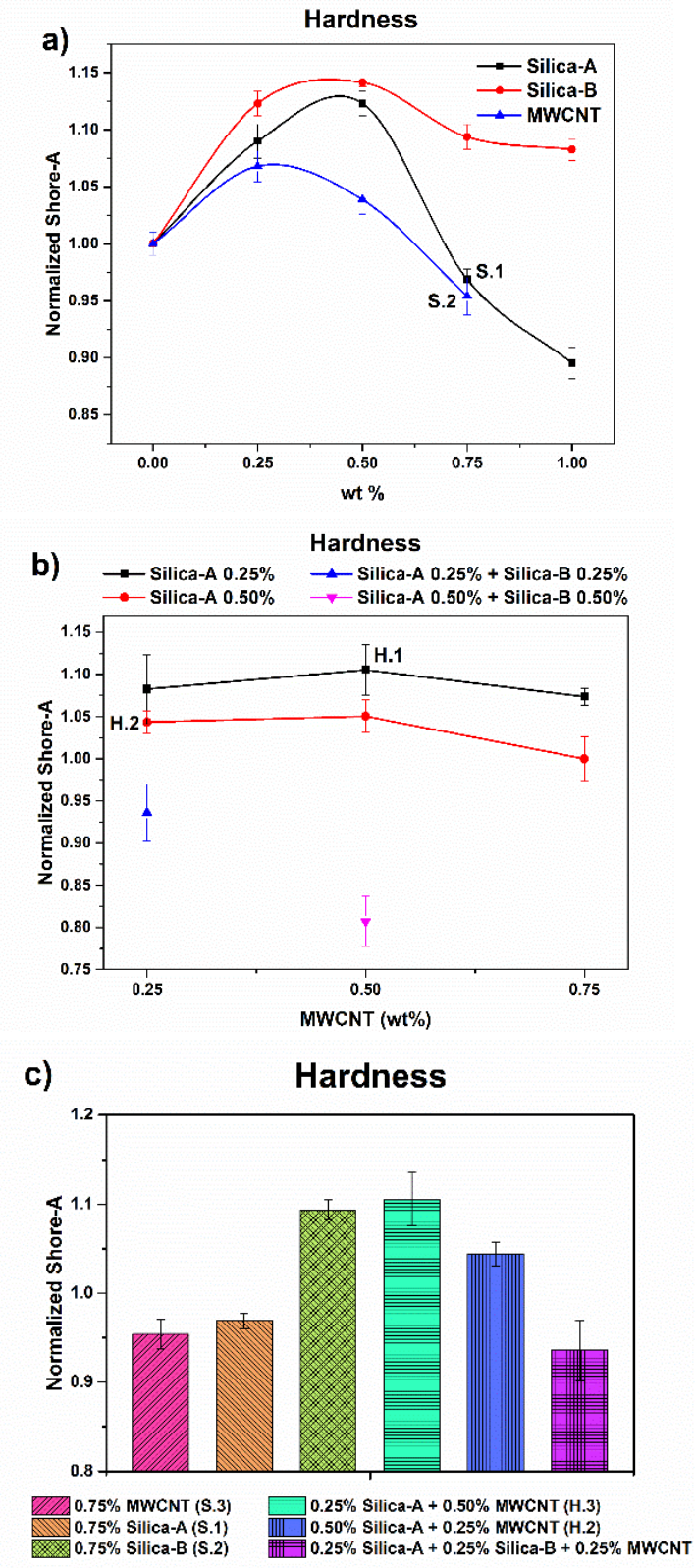

Figure 2.7 : Normalized hardness of (a) PU with various nanoparticles, (b) hybrid nanocomposites and (c) PU with 0.75 wt% nanoparticles.

2.4.5 Thermal stability

The thermal stability of studied nanocomposites was evaluated by TGA and degradation temperatures of 50% weight losses and charred residue of the different PU nanocomposites at 600 ºC are illustrated in Figure 2.8(a). The temperature for 50% weight loss decreased for nanocomposites with a single filler with 0.75 wt% content, in comparison to neat PU. Among nanoparticles, Silica-B shows a higher temperature for 50% weight loss. It is apparent that MWCNTs and Silica nanoparticles accelerate the thermal degradation due to low dispersion at 0.75 wt% loadings. However, hybrid nanocomposites indicate an enhancement in thermal stability in comparison with single fillers due to better dispersion of MWCNT in the PU matrix.

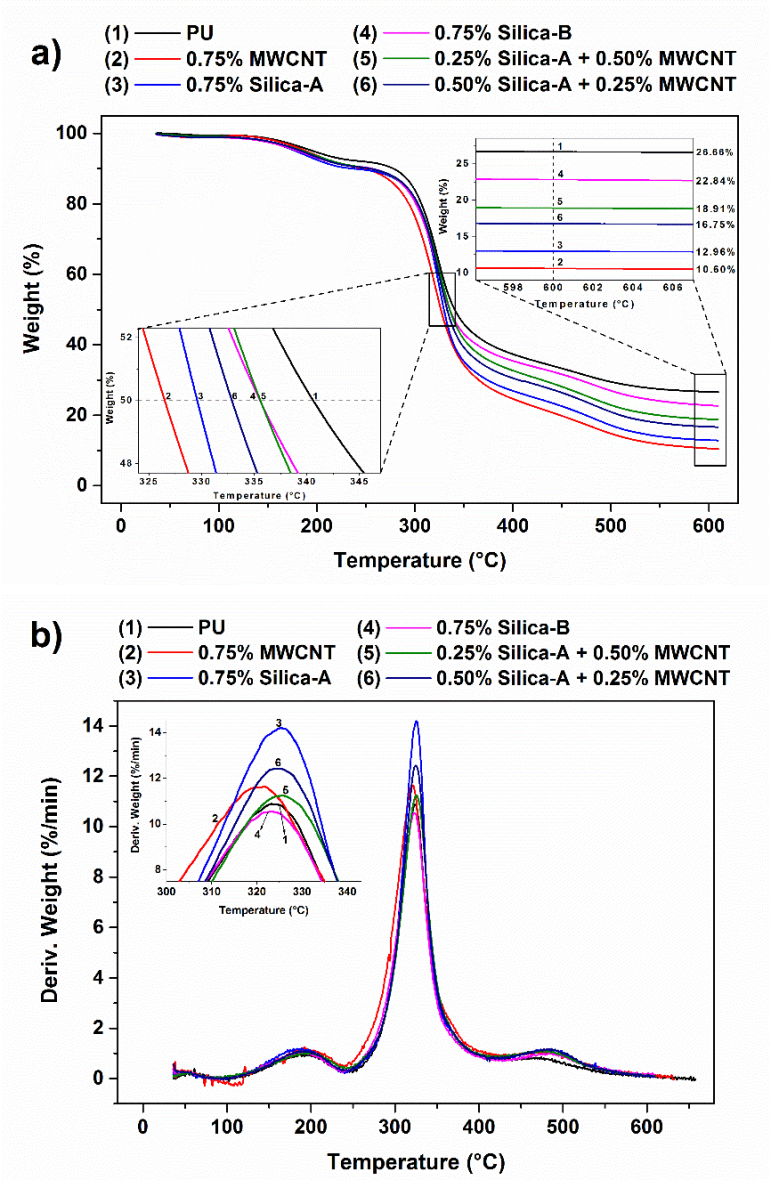

Figure 2.8 : (a) TGA and (b) DTG curves of nanocomposites.

According to Figure 2.8(a), PU with 0.50 wt% MWCNT and 0.25 wt% hybrid nanocomposite shows a more delayed decomposition compared to other nanocomposites. On the other hand, the residue of hybrid nanocomposite foams at 600 ^{o}C is higher than that of nanocomposites containing MWCNT or Silica-A, especially hybrid nanocomposite with 0.50 wt% MWCNT and 0.25 wt% Silica-A shows a residue of 18.91 wt%. The third evidence of synergistic effect in hybrid nanocomposite was seen in DTG curves (Figure 2.8(b)). The decomposition velocity of hybrid samples was slower than those of PU/MWCNT and PU/Silica-A (Zhengzhou Wang & Li, 2017).

2.4.6 FTIR spectroscopy

FTIR spectra of pure polyurethane and nanocomposites are presented in Figure 2.9. Typical peaks of PU can be seen in the figure and the results are in agreement with literature results (X. Gao et al., 2011). The comparison of the pure PU and nanocomposites spectra indicates that the positions of peaks for the nanocomposites are identical with pure PU, which means that the segmented structure of PU is not affected by the dispersion of nanoparticles in the polymer matrix. These consequences show that there are no major changes in the chemical structure of PU with the presence of carbon nanotubes and silica nanoparticles.

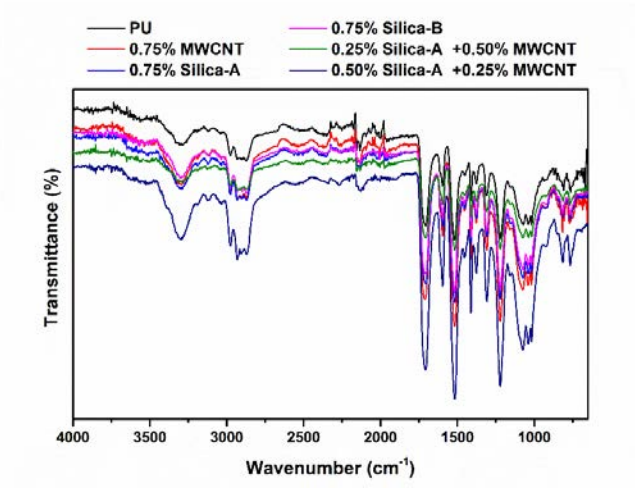

Figure 2.9 : FTIR spectra of PU and nanocomposite foams.

2.5 Conclusion

In order to determine thermal stability and mechanical properties of polyurethane reinforced with multi-walled carbon nanotubes and/or silica nanoparticles, tensile test,

Charpy impact test, hardness and TGA were carried out. For this aim, MWCNTs, Silica-A and Silica-B with varied content up to 1 wt% were added to polyol-isocyanate combinations and then poured into the wooden mold. Carbon nanotubes were first functionalized with H_2O_2 for making better interfacial adhesion and improve dispersion. After cutting and preparing desired specimens, tests were performed.

According to experiments, adding 0.25 wt% of Silica-A, Silica-B and MWCNT improved the tensile strength of PU about 33%, 27%, and 15%, respectively, but further nanoparticle adding decreased the strength. Impact test results reveal that maximum strength can be seen in the nanocomposite containing 0.5 wt% MWCNT with approximately 96% improvement in comparison to neat PU. Furthermore, adding 0.75 wt% of Silica-B and 1 wt% of Silica-A improved the impact strength of PU by about 82% and 75%, respectively. Regarding Shore-A hardness, the nanocomposite foam with 0.5 wt % Silica-B has the highest amount.

In order to produce nanocomposites with higher MWCNT content and prevent the appearance of large agglomerations, hybrid nanocomposites were produced, which could lessen large agglomerations. Thereby hybrid nanocomposites can provide a synergistic effect, which can be seen when MWCNTs and silica nanoparticles are simultaneously added to the PU matrix. The hybrid nanocomposite with 0.25 wt% Silica-A and 0.5 wt% MWCNT showed the maximum tensile strength, elastic modulus and hardness, whereas, in MWCNT/PU nanocomposite, these highest results were obtained in 0.25 wt% MWCNT. In constant overall content of 0.75 wt%, hybrid nanocomposites have higher tensile strength, in comparison to single filler composites. This study revealed that fabricating a hybrid nanocomposite with different fillers enhanced dispersion of nanoparticles with relatively low cost and consequently the hybrid nanocomposites exhibited synergistic effects, which proved to be more effective than single filler systems. However, after attaining an optimum level, adding further nanoparticles into the polymer matrix noticeably decreased the mechanical properties, due to the appearance of large agglomerations. It is evident from TGA results that the thermal stability of hybrid nanocomposites is higher than that of single filler nanocomposites. In addition, FTIR results demonstrate that there are no major changes in the chemical structure of PU with a dispersion of carbon nanotubes and silica nanoparticles in the polymer matrix.

3. GRAPHENE TYPE DEPENDENCE OF CARBON NANOTUBES GRAPHENE NANOPLATELETS POLYURETHANE HYBRID NANOCOMPOSITES: MICROMECHANICAL MODELING AND MECHANICAL PROPERTIES [5]

3.1 Abstract

Micromechanical modeling and mechanical properties of polyurethane (PU) hybrid nanocomposite foams with multi-walled carbon nanotubes (MWCNTs) and graphene nanoplatelets (GNPs) were investigated by mean of tensile strength, hardness, impact strength and modified Halpin–Tsai equation. Three types of graphene, with varied flake sizes and specific surface areas (SSA), were utilized to study the effect of graphene types on the synergistic effect of MWCNT/GNP hybrid nanofillers. The results indicate a remarkable synergetic effect between MWCNTs and GNP-1.5 (1:1) with a flake size of 1.5 μm and a higher SSA (750 m^2/g), which tensile strength of PU was improved by 43% as compared to 19% for PU/MWCNTs and 17% for PU/GNP-1.5 at 0.25 wt% nanofiller loadings. The synergy was successfully predicted using unit cell modeling, in which the calculated data agrees with the experimental results.

3.2 Introduction

Polyurethane (PU) foams, which are economic due to their low density, are frequently used in a wider range of applications, such as insulation goals, automotive and electronic industries. However, their applications are limited because of their poor mechanical properties. Therefore, it seems attractive to modify PUs using nanoparticles to modify their mechanical properties (Ayub Karimzad Ghavidel et al., 2015; Ayob Karimzad Ghavidel, Azdast, Shabgard, Navidfar, & Shishavan, 2015; Ayub Karimzad Ghavidel et al., 2016; Amir Navidfar, Sancak, Yildirim, & Trabzon,

[5] **A.Navidfar**, L. Trabzon, "*Graphene type dependence of carbon nanotubes/graphene nanoplatelets polyurethane hybrid nanocomposites: Micromechanical modeling and mechanical properties*" Composites Part B: Engineering". 176, 2019, 107337.

2018; Yan et al., 2012; Yıldırım, Sancak, Navidfar, Trabzon, & Orfali, 2018). In addition, components of PUs (polyol and isocyanate) are in a liquid form, which allows for the simple integration of solid nanofillers.

One-dimensional (1D) MWCNTs and two-dimensional (2D) GNPs owing to their superior properties can be used as hybrid nanofillers to form well-dispersed three dimensional (3D) networks, which can overcome the dispersion problem of single nanofillers (Benzait & Trabzon, 2018; Chatterjee et al., 2012; Eungkee Lee, Afsari Ghazi, Azdast, Hasanzadeh, & Mamaghani Shishavan, 2018; Faraji et al., 2017; Amir Navidfar et al., 2016a; Rashahmadi et al., 2017). In order to solve the problem, acid functionalization of nanofillers can improve the dispersion, but the reaction conditions of acid oxidations are severe and may damage the graphitic structure (S.-Y. Yang et al., 2010). Hybrid nanocomposites possess better mechanical properties in comparison with conventional nanocomposites that lead to the formation of an effective network for strain transferring (W. Li, Dichiara, & Bai, 2013; Amir Navidfar et al., 2018; S.-Y. Yang et al., 2011; Zarasvand & Golestanian, 2017). MWCNTs and graphene have a high ability to self-assemble due to π–π interactions, which could inhibit aggregates resulting in enhancing the contact area between nanofillers and polymer matrixes (Aghadavoudi, Golestanian, & Zarasvand, 2018; Verma, Chauhan, Dhawan, & Choudhary, 2017).

Recently, carbon nanotubes/graphene hybrid nanofillers were used in polymer nanocomposites to improve the mechanical properties (Bagotia et al., 2019; Chatterjee et al., 2012; Kong, 2013; W. Li et al., 2013). Weikang et al. (Kong, 2013) uniformly dispersed CNT-graphene hybrids into epoxy. Their results demonstrated that the tensile strength of the hybrid nanocomposite obtained an enhancement of 36%. Combining carbon nanotubes and graphene for improving the performance of epoxy nanocomposites was also studied by Shin-Yi Yang et al. (S.-Y. Yang et al., 2011). The tensile strength and modulus of CNT+GNP/epoxy were increased by 14.5% and 22.6% at 1 wt% loading, respectively, which is obviously higher than the results of graphene/epoxy nanocomposites. The synergistic effect of the combinations did not completely understand. It is vital to determine the effect of nanofillers size on the properties of the hybrid nanocomposites. In addition, the ratio of the nanofillers is a significant parameter regarding the reinforcing capabilities of the nanocomposites (Prasad, Das, Maitra, Ramamurty, & Rao, 2009; S.-Y. Yang et al., 2011). Chatterjee

et al. (Chatterjee et al., 2012) reported that the particle size of graphene has a noticeable influence on the mechanical and thermal properties of the nanocomposites. They also exhibited that synergistic effects can be obtained using hybrid nanofillers especially for the CNT/graphene (9:1) and CNT/graphene (5:1), which are more effective than single nanofillers. Gao et al. (Y. Gao, Picot, Bilotti, & Peijs, 2017) added two types of GNPs, xGnP-C750 (with an average diameter of 1 μm and a surface area of 750 m^2/g) and xGnP-M15 (a larger diameter of 15 μm but a lower surface area of 150 m^2/g) in PLA and indicated the highest reinforcement of 24% for 5 wt% xGnP-M15. However, in that study works were focused on single graphene nanofillers rather than on the effect of particle size on hybrid nanocomposites, which have not discussed in any detail.

A key question is which types of graphene are best suited to show a synergistic effect with MWCNTs to reinforcing polymeric nanocomposites. To investigate this, we compared three commercially available varieties of graphene with different flake sizes (24, 5 and 1.5 μm), aspect ratios and specific surface areas (150 and 750 $m^{2/}g$) to study the synergistic effect of GNP with MWCNTs on tensile, hardness and impact properties of PU hybrid nanocomposites. We have observed a high synergistic effect and substantial improvement using GNP-1.5 with a lower flake size and a higher specific surface area at a low concentration of 0.25 wt%. Various nanofiller ratios were tested to find the optimal loading for mechanical properties and the highest synergy. The tensile strength of the single and hybrid nanocomposites was also compared with the predictions of the well-established Halpin-Tsai model, which was modified by adding an exponential shape factor, and the results fitted the experimental data successfully (Montazeri et al., 2010; Yeh et al., 2006). In addition, a unit cell comprising graphene and MWCNTs was considered, which the synergistic effect was successfully predicted.

3.3 Materials and experimental setup

3.3.1 Materials

Fabrication of PUs was done by mixing the polyol and isocyanate in a weight ratio of 1:1.25, as recommended by the manufacturer according to Table 3.1. Graphene and MWCNTs were purchased from Nanografi Co.Ltd. MWCNTs were grown by chemical vapor deposition with an average diameter of 8 - 10 nm, the length of 1-3

μm, a specific surface area of 290 m^2/g and purity of more than 92%. GNP-24 refers to graphene nanoplatelets with a diameter of 24 μm, a thickness of 6 nm and a specific surface area of 150 m^2/g, according to the manufacturer datasheet. GNP-5 has a smaller diameter of 5 μm, a lower thickness of 3 nm and a specific surface area of 150 m^2/g. According to the manufacturer, GNP-1.5 has a smaller diameter of 1.5 μm, a thickness of 3 nm, but a higher specific surface area of 750 m^2/g.

Table 3.1 : Properties of polyol and isocyanate components.

Physical properties	Unit	Polyol	Isocyanate	Standards
Density (25°C)	g/cm^3	1.11	1.23	DIN 51 757
Viscosity (25°C)	MPa.s	600 ± 200	210	ASTM D4878-98
OH content	Mg KOH/g	300	-	ASTM D 4274-99
NCO content	H_2O	-	%30.8 -%32	ASTM 5155-01
Storage life	Month	3	6	-

3.3.2 Nanocomposites preparation

Prior to the synthesis of PU foams, 1.5 g of MWCNTs were added to 500 mL of 35% hydrogen peroxide (H_2O_2) at room temperature and mixed for 90 min. Subsequently, the solution was filtered and washed twice with distilled water to eliminate any H_2O_2 and then dried in an oven at 80°C for 12 h. Two sets of nanocomposites were fabricated with; (1) different contents of single MWCNTs and graphene, (2) different contents and ratios of carbon nanotubes/graphene hybrid nanocomposites at 0.25 to 0.75 wt% nanofiller contents. Nanofillers were added to the polyol and were stirred at 200-2000 rpm for 5 min. Then the mixture was ultrasonically dispersed for 5 min using an ultrasonic bath and stirred again at 2000 rpm for 5 min. Finally, the isocyanate was added to the nanofiller/polyol mixture and stirred for 20 s, as shown in Figure 3.1. The details of the fabricated nanocomposites with MWCNTs, graphene and their combinations are given in Table 2. The ratio of carbon nanotubes/graphene is vital for hybrid nanocomposites and thus specimens with three different ratios were fabricated for each graphene type.

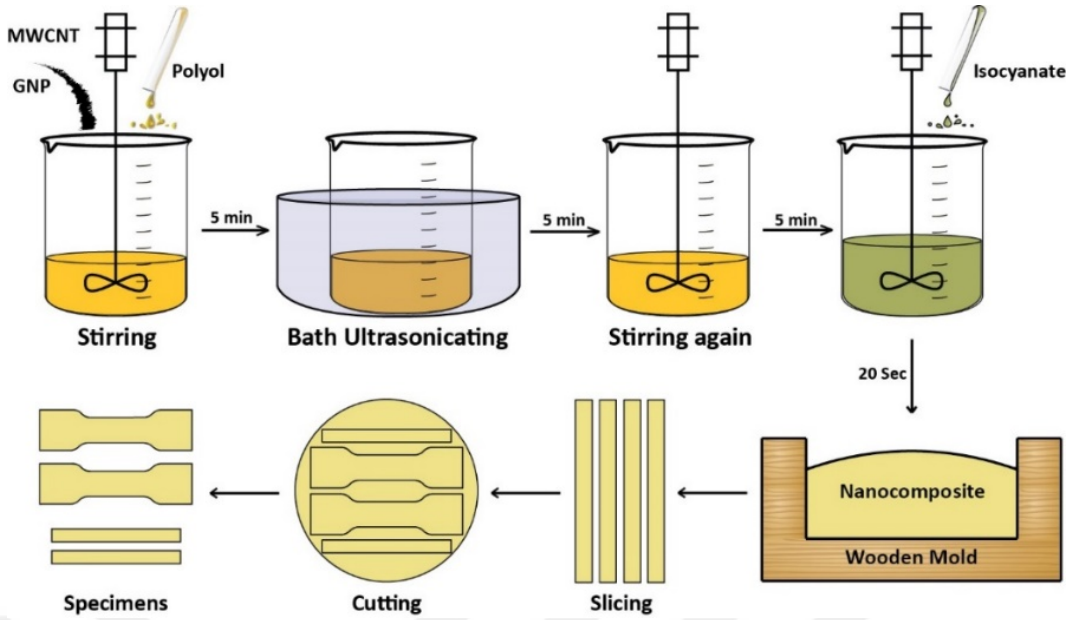

Figure 3.1 : The scheme of the nanocomposites fabrication steps.

Table 3.2 : Levels of fabricated nanocomposites.

Nanofillers	Concentrations (wt %)		
MWCNT	0.25	0.50	0.75
GNP-24	0.25	0.50	0.75
GNP-5	0.25	0.50	0.75
GNP-1.5	0.25	0.50	0.75
MWCNT + GNP-24 (1:3, 1:1, 3:1)	0.25	0.50	0.75
MWCNT + GNP-5 (1:3, 1:1, 3:1)	0.25	-	-
MWCNT + GNP-1.5 (1:3, 1:1, 3:1)	0.25	-	-

3.3.3 Characterization and instruments

A turning machine was used for cutting slices of cured nanocomposites with a thickness of 10 mm. The slices were cut in a CNC machine according to ASTM 6110 for Charpy impact tests and ISO 1926 for tensile tests of rigid cellular plastics. Tensile properties were performed on at least five samples of each nanocomposite using Shimadzu, a UTS machine equipped with a 1 kN load cell under a strain rate of 5 mm/min at room temperature. The impact strength of unnotched samples was obtained with a Devotrans Charpy impact machine. XF hardness tester is used to investigate Shore-0 hardness tests and at least six points of a sample were examined perpendicular to blowing direction. Raman spectroscopy was performed for the structure analysis of graphene nanoplatelets using a Renishaw inVia Raman spectrometer with a 532 nm

laser. X-ray diffraction (XRD) analysis was performed on a RIGAKU Diffractometer using Cu (Ka) radiation. Thermogravimetric analysis was done under a nitrogen atmosphere on a Q600, TA Instruments with a heating rate of 5°C min^{-1}. Fourier transform infrared spectroscopy of the specimens was studied in the wavenumber range from 4000 to 650 cm^{-1} at a resolution of 4 cm^{-1} using a Thermo Scientific iS10 FTIR at room temperature. Dispersion states of hybrid nanofillers were investigated using Hitachi HighTech HT7700 transmission electron microscopy (TEM).

3.4 Results and discussion

3.4.1 Characterization

XRD spectra of graphene nanoplatelets are shown in Figure 3.2 (a). A typical (002) peak at $2\Theta = 26^{o}$ is clear for all graphene while GNP-24 and GNP-5 have a much sharper peak than GNP-1.5, demonstrating that GNP-24 and GNP-5 are more crystalline than GNP-1.5. The structural defects of graphene play a critical role in the properties of nanofillers and their nanocomposites (Tian, Li, Yu, & Liu, 2017). Raman spectra are a useful tool for the characterization of crystal structure, disorder and defects in graphene-based materials. The graphene nanoplatelets exhibit D-band and G-bands which indicate defects and the sp^2 carbon networks of the sample, respectively (Y. Gao et al., 2017). Compared with GNP-24 and GNP-5, Raman analysis (Figure 3.2(b)) shows a high intensity of D-band at 1342 cm^{-1} for GNP-1.5, suggesting more defects on the graphene sheets. Furthermore, the intensity ratio of D-band to G-band ($I_D/I_G = 0.49$) of GNP-1.5 is much higher than those of GNP-24 and GNP-5 ($I_D/I_G = 0.08$), representing more defects and porous graphene (Fan et al., 2013).

Fourier transform infrared spectra of neat PU and nanocomposites are illustrated in Figure 3.2 (c). There are no visible changes in the FT-IR spectra of PU because MWCNTs and graphene display no obvious absorption in the infrared range [2]. Figure 3.2 (d) shows TGA results of PU and their nanocomposites with 0.25 wt% nanofiller loadings. It is apparent that graphene decelerates the thermal degradation and PU/GNP-1.5 indicates the highest thermal stability in comparison with other nanofillers due to the better dispersion in the PU matrix.

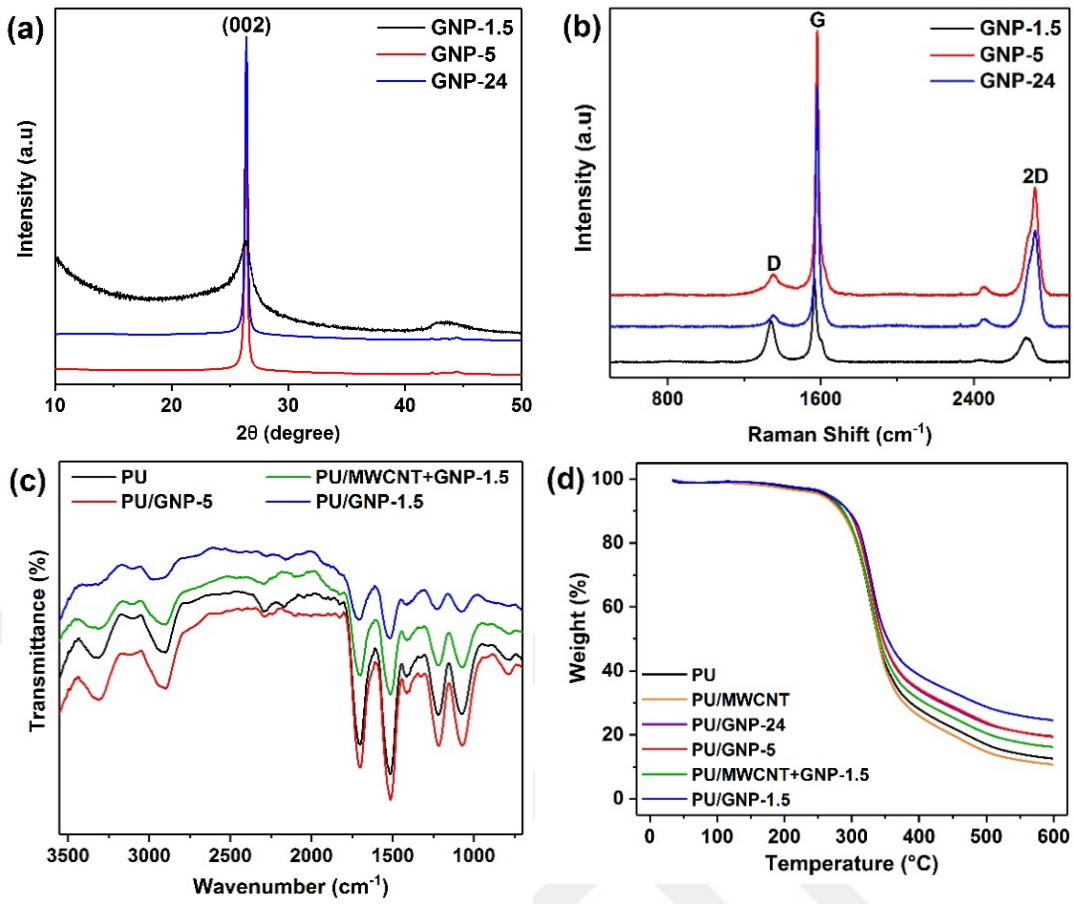

Figure 3.2 : (a) XRD patterns and (b) Raman spectra of graphene nanoplatelets, (c) FTIR spectra and (d) TGA curves of neat PU and nanocomposite foams.

3.4.2 Morphological characterization

The final properties of PU foams are severely dependent on their morphology, density, cell size, and walls thickness. In addition, the homogeneous dispersion of nanofillers in the polymer matrix is a key factor to fabricate reinforced polymer nanocomposites. Thus, it is very important to first characterize the microstructure of fabricated nanocomposites. Cross-sections of samples were fractured perpendicular to the foaming direction and fractured surfaces were coated with gold. Figure 3.3 illustrates SEM images of neat polyurethane and PU nanocomposites with 0.25 wt% nanofiller content, which provide evidence of foam cellular microstructures with the average cell size values. It has been shown that the incorporation of the nanofillers decreased cell sizes of polyurethane, proving that even small amounts of nanofillers alter the foam's morphology. The decrease in cell size can also be attributed to the higher viscosity and nucleation effect of nanofillers, which have a profound influence on the mechanical properties of foams (J.-M. Kim et al., 2018; R Verdejo et al., 2009).

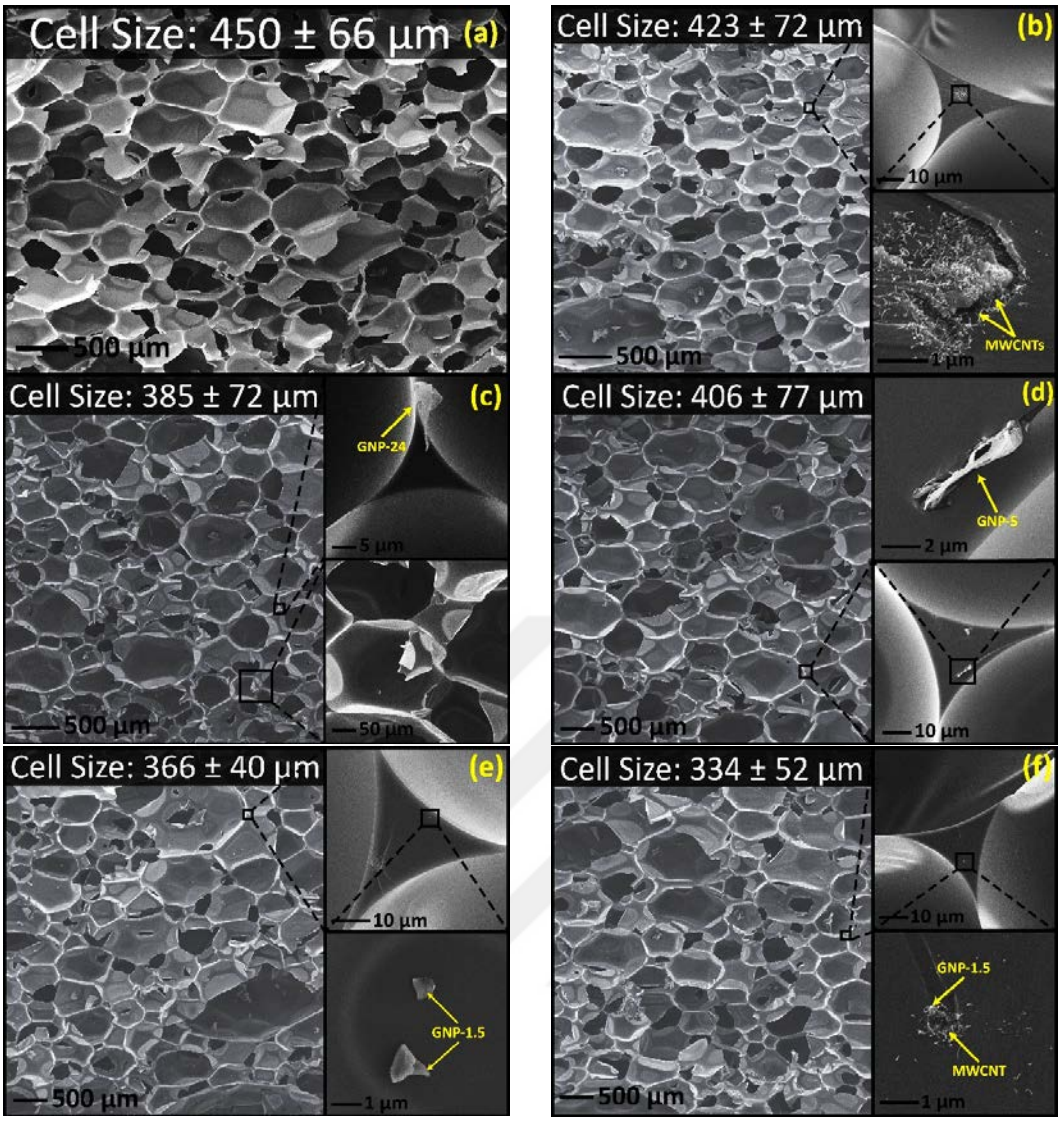

Figure 3.3 : SEM images of nanocomposite foams (0.25 wt%) (a) Polyurethane, (b) PU/MWCNT, (c) PU/GNP-24, (d) PU/GNP-5, (e) PU/GNP-1.5, (f) PU/MWCNT+GNP-1.5 (1:1).

As displayed in Figure 3.3, the neat polyurethane has a uniform closed-cell structure while the cell structure is damaged through MWCNTs and graphene addition. The hybrid nanocomposite containing MWCNT+GNP-1.5 shows the lowest cell size, which declares better dispersion (Baltopoulos et al., 2013). Consequently, it is expected that the mechanical properties of nanocomposites with carbon nanotubes/graphene hybrids could be higher than others (Amir Navidfar et al., 2018). SEM micrographs provide visual evidence of the foam microstructure consisting of three phases of the polymer, nanofillers and bubbles. Figure 3.3 also presents a series of microstructures focused on the strut area, in which carbon nanofillers are located. Several agglomerations are visible in these areas while a better dispersion in hybrid nanocomposites with GNP-1.5 and MWCNTs (Figure 3.3 (f)) is obvious that 1D

carbon nanotubes are well connected to 2D planar graphene floor via π-π stack interaction (J. Wang, Jin, Wu, & Guo, 2017) and formed a 3D structure which inhibits aggregations. This 3D structure will enhance the contact surface areas between the polymer matrix and MWCNTs/graphene structures that are favorable to their mechanical properties.

3.4.3 Tensile Properties

Uniaxial tensile testing was used to examine the mechanical properties of neat polyurethane and its nanocomposites reinforced with carbon nanotubes and graphene nanoplatelets. Figure 3.4(a) displays comparative results of MWCNTs and three types of graphene on ultimate tensile strength in various nanofiller loadings. The results show that carbon nanofillers are capable of improving the strength of PU in a low weight fraction. The tensile strength of neat polyurethane is about 0.39 MPa, whereas the addition of 0.25 wt% MWCNT, 0.25 wt% GNP-24 and 0.5 wt% GNP-1.5 enhanced the strength to about 0.468, 0.476 and 0.486 MPa with 19%, 21% and 24% improvement, respectively. The trend of strength improvement for MWCNTs is similar to GNP-24 and GNP-5, in which higher strength can be seen in the nanocomposites with 0.25 wt% nanofillers. The reinforcement efficiency of GNP-24 is obviously superior to that of GNP-5, which approves that a larger aspect ratio is beneficial for interfacial stress transfer from the matrix to graphene (M. Liu et al., 2018). Results of a similar study by Valles et al. (Valles, Abdelkader, Young, & Kinloch, 2015) showed that larger graphene provides better interfacial stress transfer with the polymer matrix, due to a more extensive contact area, which improves the mechanical properties. The nanocomposite containing 0.5 wt% GNP-1.5 has the highest tensile strength, which is attributed to the higher I_D/I_G ratio and specific surface area of GNP-1.5 (750 m^2/g) over those of GNP-24 and GNP-5 (150 m^2/g). The high specific surface area endows a better dispersion and an effective enhancement of mechanical properties in higher loadings (Hoseinabadi et al., 2017). The tensile strength of PU/MWCNTs is higher than PU/GNP-5 nanocomposites, while PU/GNP-24 shows better improvement. As a result, the superiority of graphene over MWCNTs depends on their properties such as aspect ratio, specific surface area. A study by Yan et al. (Yan et al., 2012) indicated more effective reinforcement of graphene than MWCNTs. On the contrary, Zakaria et al. (Zakaria, Kudus, Akil, & Thirmizir, 2017) concluded that carbon nanotubes possess a better reinforcement effect. As can be seen

in Figure 3.4 (a), MWCNTs, GNP-24 and GNP-5 reinforced PUs show a lower strength in higher loadings (0.5 and 0.75 wt%) because the dispersion becomes more challenging when nanofillers concentrations increased, which limits the improvement of mechanical properties (Chatterjee et al., 2012).

Due to the better reinforcement effect of GNP-24 in comparison with GNP-5, GNP-24 was used for fabricating hybrid nanocomposites with MWCNT in different ratios to investigate synergistic effects of both nanofillers. The tensile strength of pure PU and PU/MWCNT+GNP-24 hybrid nanocomposites with fixed nanofiller contents (0.25, 0.5 and 0.75 wt%) are demonstrated in Figure 3.4 (b). As expected, a synergistic effect was observed for the strength where the nanocomposite with MWCNT+GNP-24 (1:3) showed the highest increase of 23% (0.483 MPa) relative to an increase of 12% and 15% for the single MWCNTs and GNP-24 based nanocomposites in 0.5 wt% loadings, respectively. In nanocomposites with 0.75 wt% nanofiller loadings, a similar trend was observed whereas the hybrid nanocomposite containing MWCNT+GNP-24 (1:3) showed the highest strength in this content. The higher tensile strength of hybrid nanocomposites clearly presents a synergistic effect. As presented by Yang et al. (S.-Y. Yang et al., 2011) carbon nanotubes could connect to graphene to form a 3D hybrid structure, which prevents aggregations of graphene nanoplatelets. 3D hybrid structure results in better interaction between hybrid MWCNT+GNP-24 and the polymer matrix, which a larger surface area and the increased contact area between hybrid nanofillers and the matrix could help to transfer the load in the tensile test (Shin et al., 2012; Hongming Zhang et al., 2018).

In this paper, three types of graphene nanoplatelets were used to investigate the effects of graphene size, specific surface area and their defects on the mechanical properties of hybrid nanocomposites. Figure 3.4(c) represents a comparative result of graphene types on the ultimate tensile strength of hybrid nanocomposites at a constant level of 0.25 wt%. It is clear that the strength of MWCNT+GNP-1.5 hybrid nanocomposites is dramatically improved compared to the nanocomposites with other nanofillers. The tensile strength of nanocomposites with MWCNT+GNP-1.5 is increased up to about 43% (0.561 MPa) relative to that of PU. The fact that this is achieved at a nanofiller content of 0.25 wt% is remarkable. Whereas, there are moderate improvements in the PU/MWCNTs (~19%) and PU/GNP-1.5 (~17%) nanocomposites. Consequently, graphene nanoplatelets with a higher SSA and more defects have a greater ability to

self-assemble with MWCNTs, which GNP-1.5 with MWCNTs exhibit a noticeable synergistic effect in reinforcing PU.

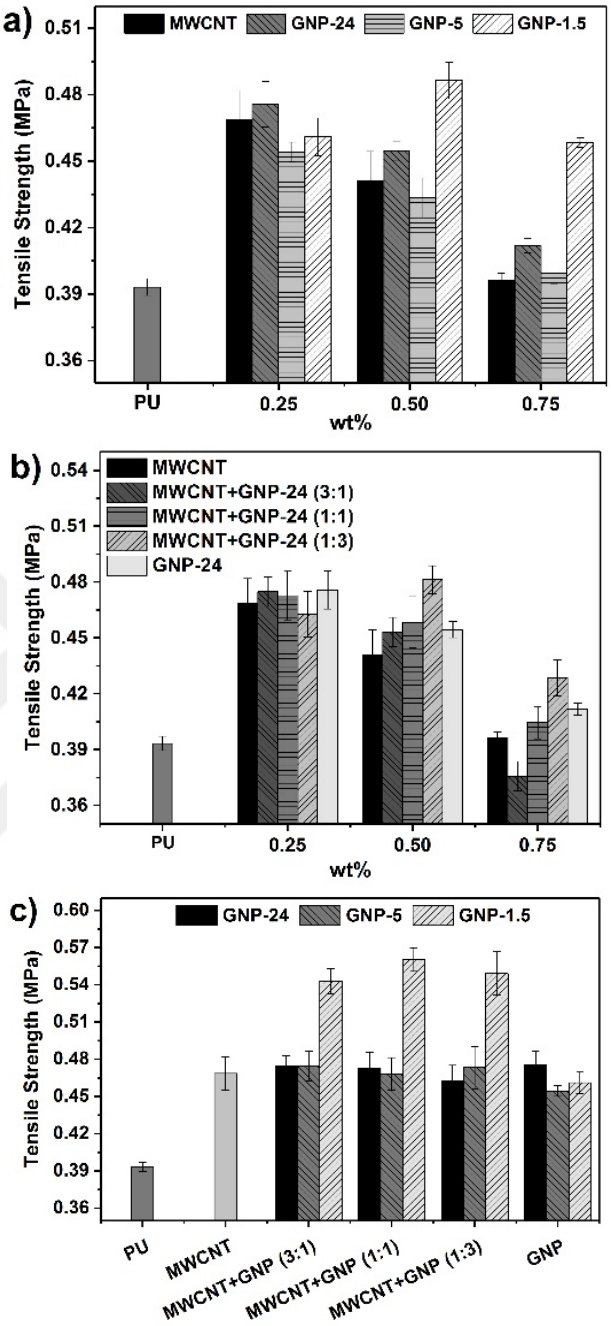

Figure 3.4 : The ultimate tensile strength of PU with (a) various nanofillers, (b) and (c) hybrid nanocomposites (0.25 wt%).

Lin Chen et al. (L. Chen et al., 2015) considered a unit cell with graphene/CNTs structure to calculate the effective thermal conductivity of the composites. A hybrid CNTs/graphene structure of the nanocomposites is displayed in Figure 3.5 (a), which is similar to that of literature (L. Chen et al., 2015; A. Yu et al., 2008). TEM image of hybrid MWCNTs/GNP-1.5 (Figure 3.5 (b)) approves the homogeneous distribution of

MWCNTs on the GNP-1.5 surface to bridge the adjacent graphene, which formed a 3D interconnecting network. In our work, the unit cell is abstracted to predict the synergistic effect of graphene/CNTs hybrids, which is the periodic structure of the nanocomposites. Each unit cell comprises two half graphene with some MWCNTs between them and it has the same length and width of L and height of H. Both the GNPs and MWCNTs are considered as cylinders and are uniformly dispersed in the polymer matrix, in which the volume fraction of graphene in the unit cell equals to that in the nanocomposites, as follow:

$$V_{f,G} = \frac{V_G}{L^2.H} \tag{3.1}$$

Where, $V_{f,\,G}$ and V_G are the volume fraction of graphene in nanocomposites and volume of single graphene, respectively. Assuming the graphene are located at the center of the cuboid as illustrated in Figure 3.5, the following equating can be written (L. Chen et al., 2015):

$$\mathrm{L} = \mathrm{D}_G + 2 \times \frac{1}{2} H_G = \mathrm{D}_G + (\mathrm{H} - t_G) \tag{3.2}$$

Where D_G and t_G are the diameter and thickness of graphene, respectively and H_G corresponds to the distance between two half graphene. By simultaneously solving equations (1) and (2), L, H and H_G can be found. Since MWCNTs are distributed between graphene to form 3D hybrid structure, only carbon nanotubes with the length $L \geq H_G$ can attach to graphene in the unit cell. Used MWCNTs have an average length of 2000 nm. According to this model, nanocomposites with $H_G \leq 2000$ nm could show the synergistic effect in the tensile strength improvement of the nanocomposites with hybrid nanofillers, which outcomes of Table 3 and Figure 3.4 prove the precision of this model. As a result, the synergistic effect could be obtained by increasing the ratio and content of graphene in the nanocomposites, in which the distance between the graphene, H_G, decreases according to equations (1) and (2). Thus, larger fractions of MWCNTs can connect graphene to form the 3D structure. Moreover, to achieve the synergistic effect in nanocomposites with larger flake graphene, either CNTs with a larger length should be used or the H_G should decrease by enhancing the ratio and content of graphene.

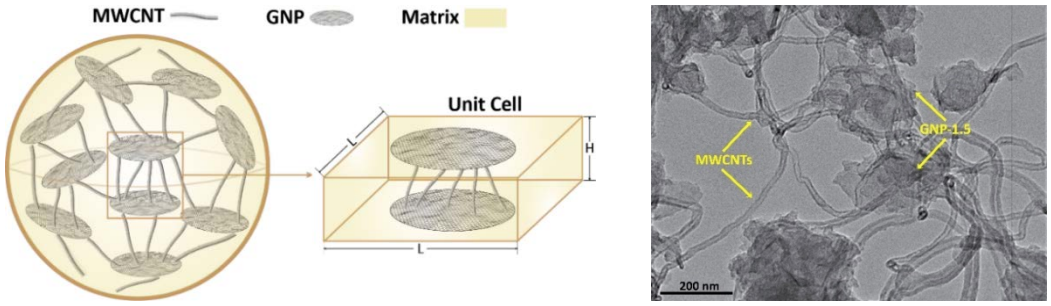

Figure 3.5 : a) Schematic diagram of the nanocomposite and a unit cell with a GNPs/MWCNTs structure, b) TEM images of GNP-1.5 and MWCNTs hybrids.

Table 3.3 : Calculated H_G of the nanocomposites, their synergistic effects and the strength enhancement.

Loading	Nanofillers	Calculated H_G (nm)	Synergy	Enhancement (%)
0.25 wt%	MWCNT/GNP-24 (3:1)	8061	×	20.7
	MWCNT/GNP-24 (1:1)	4943	×	20.2
	MWCNT/GNP-24 (1:3)	3618	×	17.7
	MWCNT/GNP-5 (3:1)	4224	×	20.6
	MWCNT/GNP-5 (1:1)	2887	×	19
	MWCNT/GNP-5 (1:3)	2266	×	20.3
	MWCNT/GNP-1.5 (3:1)	**1640** ($\leq$ 2000)[6]	✓	**38**
	MWCNT/GNP-1.5 (1:1)	**1150** ($\leq$ 2000)*	✓	**43**
	MWCNT/GNP-1.5 (1:3)	**919** ($\leq$ 2000)*	✓	**40**
0.50 wt%	MWCNT/GNP-24 (3:1)	4939	×	15.2
	MWCNT/GNP-24 (1:1)	2863	×	16.6
	MWCNT/GNP-24 (1:3)	**1992** ($\leq$ 2000)*	✓	**22.8**
0.75 wt%	MWCNT/GNP-24 (3:1)	3611	×	- 4.5
	MWCNT/GNP-24 (1:1)	2030	×	2.9
	MWCNT/GNP-24 (1:3)	**1388** ($\leq$ 2000)*	✓	**9**

3.4.4 Impact Properties

Aside from tensile strength, impact properties are crucial in foam applications, which is related to fracture toughness (Amir Navidfar et al., 2016a). Figure 3.6(a) represents the impact strength of unnotched PU nanocomposite specimens. The maximum value of impact strength is achieved at 0.5 wt% loadings for PU/MWCNTs nanocomposite with an enhancement of 21%, compared to that of pure polyurethane (0.794 kJ/m^2). Incorporating a 0.25% weight fraction of GNP-24 and GNP-5 increased the impact strength of PU by about 13.4% and 5.4%, respectively. Whereas, the maximum strength of GNP-1.5 reinforced nanocomposites can be seen at 0.75 wt% with an

[6] Used MWCNTs have an average length of 2000 nm.

enhancement of 13.6%, which is attributed to the homogeneous dispersion of GNP-1.5 due to its higher specific surface area. Figure 3.6(b) and (c) display the effects of hybrid nanofillers on the impact strength of PU nanocomposites. Synergistic effects cannot be seen in the impact strength, unlike tensile results. As reported in our previous works (Amir Navidfar, 2014; Amir Navidfar et al., 2016a; A Navidfar et al., 2014; Amir Navidfar et al., 2018), this is attributed to the dominant reinforcement effect of MWCNTs on the impact strength due to their folding and shock absorbance properties (Reich et al., 2008).

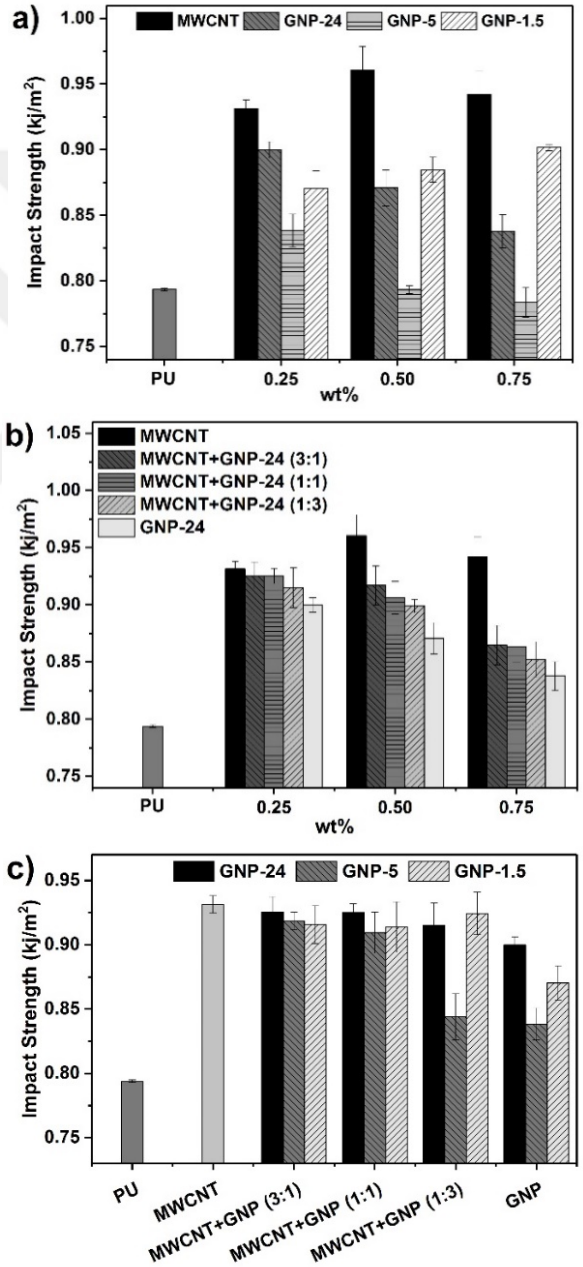

Figure 3.6 : The impact strength of PU with (a) various nanofillers, (b) and (c) hybrid nanocomposites (0.25 wt%).

3.4.5 Hardness

Figure 3.7(a) illustrates the changes in Shore-0 hardness of PUs with graphene, MWCNTs and their different concentrations. The highest hardness values can be seen in the nanocomposites with 0.25 wt% GNP-24, MWCNT, GNP-1.5 and GNP-5 with 14%, 13.4%, 10.5% and 9.3% enhancements, respectively. This improvement in the hardness of nanocomposites may be due to the presence of a strong interaction between MWCNTs/graphene and PU. However, the hardness decreased in higher loading due to the uneven dispersion of nanoparticles. As mentioned in tensile results, agglomerations occurred in higher contents, which have an undesirable effect on the hardness. GNP-24 has a superior reinforcement effect in comparison with other nanofillers that approves a larger aspect ratio is advantageous for interfacial stress transfer from the matrix to nanofillers (M. Liu et al., 2018). In the case of GNP-1.5, the higher specific surface area endows a better dispersion and an effective enhancement (Hoseinabadi et al., 2017).

Nanocomposites show lower hardness in higher loadings (0.50 and 0.75 wt%) due to agglomerations. The hybrid nanocomposites were fabricated to overcome this challenge, which synergistic effect among nanofillers could reduce agglomerations. In Figure 3.7(b), it is observed that the value of hardness increases in hybrid nanocomposites. Polyurethane with MWCNT+GNP-24 (1:3) showed the maximum reinforcement of 15.4% compared to an increase of 10% and 11% with single MWCNTs and GNP-24 based nanocomposites in 0.5 wt% loadings, respectively. In nanocomposites with 0.75 wt% nanofillers, a similar trend was observed whereas the hybrid nanocomposite containing MWCNT+GNP-24 (1:3) indicates the highest hardness in this content. These results exhibited that MWCNTs and graphene showed the highlighted synergistic effect in enhancing the hardness of the nanocomposite foams.

Three types of graphene nanoplatelets were used to examine the influence of graphene size, specific surface area and defects on the mechanical properties of hybrid nanocomposites. Figure 3.7(c) depicts comparative results of graphene types on the hardness of hybrid nanocomposites at a constant level of 0.25 wt%. It is observed that the hardness of MWCNT+GNP-1.5 hybrid nanocomposites is dramatically improved as compared to the nanocomposites with other graphene. The hardness of nanocomposites with hybrid MWCNT+GNP-1.5 is increased up to about 21%

comparative to that of PU (41 Shore-0), while foams with single MWCNTs and GNP-1.5 improved the hardness by about 13% and 10%, respectively. Therefore, graphene with a higher specific surface area and more defects facilitate synergistic effects and the formation of 3D hybrid structures.

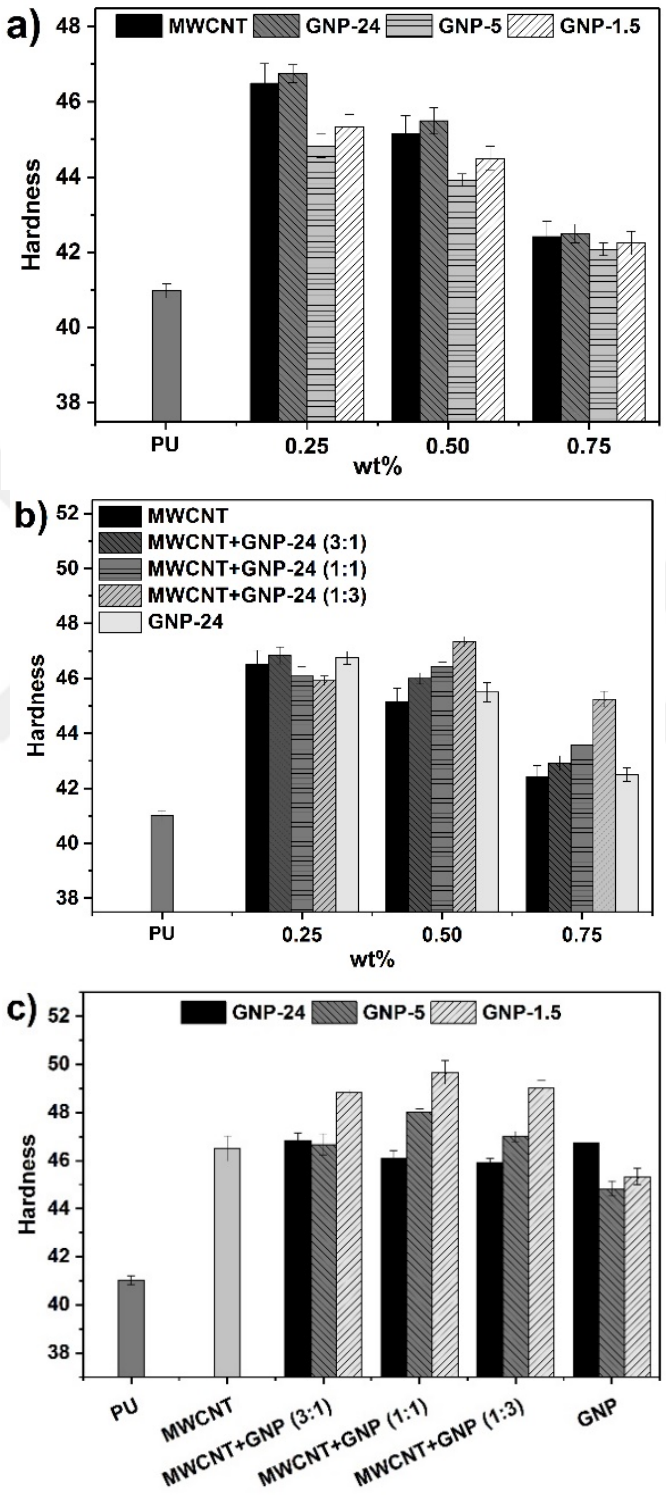

Figure 3.7 : Hardness of PU with (a) various nanofillers, (b) and (c) hybrid nanocomposites (0.25 wt%).

3.4.6 Micromechanical Analysis

The well-established Halpin-Tsai model, which can be widely utilized for predicting the tensile strength of randomly distributed nanofiller reinforced nanocomposites, was usually employed to calculate the theoretical tensile strength of the perfect dispersed nanocomposites. The experimental results of the nanocomposites are compared with the calculated values using the Halpin–Tsai equations as follows:

$$\sigma_C = \frac{3}{8}\sigma_L + \frac{5}{8}\sigma_T \tag{3.3}$$

Where σ_C, σ_L and σ_T are the nanocomposite, the longitudinal and transverse tensile strength, respectively. In our equations, graphene was assumed as effective rectangular fibers and MWCNTs were considered as discontinuous fibers, given by (Srivastava, 2012):

$$\sigma_L = \left[\frac{1 + C\eta_L V_f}{1 - \eta_L V_f}\right]\sigma_{PU} \qquad \sigma_T = \left[\frac{1 + 2\eta_T V_f}{1 - \eta_T V_f}\right]\sigma_{PU} \tag{3.4}$$

In the above relations, V_f is the volume fraction of MWCNTs and graphene, which can be calculated based on the density and weight fraction of nanofillers and neat PU (Rafiee et al., 2009). Based on the manufacturer datasheet, the graphene and MWCNTs densities were considered 2250 kg/m^3 and 2100 kg/m^3, respectively. The density of the PU matrix was measured at 40.51 kg/m^3. C is a constant shape factor related to the aspect ratio of fillers. For MWCNTs, C_{CNT} = 2(l/d), where l and d refer to the average length and diameters of MWCNTs, which are about 2 μm and 9 nm, respectively. For graphene, C_{GNP} = (2/3)(l/t), where l and t refer to the diameter and thickness of graphene. The parameters η_L, ζ_L η_T and ζ_T are given by;

$$\zeta_L, \eta_L = \frac{\left(\sigma_f/\sigma_{PU}\right) - 1}{\left(\sigma_f/\sigma_{PU}\right) + C} \qquad \zeta_T, \eta_T = \frac{\left(\sigma_f/\sigma_{PU}\right) - 1}{\left(\sigma_f/\sigma_{PU}\right) + 2} \tag{3.5}$$

Where σ_f and σ_{PU} are tensile strengths of nanofillers and the polyurethane matrix, respectively. The parameters η_L and η_T were used for MWCNTs, while ζ_L and ζ_T were utilized for graphene nanocomposites. The tensile strength of PU is σ_{PU} = 0.3933 MPa and the strength of MWCNTs and graphene are assumed 63 GPa and 130 GPa, respectively (C. Lee, Wei, Kysar, & Hone, 2008). The constant shape factor C was modified as an exponential shape factor ψ to fit nonlinear region for higher nanofiller

contents due to agglomerations of nanofillers, which Halpin-Tsai equation was not assumed. The exponential shape factor ψ has the formula (Montazeri et al., 2010):

$$\psi = CK = Ce^{-aV_f - b} \tag{3.6}$$

The constants a and b are the degree of nanofiller aggregations, accounting for the nonlinear behavior of the Halpin–Tsai equation and are found with respect to experimental results. The modified Halpin-Tsai equation may be rewritten as follows:

$$\sigma_L = \left[\frac{1 + \psi\eta_L V_f}{1 - \eta_L V_f}\right]\sigma_{PU} \qquad \zeta_L, \eta_L = \frac{\left({}^{\sigma_f}/_{\sigma_{PU}}\right) - 1}{\left({}^{\sigma_f}/_{\sigma_{PU}}\right) + \psi} \tag{3.7}$$

After an organized variation of aggregation-related a and b constants, ψ relations become equal to:

$$\psi = C_{CNT}e^{-1030.56V_f + 1.26} \quad \text{For PU/MWCNT} \tag{3.8a}$$

$$\psi = C_{GNP}e^{-905.64V_f - 0.63} \quad \text{For PU/GNP-24} \tag{3.8b}$$

$$\psi = C_{GNP}e^{-1048.93V_f + 0.817} \quad \text{For PU/GNP-5} \tag{3.8c}$$

$$\psi = C_{GNP}e^{-444.43V_f + 0.696} \quad \text{For PU/GNP-1.5} \tag{3.8d}$$

Experimental results and theoretical fits by Halpin-Tsai equation (equation (4) and (5)) and modified Halpin-Tsai equation with the exponential shape factor (equation (7) and (8)) were plotted in Figure 3.8. Comparisons indicate that there is an obvious difference between the experimental strength results and Halpin–Tsai equation, while the predictions of the modified Halpin–Tsai equation correlates well with the experimental data. It is noteworthy that the experimental results of nanocomposites with GNP-24 and GNP-5 are far from the Halpin-Tsai equation (blue lines in Figure 3.8) in comparison with PU/GNP-1.5, due to the higher folding and breaking tendency of larger graphene. Gao et al. (Y. Gao et al., 2017) reported that graphene with a larger flake is more susceptible to shortening during mixing and to bending after combining, which could lower their aspect ratio even more. The modified Halpin–Tsai with exponential shape factor is a semi-empirical method that can be utilized to calculate the results slightly outside of tested nanofillers concentration considered by extrapolation.

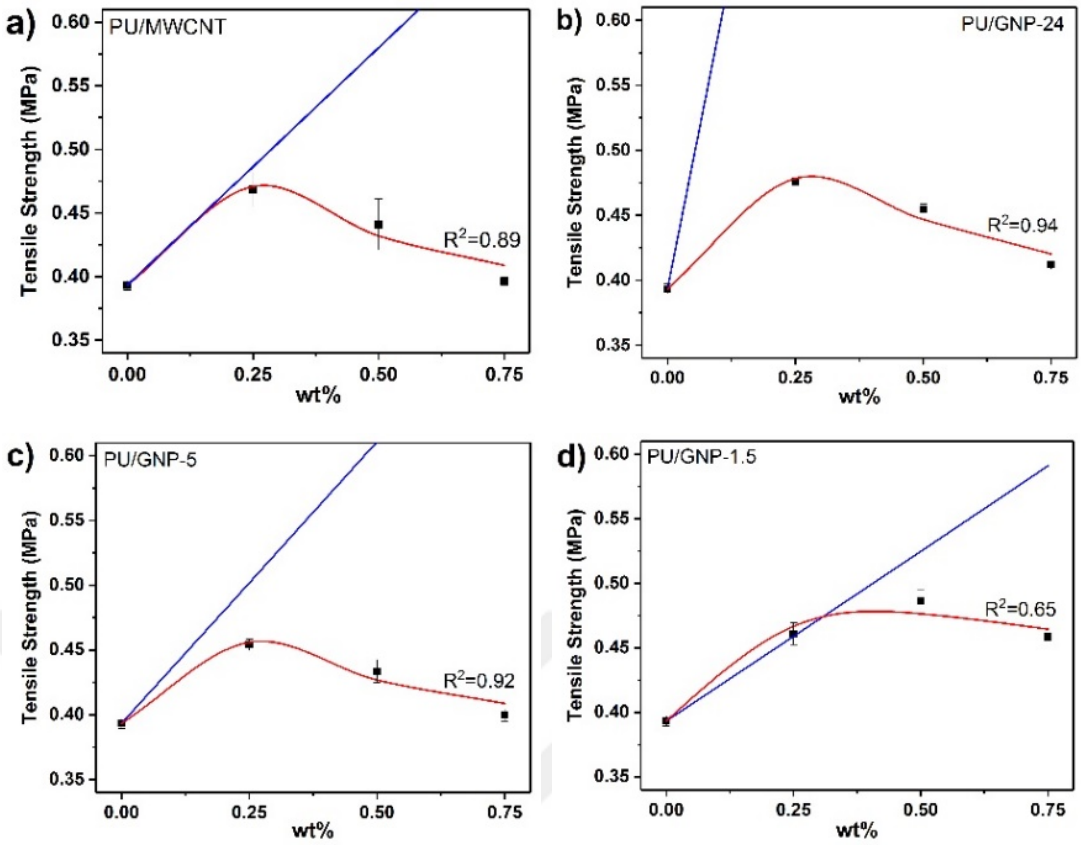

Figure 3.8 : Experimental data (■), Halpin-Tsai (blue) and modified Halpin-Tsai equations (red), for (a) PU/MWCNT, (b) PU/GNP-24, (c) PU/GNP-5, (d) PU/GNP-1.5 nanocomposites.

For hybrid nanofillers reinforced nanocomposites Halpin–Tsai equation could be rewritten as (W. Li et al., 2013):

$$\sigma_L = \left[\frac{1 + C_{CNT}\eta_L V_{CNT} + C_{GNP}\zeta_L V_{GNP}}{1 - \eta_L V_{CNT} - \zeta_L V_{GNP}}\right]\sigma_{PU}$$
$$\sigma_T = \left[\frac{1 + 2\eta_L V_{CNT} + 2\zeta_L V_{GNP}}{1 - \eta_L V_{CNT} - \zeta_L V_{GNP}}\right]\sigma_{PU} \quad (3.9)$$

In addition, the modified Halpin-Tsai equation can be used for hybrid nanocomposites using ψ instead of C_{CNT} and C_{GNP} in equation 9. For example, ψ for the modified Halpin-Tsai model for the hybrid nanocomposite with MWCNT+GNP-24 (1:1) equals to:

$$\psi = Ce^{-846.36V_f - 0.141} \quad (3.10)$$

Figure 3.9 (a) shows experimental results, Halpin-Tsai equation and modified Halpin-Tsai equation with the exponential shape factor (equation 10). The predictions of the modified Halpin–Tsai equation correlates well with the experimental results.

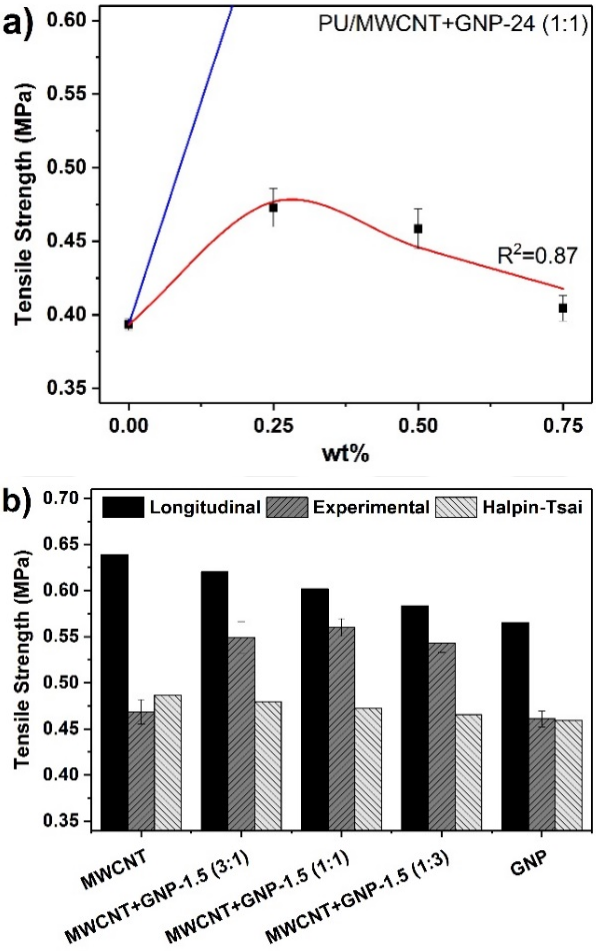

Figure 3.9 : (a) Experimental data (■), Halpin-Tsai (blue) and modified Halpin-Tsai equations (red) for PU/MWCNT-GNP-24 (1:1) and (b) Longitudinal, Halpin-Tsai model and experimental data for PU/MWCNT-GNP-1.5 hybrids

As mentioned in Figure 3.4 (c), MWCNT+GNP-1.5 hybrid nanofillers displayed an outstanding synergistic effect on tensile strength, which can be mostly attributed to the homogeneous 3D dispersion of MWCNTs and GNP-1.5 in the PU matrix. 3D distribution of MWCNT+GNP-1.5 hybrid nanofiller can be defined by the Halpin-Tsai equation. Figure 3.9 (b) reveals that the Halpin-Tsai equation under-predict the experimental data of the nanocomposites with MWCNT+GNP-1.5 hybrid nanofillers, while the experimental values of the single PU/MWCNTs, PU/graphene and other hybrid nanofillers are generally lower than their values estimated using the Halpin-Tsai model. As shown in Figure 3.9 (b), the experimental results of MWCNT+GNP-1.5 hybrid nanofillers are closer to the longitudinal tensile strength of the theory (black

columns), which approves the 3D uniform dispersion (W. Li et al., 2013). In this case, a higher reinforcement effect is achieved by adding MWCNT+GNP-1.5 to the PU matrix, which provides a synergistic effect and a higher tensile strength [45-47].

3.5 Conclusion

In summary, graphene type dependence of three-dimensional graphene/MWCNTs hybrid nanofillers on mechanical properties improvement of polyurethane nanocomposites was studied using tensile test, impact strength, hardness and micromechanical modeling. Three types of graphene with various flake sizes and specific surface areas were used to achieve a synergistic effect at 0.25 to 0.75 wt% loadings. MWCNTs and GNP-1.5 (1:1) with a flake size of 1.5 µm and a higher SSA (750 m^2/g) exhibited the highest synergistic effect at a low nanofiller content of 0.25 wt%, which the tensile strength was improved about 43%, in comparison with pure PU. Modified Halpin-Tsai modeling with an exponential shape factor was used to fit with the tensile strength results of the single and hybrid nanocomposites. A unit cell containing graphene and MWCNTs structure was introduced to predict the optimal ratio and content of the nanofillers in hybrid nanocomposites to attaining the synergism, which the modeling results were extremely compatible with the experimental data. The connections between the graphene and MWCNTs were more possibly formed when the length of carbon nanotubes is higher than the gap between graphene in the unit cell. The presented model could provide guidance for achieving the synergistic effect between different CNTs and graphene without many experiments.

4. ANALYTICAL MODELING AND EXPERIMENTALLY OPTIMIZING SYNERGISTIC EFFECT ON THERMAL CONDUCTIVITY ENHANCEMENT OF POLYURETHANE NANOCOMPOSITES WITH HYBRID CARBON NANOFILLERS [7]

4.1 Abstract

Combining various carbon nanofillers with different dimensions can lead to a synergistic effect through the formation of an efficient conductive network. Hybrid polyurethane (PU) nanocomposites containing multi-walled carbon nanotubes (MWCNTs) and graphene nanoplatelets (GNPs) were fabricated to study experimental and theoretical aspects of thermal conductivity (TC) enhancement. The optimization of hybrid nanofillers combinations was done to synergically enhance the TC using various types of graphene, nanofillers concentrations and ratios. A synergistic thermal conductivity improvement with MWCNTs and GNPs was confirmed at low nanofillers contents. The TC of hybrid nanocomposite at 0.25 wt% is approximately equivalent to the TC of individual nanofillers at 0.75 wt%. An analytical model for the effective thermal conductivity of single and hybrid nanocomposites was considered with variables of volume fraction, interfacial thermal resistance, straightness of the nanofillers and the percolation effect, in which the predictions of the modified models agreed with the experimental results.

4.2 Introduction

Lightweight thermally conductive polymers have attracted a great deal of attention in some fields, such as electronic packaging, heat exchangers and flexible electronics, in which the low thermal conductivity is one of the main technical limitations (Antunes & Velasco, 2014; Hamidinejad, Chu, Zhao, Park, & Filleter, 2018; C. Huang, Qian, &

[7] **A.Navidfar**, L. Trabzon, "*Analytıcal modelıng and experımentally optımızıng synergıstıc effect on thermal conductıvıty enhancement of polyurethane nanocomposıtes wıth hybrıd carbon nanofillers*", Polymer Composıtes, 42(2), (2021), 944-954.

Yang, 2018). Polyurethane (PU) foams were considered due to their low density, high global volume production, low cost and solid nanofillers inclusion facility.

Polymeric foams thermal conductivity is mainly transferred by the solid fraction and the gas encompassed in its cells controls thermal insulating properties (Espadas-Escalante, Avilés, Gonzalez-Chi, & Oliva, 2017; Hasanzadeh, Azdast, & Doniavi, 2020). To enhance the thermal conductivity (TC) of polymeric composites, introducing high thermally conductive nanofillers is a simple and common technique. Nanocarbon fillers owing to their lightweight, high thermal conductivity and high aspect ratio are receiving significant attention (Chu, Li, Jia, & Tang, 2012; Faraji et al., 2017; Ayub Karimzad Ghavidel et al., 2016; Amir Navidfar, 2014; Amir Navidfar et al., 2016a; A Navidfar et al., 2014; Tessema et al., 2017). Among them, graphene nanoplatelets (GNPs) and carbon nanotubes (CNTs) due to their two-dimensional (2D) and one-dimensional (1D) structure and ultrahigh surface areas offer exceptional thermal conductivity to the polymer nanocomposites (H. Lu et al., 2017). Thermal conductivities of CNTs and graphene have been informed to reach in the range of 1950–5000 and 3000–6500 W/m K, respectively (Chu, Li, & Dong, 2013; Chu, Li, & Tang, 2013; Deng, Zheng, Wang, & Nan, 2007; Zhengzhou Wang & Li, 2017; J. Yu, Choi, Kim, & Kim, 2016).

Recent experimental results indicate that combining two different nanocarbon fillers with varied sizes as hybrid fillers could lead to a synergistic effect because of a three-dimensional (3D) thermally conductive network formation, which exceeds the thermal properties of the individual graphene or carbon nanotubes filled nanocomposites (Badakhsh et al., 2019; Bagotia et al., 2019; Burgaz & Kendirlioglu, 2019; Guo, Ruan, Shi, Yang, & Gu, 2020; He et al., 2018; min Kim et al., 2019; Amir Navidfar et al., 2018; Amir Navidfar & Trabzon, 2019; Zhengzhou Wang & Li, 2017; X. Yang et al., 2020). Yu et al. (A. Yu et al., 2008) achieved a significant thermal conductivity enhancement for graphene and single-walled CNTs hybrid fillers with a weight ratio of 3:1. He et al (He et al., 2018) reported that the thermal conductivity was enhanced with 3D hybrid GNPs/CNTs inclusion in the polymer matrix at very low nanofiller loading. Enhancing thermal conductivity at low nanofiller loadings is essential for improving processability and reducing the viscosity and the cost of fabricated nanocomposites. On the other hand, several analytical predictions on the thermal conductivity of carbon nanofillers reinforced nanocomposites have been proposed

(Chu, Jia, & Li, 2012; Chu, Li, & Dong, 2013; Chu, Li, et al., 2012; Chu, Li, & Tang, 2013; Deng et al., 2007). Chu et al. (Chu, Li, & Dong, 2013) theoretically analyzed the thermal conductivity of graphene nanocomposites with considering the flatness influence of GNPs. Their experiments indicated that the waviness of graphene considerably affects the thermal conductivity of nanocomposites. In other work, Chu et al. (Chu, Li, et al., 2012) developed a theoretical model for anticipating the effective thermal conductivity (ETC) of hybrid CNT/GNP nanocomposites with incorporating the percolation effect. Although there are a few studies on the thermal conductivity improvement of single or hybrid carbon nanofillers based nanocomposites, simultaneously theoretical modeling and experimental studies on the thermal conductivity of individual and hybrid nanocomposites are still lacking. In addition, thermal conductivity analysis of these nanocomposites has not been systematically considered using varied types of graphene, nanofillers contents and ratios, as well as utilizing variables of volume fraction, interfacial thermal resistance, nanofillers straightness and the percolation effect at the same time.

In this work, we used three types of graphene nanoplatelets with different physical properties e.g. flakes size, aspect ratio and specific surface areas to investigate graphene type dependence of hybrid GNPs/MWCNTs nanofillers on synergistic thermal conductivity of PU nanocomposites. The optimization of hybrid nanofillers was done to maximize the synergistic effect and the thermal conductivity improvement of the nanocomposites. It was expected that graphene with MWCNTs would form a 3D heat conduction pathway. Thus, synergistic thermal conductivity improvement was observed through GNP-S750 with a smaller flake dimension and a higher specific surface area at a low content of 0.25 wt%. Structures and morphologies of nanocomposites were studied by scanning and transmission electron microscopy (SEM and TEM), X-ray diffraction (XRD) and Raman spectroscopy. A theoretical study on the ETC of single and hybrid nanocomposites by incorporating the straightness factor and percolation effect as fitting parameters is presented. Our analytical results are found to be in reasonable agreement with experimental data, which well describe the thermal conductivity improvement of single and hybrid nanocomposites.

4.3 Experimental

4.3.1 Materials and Sample preparation

As suggested by the supplier (Table 4.1), PU fabrication was carried out by blending the polyol and isocyanate with a weight ratio of 1:1.25. MWCNTs and graphene were bought from Nanografi Co.Ltd, which MWCNTs (purity ≥ 92%) were grown by chemical vapor deposition (CVD). The specific surface areas and geometries of used MWCNTs and graphene were listed in Table 4.2, according to the manufacturer datasheet. The density of used MWCNTs and GNPs are 2.1 and 2.25 g/cm^3, respectively.

Table 4.1 : Properties of polyol and isocyanate components.

Physical properties	Unit	Polyol	Isocyanate	Standards
Density (25°C)	g/cm^3	1.11	1.23	DIN 51 757
Viscosity (25°C)	MPa.s	600 ± 200	210	ASTM D4878-98
OH content	Mg KOH/g	300	-	ASTM D 4274-99
NCO content	H_2O	-	%30.8 -%32	ASTM 5155-01
Storage life	Month	3	6	-

Table 4.2: Properties of carbon nanofillers.

Nanofiller	Diameter (nm)	Thickness/Length (nm)	Specific Surface Area (m^2/g)
MWCNT	D_{CNT} = 8-10	L =1000-3000	290
GNP-L150	D_{GNP} = 24000 (Large)	t = 6	150
GNP-M150	D_{GNP} = 5000 (Medium)	t = 6	150
GNP-S750	D_{GNP} = 1500 (Small)	t = 3	750

Before the PU synthesis, used MWCNTs were functionalized with hydrogen peroxide (H_2O_2) to better interconnecting GNPs and formation of 3D structure in the polymer matrix, as reported elsewhere (Amir Navidfar et al., 2018; Amir Navidfar & Trabzon, 2019; Yıldırım et al., 2018). Different contents and ratios of MWCNTs and graphene were first mixed with polyol at 200-2000 rpm for 5 min using overhead stirrer equipment. Subsequently, the combination was ultrasonically dispersed for 5 min

using ultrasonication and stirred again at 2000 rpm about 5 min. The isocyanate was finally added to the carbon nanofiller/polyol composition, which was stirred for 20 s and then poured into a two-part wooden mold with a diameter of 180 mm to form free-rise PU foam (Figure 4.1) (Amir Navidfar et al., 2018; Amir Navidfar & Trabzon, 2019; Yıldırım et al., 2018). Table 4.3 summarizes the fabricated nanocomposites with MWCNTs, graphene, and their compositions. For hybrid nanocomposites, the ratio of carbon nanotubes and graphene nanoplatelets was varied for each graphene type to investigate their effectiveness in the thermal conductivity of the nanocomposites.

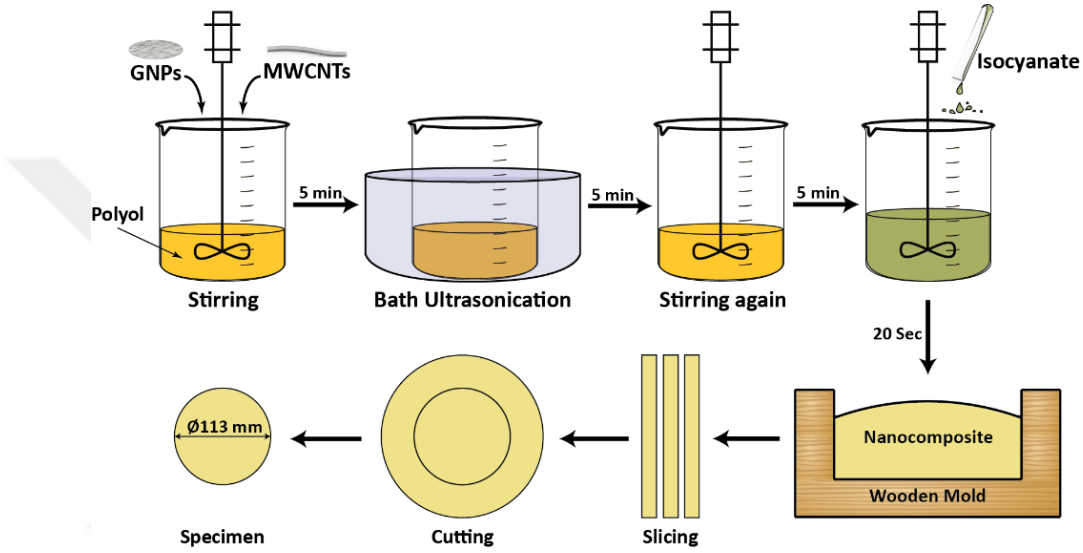

Figure 4.1 : The scheme of nanocomposites fabrication steps.

Table 4.3 : Levels of fabricated nanocomposites.

Nanofillers	Levels (wt %)		
MWCNT	0.25	0.50	0.75
GNP-L150	0.25	0.50	0.75
GNP-M150	0.25	0.50	0.75
GNP-S750	0.25	0.50	0.75
MWCNT/GNP-L150 (1:3, 1:1, 3:1)	0.25	0.50	0.75
MWCNT/GNP-M150 (1:3, 1:1, 3:1)	0.25	-	-
MWCNT/GNP-S750 (1:3, 1:1, 3:1)	0.25	-	-

4.3.2 Characterizations

For cutting slices of cured nanocomposites with a thickness of 10 mm, a lathe machine was used. A cylindrical metal piece with sharp edges and a diameter of 113 mm were pressed over sliced PU foams to shaping thermal measurement specimens. The thermal

conductivity analysis was carried out employing the guarded comparative-longitudinal heat flow technique according to the ASTM-E1225 test method. XRD analysis was determined on a RIGAKU Diffractometer using Cu (Ka) radiation. Structure analysis of carbon nanofillers was studied using a Renishaw inVia Raman spectrometer with a 532 nm laser. Morphologies of the nanocomposites composed of PU, graphene and MWCNTs were observed by FEI Nova NanoSEM. HighTech HT7700 TEM was used to investigate the dispersion states of carbon nanofillers and their hybrids.

4.4 Results and Discussion

4.4.1 Morphology and Characterization

Figure 4.2 (a) and (b) display XRD patterns of carbon nanofillers, PU and PU/GNP-S750+CNT nanocomposites in the range of 2θ =10-50˚. An intense peak at 2θ = 26.4° is obvious for all graphene, in which GNP-L150 and GNP-M150 have a much sharper peak, representing that GNP-L150 and GNP-M150 are more crystalline than MWCNTs and GNP-S750. The XRD spectra of MWCNTs exhibit a diffraction peak at 25.8˚ (002) and 43.3˚ (100), corresponding to an inner-walls distance in the radial direction of CNTs (H. Liu et al., 2016). Moreover, the pristine MWCNTs and functionalized MWCNTs (f-MWCNT) demonstrate the same XRD spectra, proving that the functionalization by H_2O_2 did not alter the crystalline structure of CNTs (Figure 4.2 (b)), in contrast to the results of acid treatment such as HNO_3/H_2SO_4 (S.-Y. Yang et al., 2011). A broad amorphous peak of PU was seen around 19˚, which confirms an amorphous microstructure of polyurethane (Figure 4.2 (b)). In PU/GNP-S750+CNT hybrid nanocomposite, the broad diffraction peak of the polymer matrix can be observed, while the peaks assigned to MWCNTs and GNP-S750 are disappeared, demonstrating that the carbon nanofillers are well dispersed in the PU matrix at 0.25 wt% content (Hongming Zhang et al., 2018). Raman spectroscopy was carried out to characterize crystal structure, disorders and defects in carbon-based materials. Figure 4.2 (c) illustrates the characteristic peaks of carbon nanofillers, including D-band, G-band and 2D-band, which are relevant to defects and carbon structures. The D-band to G-band intensity ratio of GNP-S750 (I_D/I_G = 0.49) shows a higher value compared to GNP-L150 and GNP-M150 (I_D/I_G = 0.08), indicating more defects and porous graphene. This can be ascribed to the lower flake size of GNP-S750 and more functional groups on the GNP-S750 surface and edges, which increased the

degree of disorders (F. Wang, Drzal, Qin, & Huang, 2015). XRD analysis that reveals the higher crystalline structure of GNP-M150 and GNP-L150 supports this statement. Besides, the I_D/I_G value of MWCNTs (I_D/I_G = 1.19) is higher than that of graphene, which is attributed to sp^3 defects and twist structure of carbon nanotubes (Zakaria et al., 2017).

TEM micrographs of graphene and MWCNTs and their hybrid are shown in Figure 4.2 (d-f), where the wrinkled or crumpled structure of graphene nanosheets can be observed. In MWCNT/GNP-S750 hybrid (Figure 4.2 (f)), MWCNTs interconnected adjacent graphene to form a 3D hybrid network structure, which inhibited the aggregation of graphene and CNTs. Thus, the hybrid MWCNT/GNP-S750 combination is anticipated to provide an outstanding improvement in the mechanical and thermal properties of nanocomposites (Ma, Wang, & Dai, 2017; Amir Navidfar & Trabzon, 2019; Pradhan & Srivastava, 2014).

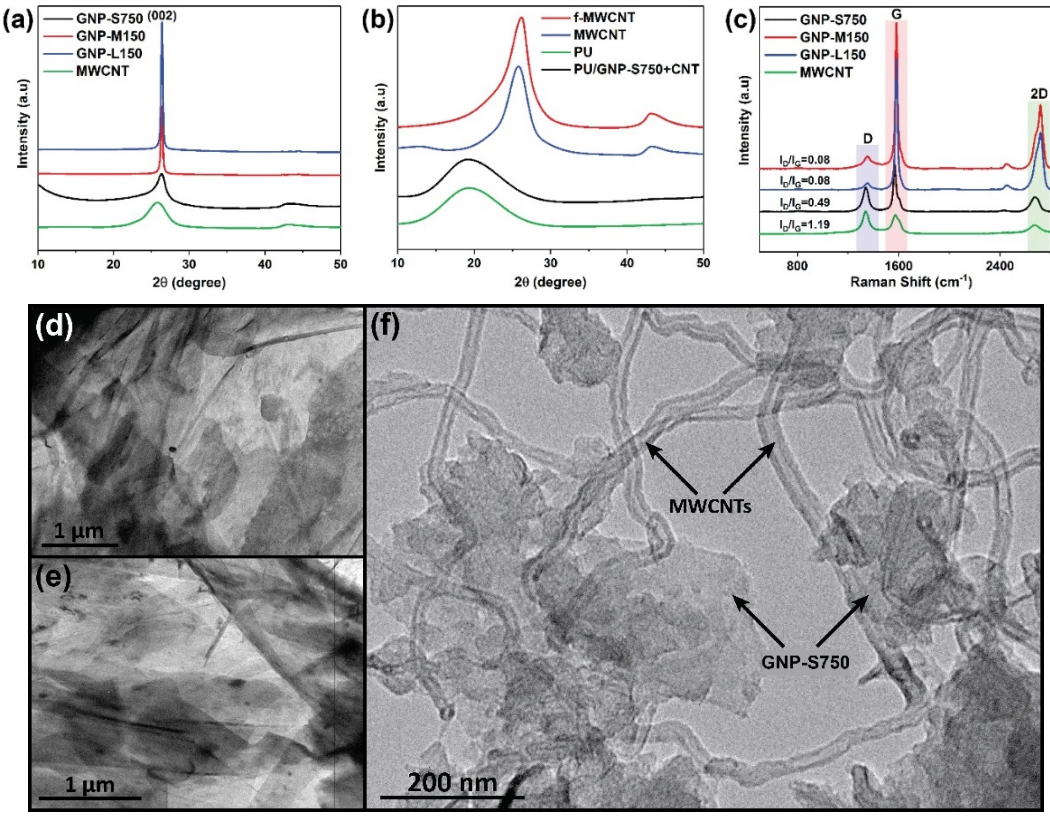

Figure 4.2 : (a) and (b) XRD patterns and (c) Raman spectra of carbon nanofillers and TEM images of (d) GNP-L150, (e) GNP-M150 and (f) GNP-S750/MWCNTs hybrids (an efficient 3D conductive network).

Samples cross-sections were cryogenically fractured and coated with gold to observe the surface of nanocomposites. Figure 4.3 demonstrates SEM images of PU

nanocomposites with different carbon nanofillers, as well as hybrid GNP-S750/MWCNTs inclusion at low content of 0.25 wt%. Several aggregations are evident in PU/MWCNTs (Ayub Karimzad Ghavidel et al., 2015; Ayob Karimzad Ghavidel et al., 2015; Amir Navidfar et al., 2016a; Amir Navidfar et al., 2018), while a better nanofiller distribution in hybrid GNP-S750 and MWCNTs nanocomposites is obvious, according to Figure 4.3 (e). 1D MWCNTs interconnected to the 2D graphene surface, which formed a 3D structure and hindered agglomerations (C. Huang et al., 2018; J. Wang et al., 2017). This 3D architecture improves the contact surface areas among MWCNTs/GNP-S750 structures and the polymer matrix that is promising for heat transferring. The folded shape of GNP-L150 with a larger flake size is clear in Figure 4.3 (b), which weakens the thermal conductivity of GNP-L150 in the polymer matrix.

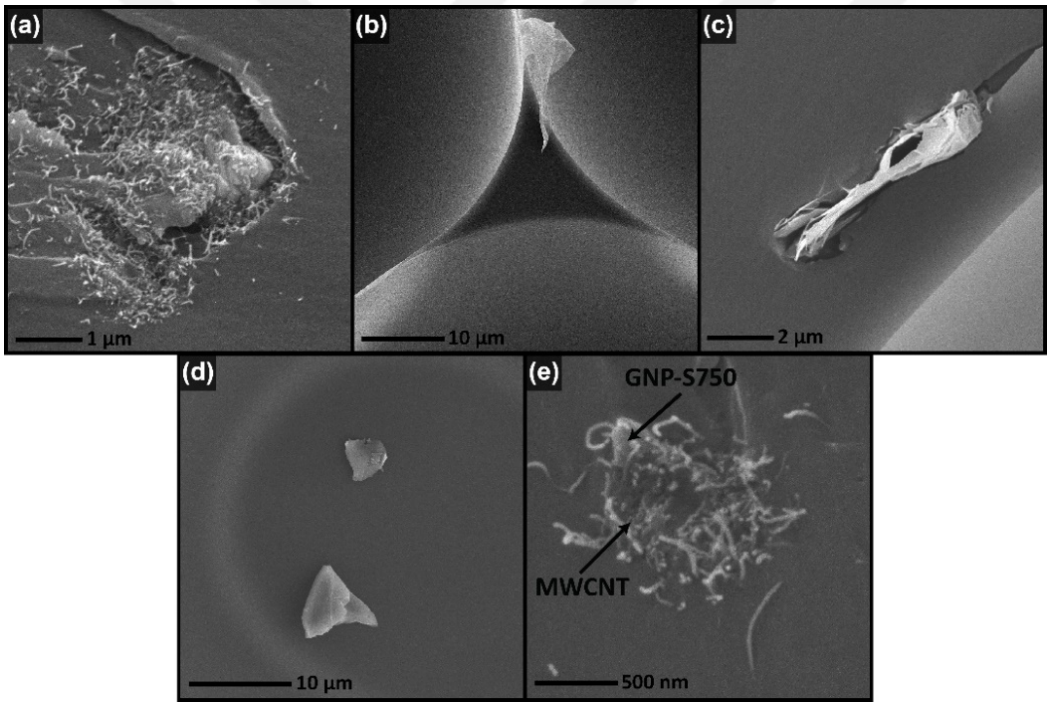

Figure 4.3 : SEM images of (a) PU/MWCNT, (b) PU/GNP-L150, (c) PU/GNP-M150, (d) PU/GNP-S750 and (e) PU with GNP-S750 and MWCNT (1:1) at 0.25 wt%.

The properties of PU foams depend on their microstructure, morphology, cell size and thickness of microcellular walls. Figure 4.4(a-e) exhibits foam microcellular structures of PU and their nanocomposites perpendicular to the foaming direction. The nanofillers decrease the average cell size of PU due to their nucleation effect and higher viscosity in fabrication, which affects the final characteristics of nanocomposites (Amir Navidfar et al., 2018).

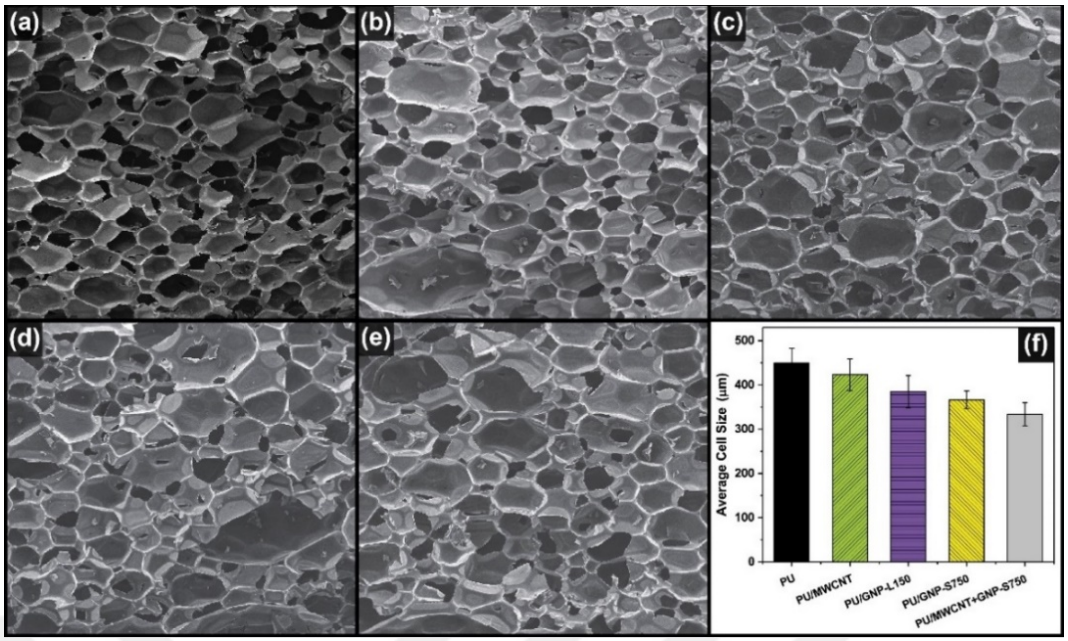

Figure 4.4 : SEM images of (a) PU, (b) PU/MWCNT, (c) PU/GNP-L150, (d) PU/GNP-S750, (e) PU with GNP-S750 + MWCNT (1:1) at 0.25 wt% and (f) average cell size of PU foams.

The PU including hybrid MWCNT/GNP-S750 demonstrates the lowest cell size that confirms their better distribution into the polymer matrix (Figure 4.4(f)). The closed-cell structure of neat PU is more uniform than nanofillers included PU so that carbon nanotubes and graphene damaged PU cell structure and enhance open-cell content (J.-M. Kim et al., 2018).

4.4.2 Thermal Conductivity

Three types of graphene and MWCNTs in various nanofiller contents up to 0.75 wt% were used to explore the effects of carbon nanofillers with different dimensions and properties on the thermal conductivity of PU. Comparative thermal conductivity results of PU with nanofillers are illustrated in Figure 4.5 (a). Pure PU has an extremely low thermal conductivity of 0.02617 W/mK. All PU nanocomposites show gradually enhanced thermal conductivity with increasing nanofiller loading. The highest thermal conductivity value was measured at 0.279 W/mK for 0.75 wt% of PU/GNP-S750 with a 6.6% improvement as compared to PU. The considerable improvement in thermal conductivity of PU/GNP-S750 at higher content (0.75 wt%) reflects the well-dispersed GNP-S750 in the PU matrix, due to their higher specific surface area and smaller flake size (Amir Navidfar & Trabzon, 2019). A uniform nanofiller dispersion is vital for enhancing the thermal conductivity of nanocomposites because a homogeneous

nanofiller network hinders high graphene-PU interface resistance and promotes phonon transport (S.-Y. Yang et al., 2010). Higher surface area causes improved heat transfer and minus thermal resistance (H. S. Kim, Bae, Yu, & Kim, 2016).

Although graphene with a higher aspect ratio showed better thermal conductivity in the polymer matrix, the higher waviness of graphene with a larger aspect ratio limited their conductive properties (Chatterjee et al., 2012; Chu, Li, & Dong, 2013; H. S. Kim et al., 2016). Thus, wrinkled graphene would increase the interfacial bonding and decreased the effectiveness of graphene as thermal conductors in the polymer matrix (Chu, Li, & Dong, 2013). Therefore a balance between nanofiller dimensions and the dispersion rate is essential in thermal conductivity. In addition, Deng et al. (Deng et al., 2007) declared that the enhancement trend of TC with an increasing aspect ratio tends to be saturated for higher than 500 using an analytical model. As a result, at low nanofiller loadings (<1 wt%), there is no major difference between carbon nanofillers in the thermal conductivity of PU nanocomposite (Zakaria et al., 2017), according to Figure 4.5 (a).

Three types of graphene were used to study the influence of graphene dimensions, specific surface area and their defects on the thermal conductivity of hybrid PU nanocomposites. Figure 4.5 (b) illustrates a comparative outcome of graphene on the thermal conductivity of hybrid nanocomposites at a constant nanofiller loading of 0.25 wt%. The thermal conductivity of the nanocomposite with hybrid MWCNT/GNP-S750 nanofiller is dramatically enhanced in a synergistic manner compared to other nanocomposites.

The thermal conductivity of nanocomposites with hybrid MWCNT/GNP-S750 is enhanced synergically up to 5% relative to that of PU, whereas PU/GNP-S750 and PU/MWCNT nanocomposites show 2.44% and 2.66% thermal conductivity improvement, respectively. It is clear that graphene with a higher SSA and more defects has a higher ability to form a more efficient 3D thermally conductive network with MWCNTs and can form a path for heat flowing (Amir Navidfar, Baytak, Bulut, & Trabzon, 2020; Amir Navidfar & Trabzon, 2019).

As an interesting outcome, the thermal conductivity of MWCNTs/GNP-S750 (1:1) hybrid nanocomposite with a synergistic effect at 0.25 wt% is approximately equal to the thermal conductivity of individual graphene and MWCNTs at 0.75 wt% (Figure

4.5 (a) and (b)). Therefore, we can conclude that hybrid nanocomposites fabrication improves processability and reduces the viscosity and the cost of nanocomposites through declining required nanofillers concentration.

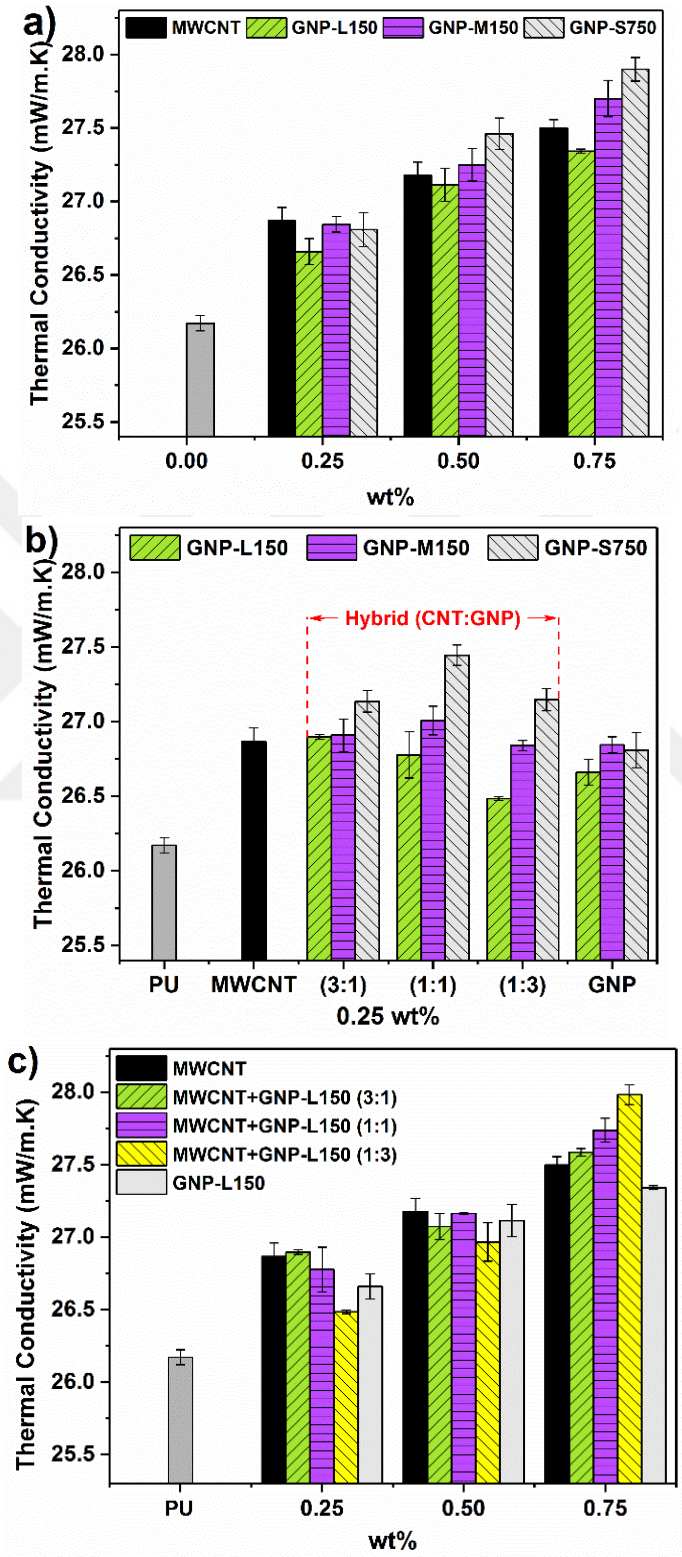

Figure 4.5 : The thermal conductivity of PU with (a) single nanofillers, (b) and (c) hybrid nanofillers.

On the other hand, GNP-L150 was used to prepare hybrid nanocomposites with MWCNT in higher contents and varied ratios to study the synergistic effects of both nanofillers. The thermal conductivity of PU with MWCNT and GNP-L150 with constant loadings (0.25, 0.5 and 0.75 wt%) are shown in Figure 4.5 (c). A synergistic effect is not seen at 0.25 wt% and 0.5wt% nanofiller contents, whereas the synergy is obtained at 0.75 wt%. The CNTs in hybrid nanofillers act as interconnectors among graphene and provide further channels for the heat flowing due to their high aspect ratio. The gap among graphene is higher in lower nanofiller loadings and consequently, CNTs cannot interconnect adjacent graphene. Our previous work showed that the synergistic effect in hybrid nanocomposites with larger graphene can be obtained using CNTs with a higher length and/or enhancing the content and ratio of graphene (Amir Navidfar & Trabzon, 2019).

4.4.3 Analytical Modeling

4.4.3.1 Single Nanofillers

To profoundly understand the thermal conductivity behavior of nanocomposites, a theoretical analysis was considered. Some factors limit the thermal conductivity of nanocomposites. The nanofiller-matrix interface resistance (R_K) has a negative influence on thermal conductivity of the nanocomposites, which ETC of CNTs and graphene is given by (Nan, Liu, Lin, & Li, 2004):

$$K_{CNT}^{eff} = \frac{K_{CNT}}{\frac{2R_K K_{CNT}}{L_{CNT}} + 1}, \qquad K_{GNP}^{eff} = \frac{K_{GNP}}{\frac{2R_K K_{GNP}}{L_{GNP}} + 1} \tag{4.1}$$

Where L_{GNP} and L_{CNT} are the width and length of the graphene and MWCNTs, respectively and *eff* express ETC. The interfacial thermal resistance, R_K, is taken as 8 x 10^{-8} m^2 K/W for both MWCNTs and graphene in this work (Deng et al., 2007; Nan et al., 2004). Microscopic analysis reveals that graphene and CNTs in nanocomposites are frequently far from straightness owing to their large aspect ratios. The CNTs are usually crooked and graphene are commonly wrinkled and folded in the matrix, which leads to a reduction in the ETC of nanocomposites (Chu, Li, & Dong, 2013; Chu, Li, & Tang, 2013; Deng et al., 2007). The straightness factor is presented as:

$$\eta = \frac{L^e}{L} = \frac{K^e}{K} \tag{4.2}$$

Where L and L^e are the original length and equivalent length of graphene or carbon nanotubes, respectively. K and K^e are the intrinsic and equivalent TC of graphene or CNTs, respectively. Chu et al. (Chu, Li, & Dong, 2013) developed an analytical model for ETC of graphene nanocomposites using an effective medium theory of Nan et al. (Nan et al., 2004). On the other side, a simple model for TC enhancement of CNT-based nanocomposites was presented by Deng et al. (Deng et al., 2007). Moreover, the waviness of incorporated CNTs and graphene is found to be a significant factor in the thermal conductivity (F. Wang et al., 2015) and thus straightness ratio (η) are added to formulas in this work, as follow:

$$\frac{K_e}{K_m} = 1 + \frac{1}{3}\frac{\eta f_{CNT}}{H(\eta p) + K_m/\eta K_{CNT}^{eff}} \tag{4.3}$$

$$\frac{K_e}{K_m} = 1 + \frac{2}{3}\frac{\eta f_{GNP}}{H(\eta p) + (\eta^2 K_{GNP}^{eff}/K_m - 1)^{-1}} \tag{4.4}$$

H(p) is a function of nanofillers aspect ratio (p) that is negligible due to the high aspect ratio of the nanofillers and can be ignored (Deng et al., 2007). To predict nonlinear thermal conductivity enhancement of the nanocomposites, a simple percolation model can be applied, which is described as $K_e \sim (f - f_p)^{\alpha}$. f_p indicates the critical volume fraction for the nonlinear conductivity variation, and α is a critical conductivity exponent, which depends on the contact among nanofillers and/or their intrinsic conductivity. It is obvious that the measurements and prediction deviation without considering the percolation effect occurred at very low nanofiller concentrations, implying that f_p may be very low and is estimated f_p=0.0001 (Chu, Li, et al., 2012; He et al., 2018). By incorporating the nonlinear influence of nanofillers, the final K_e of the nanocomposites can be obtained:

$$\frac{K_e}{K_m} = 1 + \frac{1}{3}\frac{\eta (f_{CNT} - 0.0001)^{\alpha}}{K_m/\eta K_{CNT}^{eff}} \tag{4.5}$$

$$\frac{K_e}{K_m} = 1 + \frac{2}{3}\frac{\eta (f_{GNP} - 0.0001)^{\alpha}}{(\eta^2 K_{GNP}^{eff}/K_m - 1)^{-1}} \tag{4.6}$$

Equations (5) and (6) present the thermal conductivity of the nanocomposites as a function of aspect ratio, nanofiller content, anisotropy, interfacial thermal resistance, straightness factor and interaction among nanofillers. Thermal conductivity of pure PU

measured K_m= 0.02617 W/mK and thermal conductivity of graphene and MWCNTs regarded as 2000 W/mK (Chu, Li, & Dong, 2013; Deng et al., 2007; Nan et al., 2004). The comparison between experimental measurements and theoretical calculations is shown in Figure 4.6. Our models provide the best fit for experimental data by taking α and η as fitting parameters for various nanocomposites with nonlinear TC behavior (Table 4.4). The predicted values of K_e using equations (3) and (4) versus weight fraction of nanofillers are plotted in Figure 4.6, as well as the nonlinear prediction by equations (5) and (6). As shown in Table 4.4, the amount of R-square is higher for equations (5) and (6) using the percolation effect, compared to equations (3) and (4). The results clearly show that larger graphene tends to be wavier in the polymer matrix so that the calculated straightness factor (η) is reduced by enhancing the flake size of graphene, as presented in Figure 4.6. The waviness factor (η) is equal to 0.15, 0.27 and 0.42 for PU nanocomposites with GNP-L150, GNP-M150 and GNP-S750, respectively. As a result, the straightness ratio has a dominant effect on the TC of graphene-based nanocomposites (J. Yu et al., 2016).

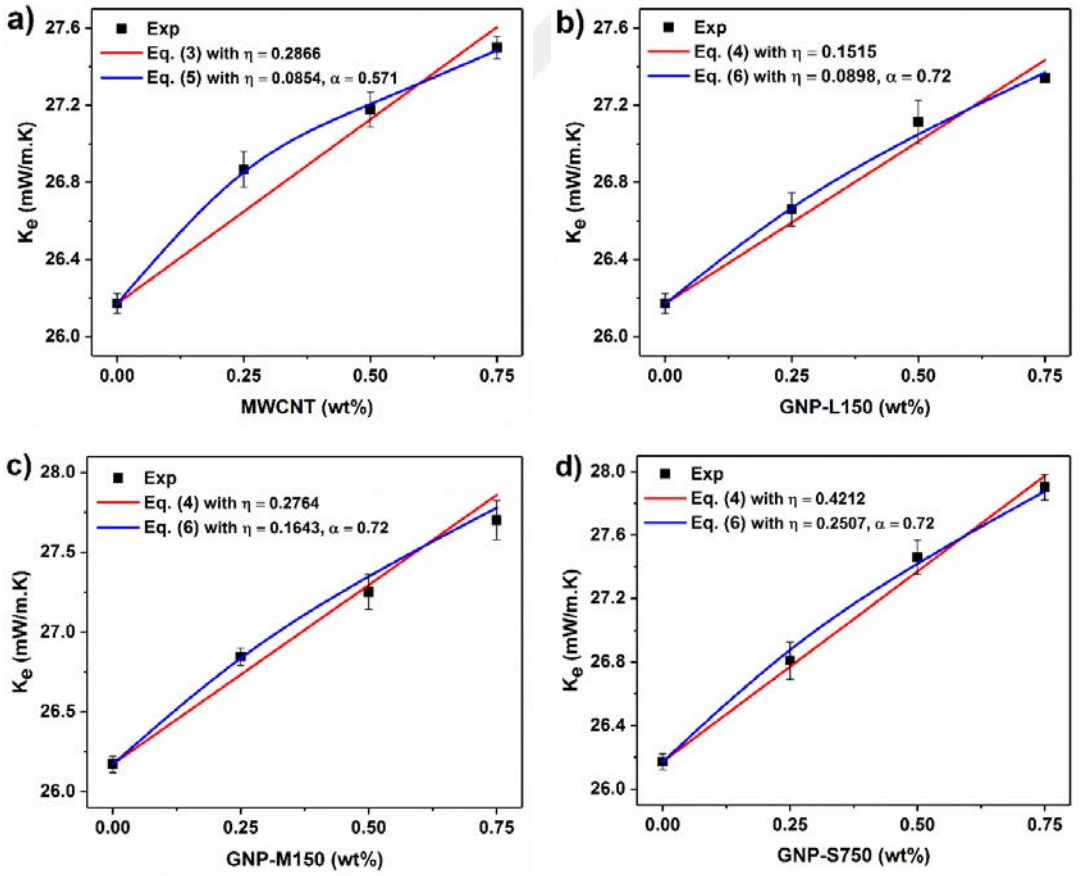

Figure 4.6 : Measured and theoretical modeling of (a) PU/MWCNT, (b) PU/GNP-L150, (c) PU/GNP-M150 and (d) PU/GNP-S750 nanocomposites.

Table 4.4 : Fitting parameters of the analytical models.

Carbon Nanofillers	η	α	R^2 (%)	Equations
MWCNT	0.2866	-	84	(3)
	0.0854	0.571	99.7	(5)
GNP-L150	0.1515	-	93.8	(4)
	0.0898	0.72	98.3	(6)
GNP-M150	0.2764	-	87.1	(4)
	0.1643	0.72	97.5	(6)
GNP-S750	0.4212	-	98.3	(4)
	0.2507	0.72	98.6	(6)
MWCNT / GNP-S750 [8]	0.34	0.89	100	(7)
MWCNT + GNP-S750 [9]	0.34	0.75	99.9	(7)
MWCNT / GNP-L150 [5]	0.27	1.22	100	(7)
MWCNT + GNP-L150 [6]	0.27	1.33	99.2	(7)

4.4.3.2 Hybrid Nanofillers

To well describe the synergistic effect on the thermal conductivity enhancement of PU with hybrid GNPs/CNTs, the experimental data are compared with the theoretical values. Chu et al. (Chu, Li, et al., 2012) proposed a theoretical model to describe the synergistic effect in thermal conductivity improvement of hybrid nanocomposites that are used to predict TC of hybrid GNPs/CNTs based PU nanocomposites in this work. As described before, the straightness factor of nanofillers, η, has a significant influence on the thermal conductivity of nanocomposites, which is added to the formula, as follow:

$$\frac{K_e}{K_m} = \frac{1 + \eta^2 f_c (K_{CNT}^{eff}/K_m)/3 + 2\eta^3 (f_g - 0.0001)^a (K_{GNP}^{eff}/K_m)/3}{1 - (2f_{CNT} + f_{GNP})/3} \qquad (4.7)$$

It is noted that carbon nanotubes and graphene are supposed to have the same η and R_K. The theoretical model by equation (7) as a function of GNPs/CNTs ratios is shown in Figure 4.7, in which the experimental results are significantly matched with predicted data. The thermal conductivity of PU with hybrid GNP-S750/MWCNTs is synergically higher than those of PU with single GNP-S750 or MWCNTs at 0.25 wt%, whereas the synergy is obtained at 0.75 wt% for MWCNT/GNP-L150. The bridging interaction of graphene and CNTs could lead to the development of a 3D thermally conductive structure that efficiently transfers the heat flow and inhibits the aggregations, as shown in Figure 4.3 (f). The factor α represents the nanofillers

[8] Individual nanofillers
[9] Hybrid nanofillers

dispersion in the polymer matrix, whereas the higher α value reflects the poor dispersion of nanofillers in the polymer matrix (J. Huang, Gao, Pan, Zhang, & Lin, 2014). It is determined that the fitting parameters of α=0.75 and η=0.34 for hybrid GNP-S750/MWCNTs nanocomposites at f_{GNP} < 0.125 wt% and α=0.89 and η=0.34 for PU with individual GNP-S750 and MWCNTs yields a good agreement with the experiments (Table 4.4 and Figure 4.7). In addition, hybrid GNP-L150/MWCNTs nanocomposites exhibited α=1.22 and η=0.27, whereas for single inclusions α=1.33 and η=0.27 are obtained (Figure 4.7 (b)). The lower value of α for hybrid GNPs/MWCNTs based nanocomposites proves the better dispersion in the PU matrix, which would contribute to thermal conductivity enhancement by forming a conductive 3D structure. On the other hand, the higher ratios of graphene in hybrid systems weaken the TC of nanocomposites. Excess loading of graphene leads to the shortage of MWCNTs that cannot effectively bridge the adjacent graphene and thus results in the breakdown of the 3D conductive network. Consequently, the remarkable synergistic effect that exhibits the best performance can be reached in an optimum ratio of GNPs/CNTs hybrids.

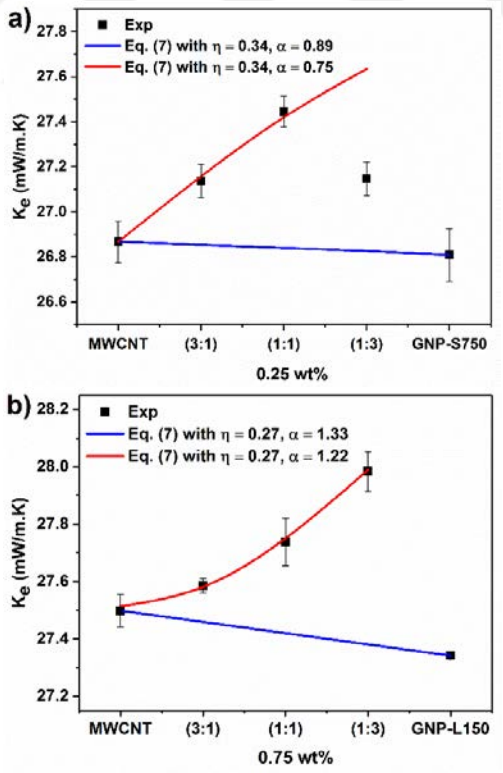

Figure 4.7 : Model predictions (equation 7) for the effective thermal conductivity (K_e) of hybrid (a) GNP-S750/MWCNTs (at 0.25 wt%) and (b) GNP-L150/MWCNTs (at 0.75 wt%) based PU nanocomposites compared with the experimental data.

4.5 Conclusion

The thermal conductivity of PU nanocomposites comprising MWCNTs and three types of graphene was studied by experimental and theoretical approaches. By combining carbon nanotubes and graphene a synergistic thermal conductivity improvement was achieved, which surpasses the performance of individual carbon nanofillers in the PU matrix. The optimization of hybrid nanofillers is essential to maximize the synergistic effect and the thermal conductivity improvement of the nanocomposites. Synergistic thermal conductivity enhancement using MWCNTs and GNP-S750 with a smaller flake size and higher specific surface area was achieved at low nanofillers contents (0.25 wt%) which is vital for reducing the viscosity and improving the processability of the nanocomposites. In addition, the synergism can be seen at higher nanofiller content (0.75 wt%) for GNP-L150 with a larger flake size. The hybrid nanofillers can effectively enhance the thermal conductivity so that 1D MWCNTs interconnected adjacent 2D graphene to form a more efficient 3D thermally conductive network. As an interesting outcome, the thermal conductivity of MWCNTs/GNP-S750 (1:1) hybrid nanocomposite at 0.25 wt% was approximately equivalent to the thermal conductivity of the individual graphene and MWCNTs at 0.75 wt%. Therefore, it can be concluded that the fabrication of hybrid nanocomposites is a cost-effective method with higher processability through declining required nanofillers content. An analytical study on the thermal conductivity of single and hybrid nanocomposites by incorporating the straightness factor and percolation effect as fitting parameters was presented, in which an outstanding agreement between the modified model predictions and experimental results was achieved. The results showed that the straightness of nanofillers profoundly affected the thermal conductivity of nanocomposites and larger graphene tends to be wavier or less straight in the polymer matrix so that the calculated straightness ratio is reduced by enhancing graphene flake size.

5. SYNERGICALLY ENHANCED DYNAMIC MECHANICAL BEHAVIOR OF BINARY NANOCARBON BASED POLYURETHANE HYBRID NANOCOMPOSITE FOAMS

5.1 Abstract

Carbon-nanofillers are known for improving the desired properties of polymers. The dispersion quality of nanofillers in the matrix is vital for the fabrication of high-performance nanocomposites. An effective approach for improving dispersion states of multi-walled carbon nanotubes (MWCNT) and graphene nanoplatelets (GNPs) was employed via hybrid inclusion of the nanofillers in polyurethane matrix to further enhancing viscoelastic properties. Nanocomposites based on MWCNTs, two groups of graphene and hybrid MWCNT/graphene with varied weight fractions and ratios were fabricated via a simple, quick and scalable approach. Dynamic mechanical analysis results indicated an improvement of up to 86% in storage modulus at 25ºC for hybrid MWCNT/GNP-S750 at only 0.25 wt% loading, whereas solely MWCNTs and graphene nanocomposites showed 9% and 15% enhancement at the same content, respectively. The glass transition temperature value was enhanced by about 9.5 ˚C with 0.25 wt% inclusion of well-dispersed three-dimensional MWCNT/GNP-S750 structure, which disclosed a noticeable synergistic effect in thermomechanical properties.

5.2 Introduction

Carbon nanofillers such as multi-walled carbon nanotubes (MWCNTs) and graphene nanoplatelets (GNPs) are one of the most promising nanomaterials. Their extraordinary mechanical strength, thermal and electrical properties make them highly demanding in reinforcing polymeric materials (Benzait & Trabzon, 2018; Ciecierska et al., 2016; Eda et al., 2008; Faraji et al., 2017; Rashahmadi et al., 2017; D. Yuan et al., 2017). However, agglomerations and the restacking tendency of these nanofillers enhanced dispersion difficulty in the polymer matrix (Ayob Karimzad Ghavidel et al.,

2015; Amir Navidfar, 2014; Amir Navidfar et al., 2016a; A Navidfar et al., 2014). Hybridization of the one-dimensional (1D) MWCNTs and two-dimensional (2D) graphene with different geometry can overcome this dispersion challenge. The synergistic effect between CNTs and graphene has been shown to enhance mechanical properties (Bagotia et al., 2019; Chatterjee et al., 2012; Amir Navidfar & Trabzon, 2019), thermal (min Kim et al., 2019; Amir Navidfar & Trabzon, 2020) and electrical conductivity (Ayub Karimzad Ghavidel et al., 2015; Ayub Karimzad Ghavidel et al., 2016; Hongming Zhang et al., 2018). Bagotia et al. (Bagotia et al., 2019) concluded an enhancement in mechanical properties, electrical conductivity and EMI shielding of nanocomposites with graphene/MWCNT hybrid fillers. In the hybrid graphene/CNT, it is believed that 1D CNTs bridge the adjacent graphene to form a three-dimensional (3D) network architecture. In this condition, graphene and CNTs exhibit a stronger synergistic effect in increasing the contact area between nanofillers and polymer matrix (Aghadavoudi et al., 2018; Verma et al., 2017), which formed an effective network to strain transferring (Amir Navidfar et al., 2018).

The energy efficiency requirements increasingly demand lightweight structures such as polyurethane (PU) foams. The simple fabrication of PU structures and composites in a single processing step is the main advantage of PU technology (Kausar, 2018). Due to their low density, PU foams have been used in versatile applications such as insulation, packaging, seating and sound-absorbing materials (Burgaz & Kendirlioglu, 2019; Hoseinabadi et al., 2017). However, PU foams have some disadvantages, such as low mechanical properties and deficient structural stability in high temperatures, which hinder their widespread application in the automobile and aerospace industries (Engels et al., 2013). Hence, graphene (D. Chen & Chen, 2013; Yousefi et al., 2013) and MWCNTs (Amir Navidfar et al., 2016a; Amir Navidfar et al., 2018; Roy, Srivastava, Pionteck, & Mittal, 2015; Yıldırım et al., 2018) have been employed in the development of mechanically enhanced and thermally stable PU nanocomposites(Amirkhosravi, Yue, & Manas-Zloczower, 2020). In our previous work, the tensile strength of PU enhanced synergically up to 43% with the addition of graphene/MWCNT hybrids, while the strength of PU/MWCNTs and PU/graphene improved 19% and 17% at the same content, respectively (Amir Navidfar & Trabzon, 2019). According to the numerous applications of PU, dynamic mechanical analysis (DMA) as a tool in the evaluation of nanocomposite structures is critical. DMA

provides the mechanical properties of viscoelastic materials under periodic loading and thermal changes for a diversity of specimen geometries. It is used to determine a variety of major material parameters containing storage (E') and loss modulus (E''), damping factor (tan δ), glass transition temperatures (T_g), creep compliance and relaxation modulus (Shamsi, Mir Mohamad Sadeghi, & Asghari, 2018). It has been verified to be an effective technique to investigate the relaxations in polymers and thereby materials behavior under several conditions of temperature, stress, nanocomposites structure and their influence in evaluating the mechanical properties. Numerous works have been investigated storage modulus, loss modulus and tan δ at a temperature range for PU nanocomposites (Burgaz & Kendirlioglu, 2019; Pokharel et al., 2015; Roy et al., 2015). However, there are limited studies on the viscoelastic properties of MWCNTs/graphene hybrid nanocomposites with a synergistic effect. Pokharel et al. (Pokharel et al., 2015) studied the DMA behavior of graphene, graphene oxide (GO) and functionalized graphene sheet (FGS) reinforced PU nanocomposites at 2 wt% concentration. Their results showed superior thermomechanical properties of FGS/PU than other nanofillers incorporation in PU, due to improved interface in FGS/PU nanocomposite. Roy et al. (Roy et al., 2015) fabricated thermoplastic PU via solution mixing method with chemically reduced GO and MWCNT hybrids, which the storage modulus at the glassy region enhanced by 51% at 0.25 wt% loadings. Wang et al (E. Wang et al., 2019) indicated an outstanding dynamic mechanical properties enhancement in waterborne epoxy via introducing graphene oxide/carbon nanotube hybrid nanofillers. Nevertheless, their works were focused on single nanofillers inclusion or limited study of hybrid nanofillers on bulk polymeric matrices instead of cellular PU foams.

The present study focused on the viscoelastic behavior of PU foam nanocomposites reinforced with graphene/MWCNTs hybrid nanofillers. Commercially available MWCNTs and GNPs with different dimensions and specific surface areas were used to investigate the synergistic effect of carbon nanofillers on the thermomechanical properties of PU. Varied nanofiller ratios and concentrations were studied to find the highest synergy, in which 86% improvement in storage modulus is achieved at 0.25 wt%, relative to pure PU. This work also reveals the capability to reach these significant results in very low loadings of low-cost commercially available GNPs and

CNTs. Successful dispersing of these hybrid carbon nanofillers in the polymeric matrix can pave the way toward low-cost and efficient composite fabrication.

5.3 Materials and Experimental Study

5.3.1 Materials

For the fabrication of polyurethane foams, the polyol and isocyanate with a weight ratio of 1:1.25, as suggested by the manufacturer were mixed. The density and viscosity of the polyol (at 25°C) are 1.11 g/cm^3 and 600 ± 200 MPa.s, respectively. The hydroxyl number of the polyol is 300 mg KOH/g. The density and viscosity of isocyanate (at 25°C) are 1.23 g/cm^3 and 210 MPa.s, respectively. The NCO content of isocyanate is about %30.8 - %32. Carbon nanofillers were purchased from Nanografi Co.Ltd, which the properties and geometries of used MWCNTs and graphene are tabulated in Table 5.1. MWCNTs (purity ≥ 92%) were grown by CVD.

Table 5.1 : Properties and geometry of nanofillers.

Nanofillers	Diameter (nm)	Thickness/Length (nm)	Specific Surface Area (m^2/g)
MWCNT	8-10	L =1000-3000	290
GNP-L150	24000 (Large)	t = 6	150
GNP-S750	1500 (Small)	t = 3	750

5.3.2 Fabrication of Nanocomposites

MWCNTs were functionalized with hydrogen peroxide (H_2O_2) before the fabrication of PU foams (Amir Navidfar et al., 2018; Amir Navidfar & Trabzon, 2019, 2020). Different contents (0.25, 0.50 and 0.75 wt%) and ratios (3:1, 1:1 and 1:3) of MWCNTs and graphene were first mixed with polyol at 200-2000 rpm for 5 min using overhead stirrer equipment. Polyol and carbon nanofiller combinations were ultrasonically dispersed for 5 min using an ultrasonic bath and then stirred at 2000 rpm for 5 min. The isocyanate was finally added to the mixture, which was stirred for 20 s and then expanded in a two-part wooden mold to form free-rise PU foam. Cured nanocomposites were cut with a thickness of 10 mm using a lathe machine.

5.3.3 Characterization

DMA technique was used to measure the viscoelastic properties of fabricated nanocomposites using TA Instruments Q800 DMA at a loading frequency of 1 Hz

from 25 °C to 180 °C with a heating rate of 3 °C/min in single cantilever mode. A desktop CNC machine was used to prepare desired DMA specimens with a size of 25 mm x 15 mm x 2 mm. The glass transition temperatures (T_g) of the samples were also obtained by DMA tests. To examine the repeatability of the DMA results, three specimens were prepared and tested for each type of nanocomposite. Thermogravimetric analysis (TGA) was carried out under a nitrogen atmosphere on a Q600, TA Instruments with a heating rate of 5 °C/min. Transmission electron microscopy (TEM) images of carbon nanofillers and their hybrids were taken using a Hitachi HighTech HT7700 with an acceleration voltage of 120 keV. Besides, scanning electron microscopy (SEM) experiments of fabricated PU nanocomposites were done by an FEI - NOVA NanoSEM 450.

5.4 Results and Discussions

5.4.1 Material characterization of carbon nanofillers and their nanocomposites

Several techniques such as Raman Spectroscopy, TGA, SEM and TEM were utilized for the characterization of MWCNTs, graphene and their nanocomposites. The decomposition behavior of fabricated nanocomposites was investigated using thermogravimetric analysis. TGA and derivative thermogravimetric (DTG) curves, as well as degradation temperature at 50% weight losses and charred residue of the nanocomposites, are illustrated in Figure 5.1 (a-d). All nanocomposites at 0.25 wt% except PU/MWCNT exhibited higher thermal stability, relative to neat PU. The decomposition temperature of hybrid MWCNT/GNP-S750 nanocomposite enhanced due to nanofillers synergistic effect. However, the enhancement in decomposition temperature was higher for the nanocomposite with solely GNP-S750, compared to hybrid MWCNT/GNP-S750 (Figure 5.1 (a) inset), which is attributed to the higher thermal conductivity of hybrid MWCNT/GNP-S750 in the PU matrix, in comparison with PU/GNP-S750. Hybrid MWCNT/GNP-S750 nanocomposite lost weight at lower temperatures compared to PU/GNP-S750, owing to higher heat flow throughout the specimen. This means that thermal conductivity enhancement dominated improved nanofillers dispersion in hybrid nanocomposites (S. Kumar et al., 2010). Figure 5.1 (c) exhibited that the thermal stability of PU improved by 3 ˚C, 7.3 ˚C and 14.5 ˚C with MWCNT/GNP-S750, GNP-L150 and GNP-S750 nanofillers at 50% weight loss, respectively. It is also noted that charred residue of PU at 600 ˚C improved, especially

in GNP-S750 included nanocomposites, as shown in Figure 5.1(d). This may be due to the homogeneous distribution of GNP-S750, as well as their strong interaction with the polymer matrix caused by their higher specific surface area (Prolongo, Jiménez-Suárez, Moriche, & Urena, 2014; Roy et al., 2015; Zixin Wang, 2018). According to Figure 5.1(d), among all nanocomposites, PU/GNP-S750 showed the highest residue of 24.4 wt% at 600 ˚C. It is reported that graphene revealed a notable barrier effect to delay the thermal degradation of nanocomposites by means of hindering the exit of volatile products during the degradation (Bagotia & Sharma, 2019; Bisht, Dasgupta, & Lahiri, 2018).

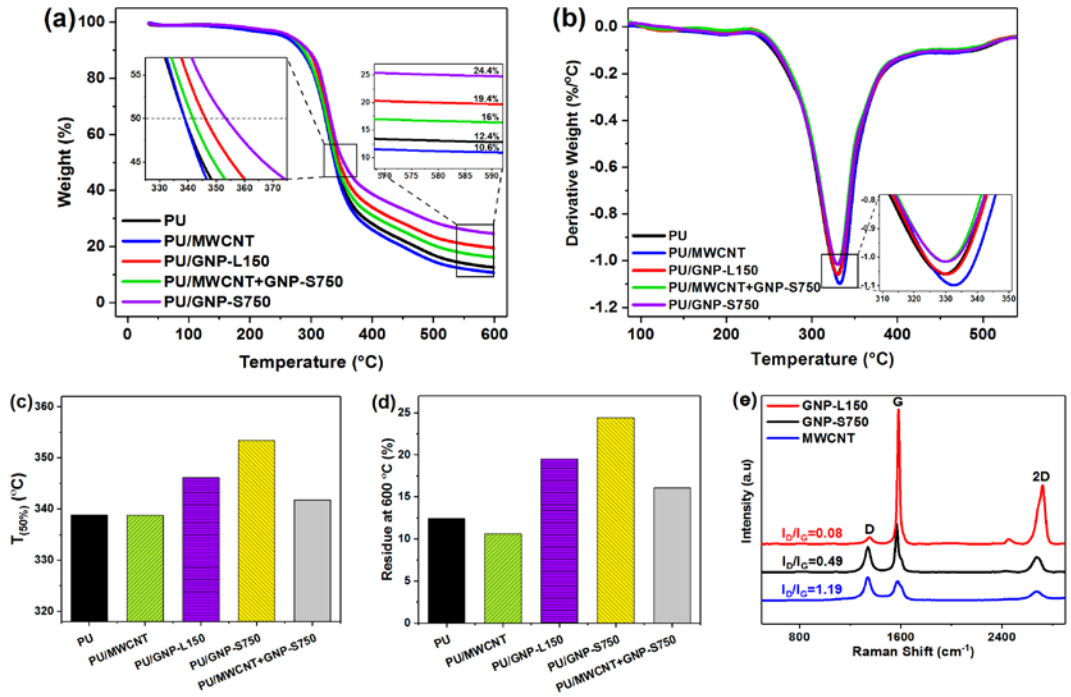

Figure 5.1 : (a) TGA curves, (b) DTG curves, (c) temperature at 50% weight loss, (d) residue at 600 ˚C of nanocomposites and (e) Raman spectra of carbon nanofillers.

The derivative thermograms (Figure 5.1(b)) indicates that the maximum decomposition rate is higher for PU/MWCNT. However, the peak intensity decline in other nanocomposites, especially in GNP-S750 and MWCNTs+GNP-S750 based nanocomposites. Raman spectra are commonly used to characterize quality, crystal structure, disorder and defects of carbon-based materials such as CNT and graphene quickly and non-destructively. Figure 5.1(e) exhibited D-bands, G-bands and 2D-bands of the carbon nanofillers, which are relevant to their defects and carbon networks (Y. Gao et al., 2017). The I_D/I_G ratio of GNP-S750 (I_D/I_G = 0.49) indicated a higher

value than those of GNP-L150 (I_D/I_G = 0.08), demonstrating extra defects and porous graphene. The lower flakes dimension and more functional groups on the surface and edge of GNP-S750 enhanced the disorder degree (Zixin Wang, 2018). Also, the D-band to G-band intensity ratio of MWCNTs (I_D/I_G = 1.19) was higher than those of graphene, which was ascribed to sp^3 defects and twist network of carbon nanotubes (Kausar, Anwar, & Muhammad, 2016).

5.4.2 Morphological Characterization

The TEM micrographs of the graphene and MWCNTs (Figure 5.2 (a-c)) displayed wrinkled and crumpled structures of graphene nanosheets, as well as randomly organized and aggregated MWCNTs due to inter-molecular Van der Waals interaction, which were entangled. Figure 5.2 (d-g) exhibits SEM images of PU with various carbon nanofillers, as well as GNP-S750/MWCNTs hybrids at 0.25 wt%. Several agglomerations are apparent in PU/MWCNTs, while a well-dispersed hybrid MWCNTs/GNP-S750 nanocomposite is obvious, according to Figure 5.2 (g). 1D MWCNTs connected to the 2D graphene surface and formed a 3D architecture, which hindered agglomerations (Johnson, Dobson, & Coleman, 2015). This 3D structure expands the contact surface areas among MWCNTs/GNP-S750 nanofillers and the PU matrix that is favorable in stress transferring.

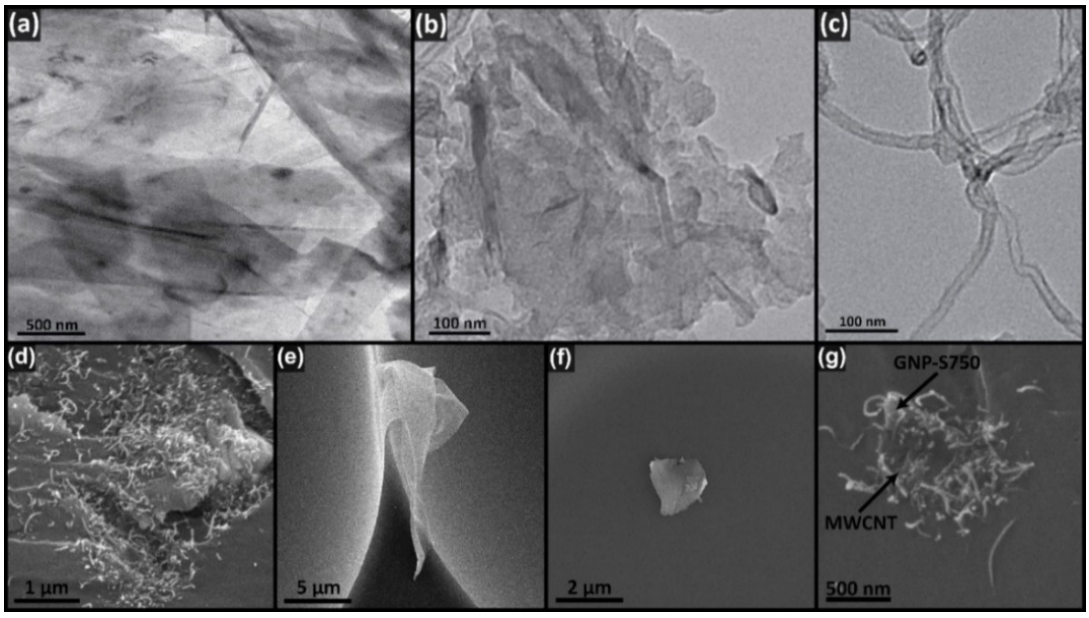

Figure 5.2 : TEM images of (a) GNP-L150, (b) GNP-S750, (c) MWCNTs and SEM of (d) PU/MWCNTs, (e) PU/GNP-L150, (f) PU/GNP-S750 and (g) PU/MWCNT+GNP-S750 nanocomposites.

5.4.3 Viscoelastic properties

5.4.3.1 Storage modulus

DMA measurements reveal the viscoelastic properties of the nanocomposites. Figure 5.3 exhibits the variation of dynamic storage modulus (*E′*) of PU with the change of temperature and its nanocomposites including carbon nanofillers, which implies nanocomposites stiffness. The results showed that the storage modulus declined very slowly in the temperature range of 25–100 °C but after 100 °C the storage modulus diminished abruptly due to the transition from a glassy to rubbery state (Burgaz & Kendirlioglu, 2019). The storage modulus improved in the glassy region (about 25 ˚C) with the carbon nanofillers loadings, being higher for the nanocomposites at 0.75 wt% contents owing to the restriction in mobility of polymer chains provided by the nanofillers (Figure 5.3(d)). The resilient properties of MWCNTs and graphene improved the storage modulus by transferring the stress under loading, besides acting as additional physical crosslinks (Araby et al., 2013).

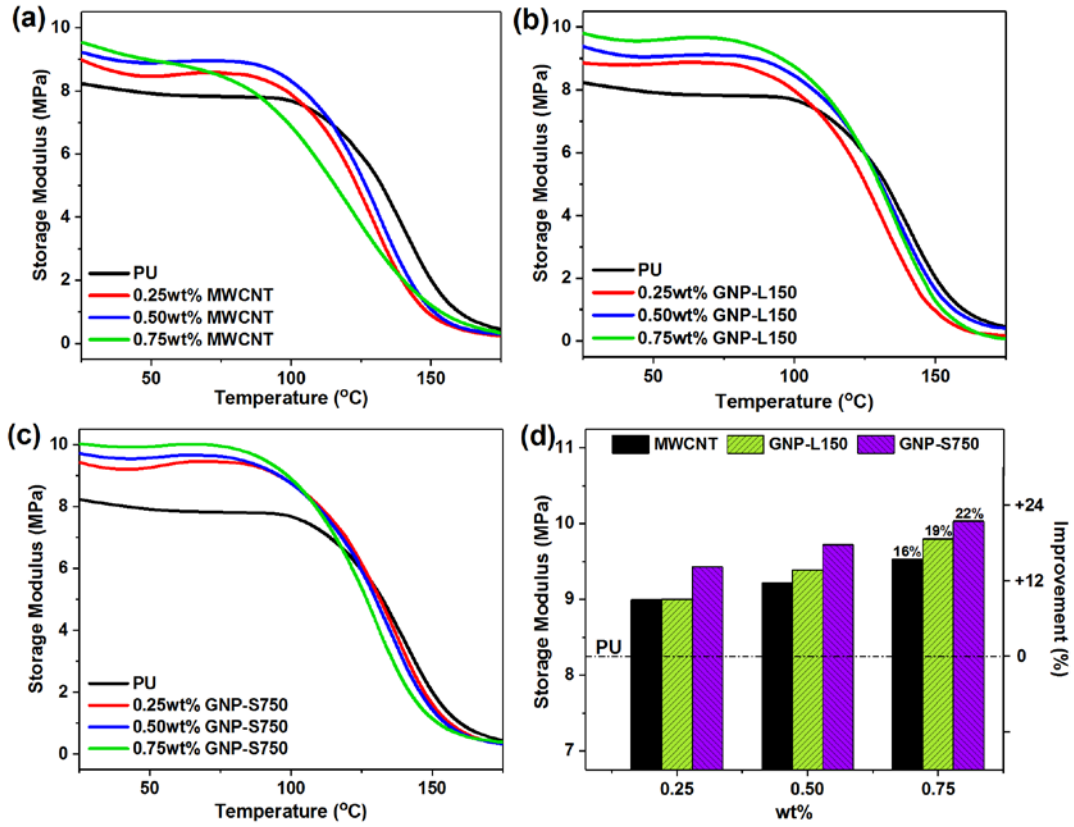

Figure 5.3 : DMA storage modulus versus temperature of (a) MWCNTs, (b) GNP-L150 and (c) GNP-S750 nanocomposites and (d) storage modulus in the glassy region (25˚C).

The storage modulus of polyurethane was improved up to around 16%, 19%, and 22% for MWCNTs, GNP-L150, and GNP-S750 nanocomposites at 0.75 wt%, respectively. Higher modulus improvement in GNP-S750 based nanocomposites is ascribed to the homogeneous distribution of GNP-S750, as well as the strong interaction with the polymer matrix due to their higher specific surface area and lower flake size (Roy et al., 2015; Zixin Wang, 2018). Moreover, GNP-S750 with smaller thickness and diameter could efficiently enter among polymer chains and restrict their mobility, as compared to GNP-L150 (Zixin Wang, 2018).

Figure 5.4(a-d) illustrates DMA storage modulus versus temperature of hybrid nanocomposites in comparison with single MWCNTs and single graphene-based PU. Besides, the storage modulus in the glassy region (25˚C) is summarized in Figure 5.4(e-f). The results revealed that hybrid nanofillers inclusion in PU promoted the storage modulus as a result of their better dispersion into the polymer matrix. It is evident that storage modulus of PU with hybrid MWCNT/GNP-S750 (1:1) dramatically enhanced up to about 86% at 0.25 wt% in the glassy region (25˚C), relative to pure PU (Figure 5.4(a) and (e)), while the moderate improvement of 22% can be seen in MWCNTs/GNP-L150 (1:3) based hybrid nanocomposites at the same content.

According to Figure 5.4(f), maximum improvement of storage modulus using MWCNTs and GNP-L150 hybrids can be obtained about 29% at 0.75 wt%. Consequently, MWCNTs with GNP-S750 showed a remarkable synergistic effect in enhancing the storage modulus of polyurethane at a low nanofillers content of 0.25 wt%. Two-dimensional GNP-S750 with lower flake dimension and higher specific surface area and defects has more ability to be interconnected by one-dimensional MWCNTs to develop a three-dimensional well-dispersed nanofillers network (Charitos et al., 2021; S. Kumar et al., 2010; Amir Navidfar & Trabzon, 2019). This three-dimensional hybrid architecture promoted the interaction of nanofillers with the polyurethane matrix, in which the enhanced contact area facilitated the load transferring through the nanofillers (Amir Navidfar & Trabzon, 2019, 2020; Roy et al., 2015).

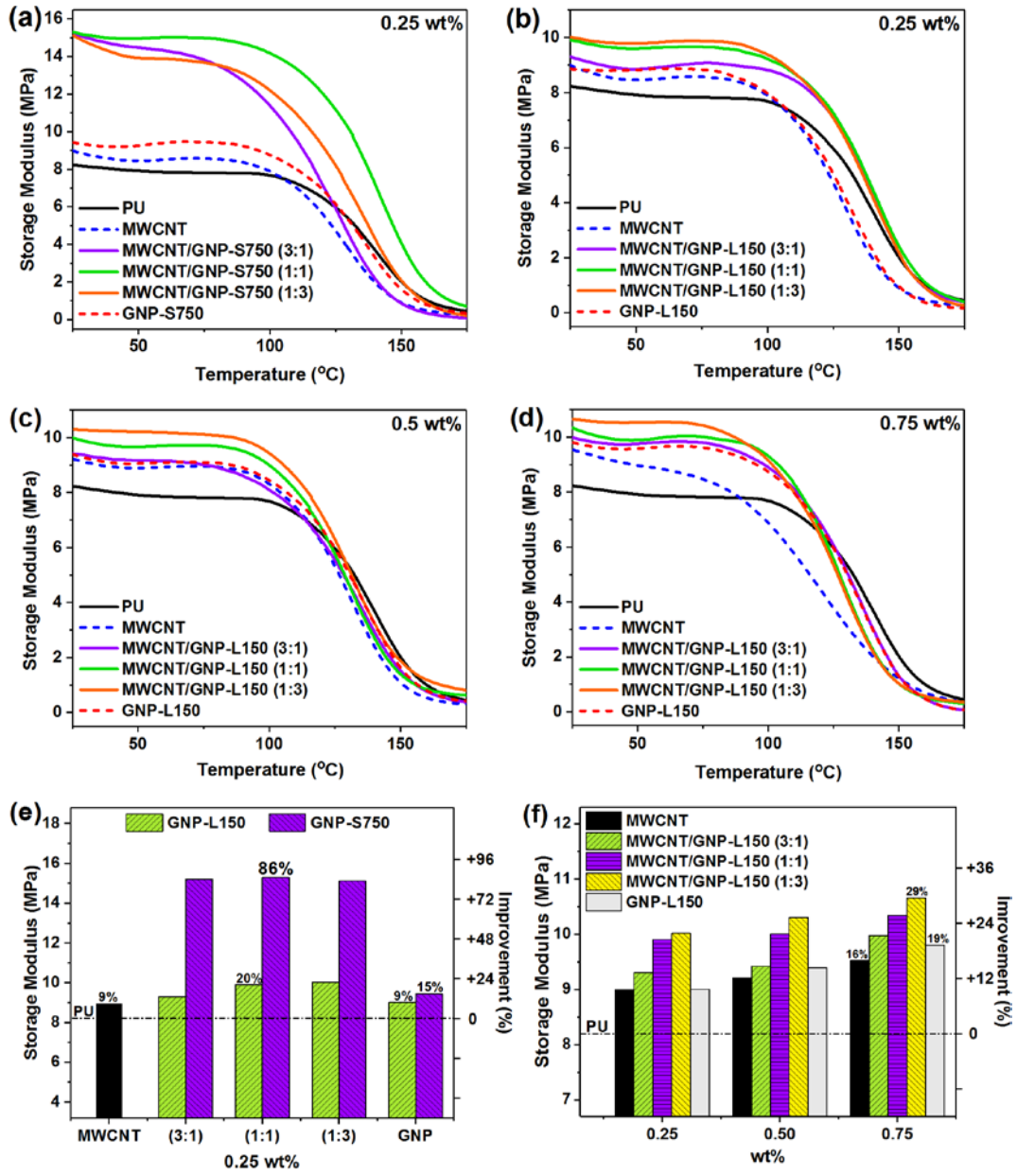

Figure 5.4 : DMA storage modulus of (a-d) hybrid MWCNTs/GNPs nanocomposites versus temperature and (e-f) storage modulus in the glassy region (25˚C).

Excitingly, the TEM image of the hybrid MWCNTs/GNP-S750 in Figure 5.5(d) demonstrates the uniform dispersion of carbon nanotubes on the GNP-S750 surface to connect the adjacent graphenes that made a 3D interconnecting structure. Hence, the hybrid MWCNT/GNP-S750 nanofillers are anticipated to provide an outstanding improvement in the mechanical and thermal properties of nanocomposites (Chong, Hinder, & Taylor, 2016; Moriche et al., 2015). To better understand the mechanism of hybrid nanocomposites in various strain conditions in DMA, a schematic illustration about the change of the 3D interconnecting network of GNP-S750/MWCNTs hybrids

in PU matrix before loading, under loading and in relaxation time is displayed in Figure 5.5 (a-c). In the primary state, well-dispersed nanofillers were formed by the interconnected MWCNTs and graphene. When the graphene/CNTs nanocomposites were stretched to a strain, the distance among nanofillers enhances (red lines), causing the higher modulus. However, the initial nanofillers condition could be found again after the relaxation. Consequently, this 3D interconnected structure caused to enhance the storage modulus of the hybrid nanocomposites under periodic strain.

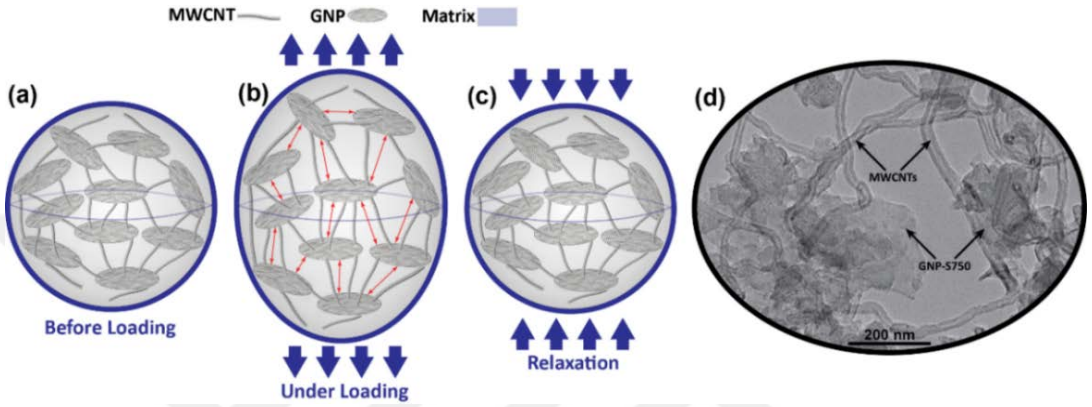

Figure 5.5 : (a-c) Schematic of the change of graphene/MWCNTs hybrid network under different strains and (d) TEM image of hybrid MWCNTs/GNP-S750.

5.4.3.2 Tan δ and glass transition temperature (T_g)

The temperature-dependent tan δ (damping factor) curves of pristine PU and carbon nanofiller-based nanocomposites are displayed in Figure 5.6(a-c), which represents the balance of dissipated energy (viscous behavior) and stored energy (elastic behavior). The temperature value in the peak of tan δ curves suggested the glass transition temperatures (T_g), as summarized in Figure 5.6(d). PU/GNP-S750 nanocomposite at 0.5 wt% showed the highest T_g value (155.5 ˚C) among all nanofillers with 5.8 ˚C enhancement compared to pure PU (149.7 ˚C) due to the better interfacial adhesion of the nanofillers and the polymer matrix (Rasana, Jayanarayanan, Deeraj, & Joseph, 2019). This T_g enhancement can be attributed to the smaller diameter of GNP-S750, which reduced the polymer chains mobility through efficiently entering to polymer chains, as well as better dispersion in PU matrix due to their higher specific surface area (Zixin Wang, 2018). PU with GNP-L150 at 0.25 wt% indicated a 2.1 ˚C shift in T_g value, in comparison with PU, but the amount of T_g declined in higher GNP-L150 loadings owing to their poor dispersion state in higher concentrations (Amir Navidfar et al., 2016a; Amir Navidfar et al., 2018; Amir Navidfar & Trabzon, 2019). The results

also presented reduced T_g with MWCNTs loadings, which is caused by large agglomerations as illustrated in SEM images (Figure 5.2(d)). These agglomerates decreased chain interaction, declined the crosslink density and enhanced free volume in the nanocomposites (Zixin Wang, 2018). As a result, graphene is more efficient than MWCNTs in enhancing the T_g value of PU (Tang et al., 2013).

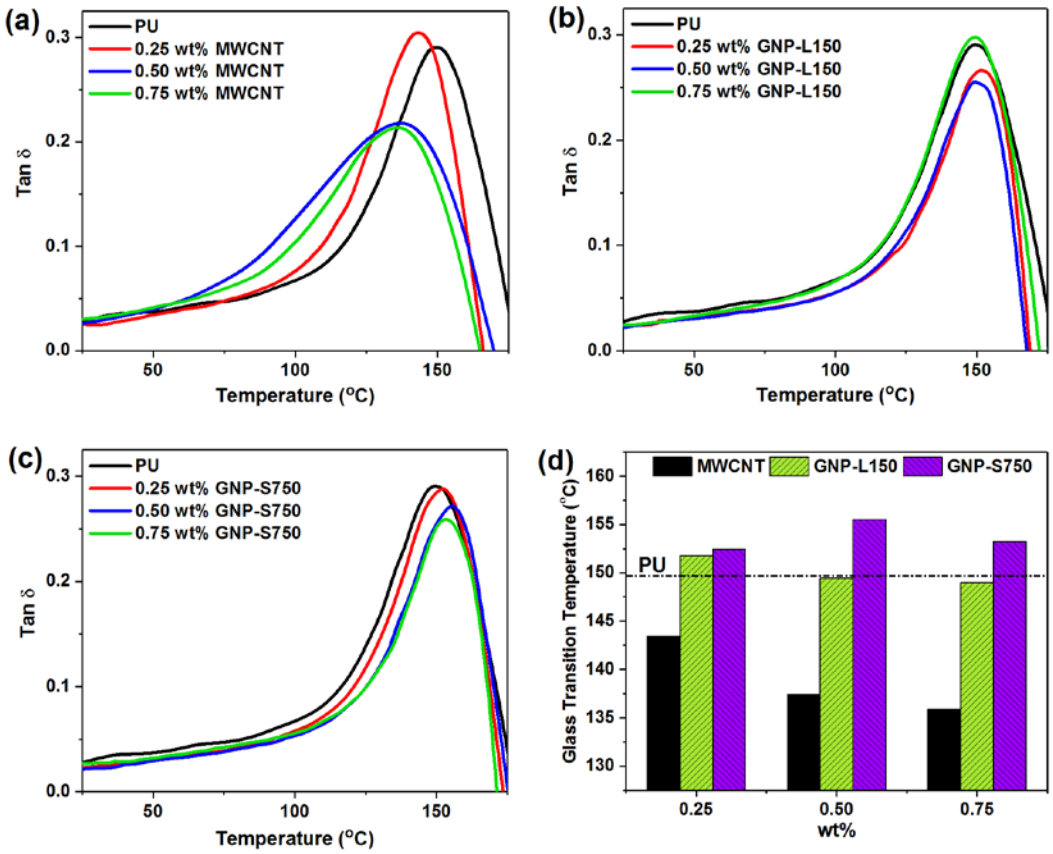

Figure 5.6 : Tan δ versus temperature of (a) MWCNTs, (b) GNP-L150 and (c) GNP-S750 nanocomposites and (d) glass transition temperature of nanocomposites.

Figure 5.7(a-d) illustrates tan δ versus temperature curves of hybrid nanocomposites, in comparison with the single nanofillers included nanocomposites and neat PU, which provides the information regarding the ratio of viscous to elastic properties of nanocomposites. The glass transition temperature of pure PU measured T_g = 149.7 ˚C. The results revealed that T_g values are shifted to higher temperatures in hybrid nanocomposites, which surpassed the T_g of single nanofillers-loaded nanocomposites (Jen & Huang, 2019). The nanocomposites with MWCNTs/GNP-L150 hybrids showed a T_g shift of 5.6 ˚C at 0.25 wt% with an MWCNT: graphene ratio of 1:3. MWCNT/GNP-S750 (1:1) hybrid nanocomposite synergistically exhibited the highest

T_g value with 9.5 ˚C enhancement (159.2 ˚C), relative to T_g of pure PU (Figure 5.7(e)). This temperature shift is caused by the immobilization effect of hybrid nanofillers on the polymer chains (Bagotia & Sharma, 2019). Homogeneous dispersion was contributed to a higher T_g because of increased contact area with polymer chains to constrain their mobility (Tang et al., 2013). Thus, the 3D well-dispersed hybrid MWCNT/GNP-S750 structure results in a rise of the surface area with the PU and a higher T_g value.

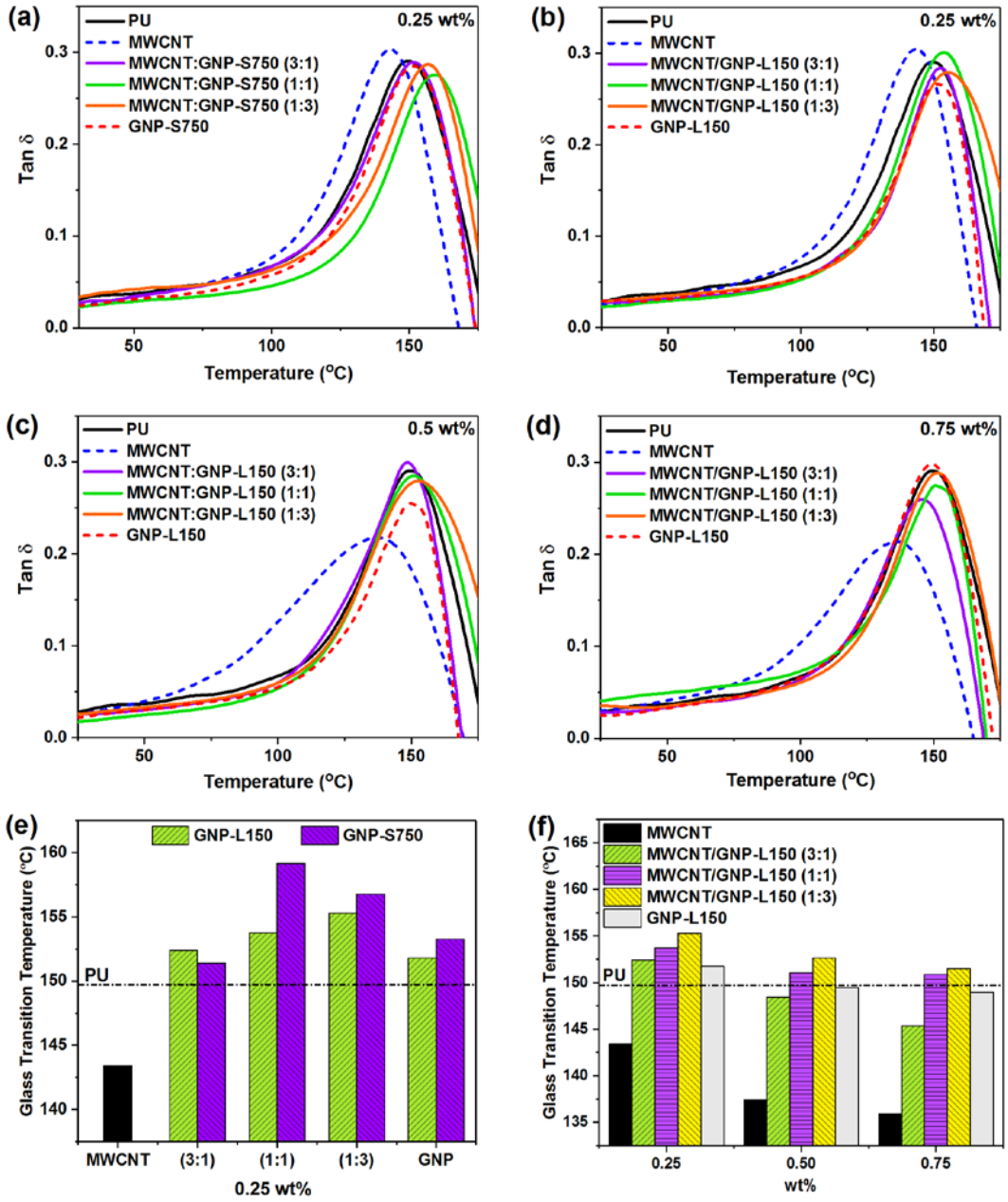

Figure 5.7 : Tan δ of (a-d) hybrid MWCNTs/graphene nanocomposites versus temperature and (e-f) glass transition temperature of nanocomposites.

5.4.3.3 C-Factor

The carbon nanofillers effectiveness on PU bases nanocomposites can be described using the C-factor coefficient (C) using the storage modulus of PU and its nanocomposites, which offers a closer outline about the interaction of nanofillers and the matrix, given by (Bagotia & Sharma, 2019; Jyoti, Babal, Sharma, Dhakate, & Singh, 2018):

$$C = \frac{\left[E'_g / E'_r\right]_{Nanocomposites}}{\left[E'_g / E'_r\right]_{PU}} \tag{5.1}$$

where E'_r and E'_g denote the storage modulus in the rubbery and the glassy regions, respectively. The C-factor value indicates a ratio of storage modulus in the glassy to rubbery regions, which is the inverse of nanofillers effectiveness in the polymer matrix. Therefore, the lower value of the C-factor represents higher nanofillers efficacy along with their better distribution within the PU matrix. The C-factor value for hybrid and single nanocomposites are illustrated in Figure 5.8 (a). Hybrid MWCNTs/GNP-S750 based nanocomposite has the lowest C-factor value, which revealed the maximum nanofillers effectiveness, in comparison with solely MWCNTs and graphene.

5.4.3.4 Degree of Entanglement

The degree of entanglement in the nanocomposites can be measured using DMA, which depends on the interaction of the nanofillers and the polymer matrix. The maximum nanofillers effectiveness in the nanocomposites was evaluated via the degree of entanglement using the storage modulus value, as follow (Bagotia & Sharma, 2019; Jyoti, Singh, Arya, & Dhakate, 2016):

$$N = \frac{E'}{6RT} \tag{5.2}$$

where E', T and R are the storage modulus at the rubbery region (175 ˚C), the absolute temperature and the universal gas constant, respectively. Figure 5.8(b) illustrates the degree of entanglement between single or hybrid carbon nanofillers and PU matrix. Hybrid nanocomposites represented higher N values, where the maximum

entanglement density (31.17 mol/m^3) was achieved in PU/MWCNT+GNP-S750 due to the physical adhesion between MWCNTs and GNP-S750, as well as the better interfacial interaction among hybrid nanofillers and PU matrix (Jyoti et al., 2018). It can be concluded that mechanical loading efficiently transferred from the PU matrix to 3D hybrid MWCNTs/GNP-S750 as a result of dominant interfacial interaction.

5.4.3.5 Cross-Link Density

The contribution of nanofillers and the PU matrix to the storage modulus of the nanocomposites that are arising from the nanofiller-matrix interface was calculated using the Maier and Goritz model, as follow (Ponnamma, Sadasivuni, Strankowski, Guo, & Thomas, 2013):

$$E' = \lambda K_B T \tag{5.3}$$

where λ, K_B and T represent cross-link density, the Boltzmann constant and the temperature in the Kelvin scale (25 ˚C), respectively. The cross-link density of single and hybrid nanocomposites at 0.25 wt% is illustrated in Figure 5.8 (c). The cross-link density of neat PU is 2 x 10^{27} m^{-3}, whereas the MWCNTs/GNP-S750 based hybrid nanocomposite presented the cross-link density of 3.72 x 10^{27} m^{-3}, which is higher than the value of other nanocomposites due to the synergistic effect between GNP-S750 and MWCNTs. It can be concluded that effective dispersion of MWCNTs/GNP-S750 formed highly cross-linked nanofillers within the PU matrix (Jyoti et al., 2018). Moreover, the interconnections of hybrid nanofillers developed further crosslinks, which enhanced the elastic properties (Ponnamma et al., 2013).

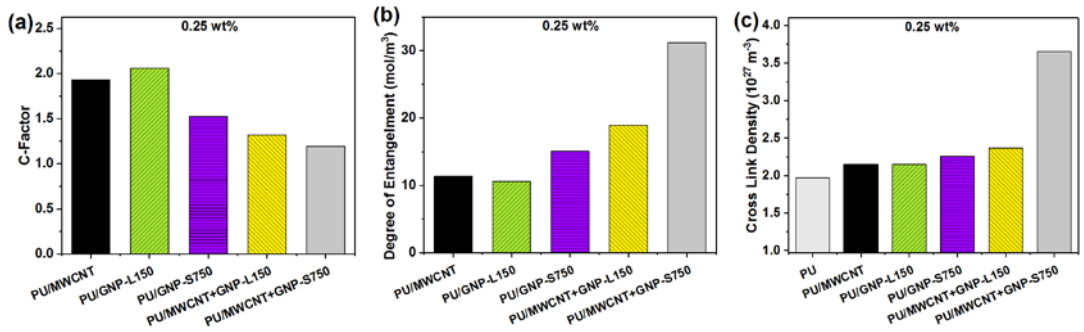

Figure 5.8 : (a) C-factor, (b) the degree of entanglement and (c) cross-link density of the nanocomposites.

5.5 Conclusion

PU foam nanocomposites including MWCNTs and two varieties of graphene were fabricated at low nanofillers loadings and various ratios via a simple, quick and scalable method. TGA, SEM, TEM, Raman spectroscopy and DMA have been performed to evaluate the most substantial enhancement in thermomechanical properties of PU foams. Uniform distribution of the interconnected graphene through CNTs was confirmed using SEM and TEM images. Accordingly, PU foams including solely GNP-S750 or both graphene and MWCNTs had much higher thermal stability relative to pure PU and the samples containing only MWCNTs. The viscoelastic properties of PU nanocomposites were carried out using DMA measurement, in which storage modulus, damping factor (Tan δ) and the glass transition temperature (T_g) were studied. The storage modulus of PU improved with single nanofillers, being higher for PU/GNP-S750 at 0.75 wt% contents with 22% enhancement, whereas the T_g value diminished at higher concentrations. Results showed that the combination of MWCNTs and graphene in the PU matrix exhibited a synergistic effect regarding storage modulus and T_g, which exceeded the influence of each nanofiller. In comparison with pure PU, the storage modulus of hybrid MWCNTs/GNP-S750 (1:1) nanocomposite improved about 86% at a low content of 0.25 wt%, while PU/MWCNTs and PU/GNP-S750 showed a 15% and 19% enhancement at the same loading, respectively. Moreover, the highest storage modulus of PU nanocomposites using single MWCNTs or graphene can be found at 0.75 wt% for GNP-S750 with a 22% improvement. A 3D hybrid network was formed in hybrid nanocomposites, in which MWCNTs interconnected adjacent graphene. When the graphene /MWCNTs hybrid nanocomposites were stretched, the nanofillers distance enhanced, however, the initial nanofillers condition was found again after relaxation, which led to enhancing the storage modulus of PU. The T_g value of PU was also synergically enhanced by about 9.5 ˚C with 0.25 wt% inclusion of well-dispersed 3D MWCNT/GNP-S750 (1:1). The C-factor (reinforcement coefficient), degree of entanglement and cross-link density of fabricated nanocomposites were also examined using the storage modulus value to evaluate the interaction of single and hybrid carbon nanofillers with PU matrix. All of these outcomes revealed that the GNP-S750 with a smaller dimension, a higher SSA and more defects have a higher ability to form a more effective 3D architecture, which further improved the storage modulus and T_g of PU

when combined with MWCNTs as hybrid nanofillers. Here, these hybrid graphene /CNTs nanocomposites are favorable for lightweight foam applications in that thermal stability and thermomechanical properties are crucial principles, such as packaging and structural damping materials.

6. ACOUSTIC AND DIELECTRIC PROPERTIES OF GRAPHENE AND CARBON NANOTUBES HYBRID NANOCOMPOSITES

6.1 Acoustic Properties

6.1.1 Introduction

Noise pollution is deleterious to human health and therefore its control has become a crucial issue with the advancement of modern industry and transportation (Xia, Wu, Guo, Sun, & Liang, 2016; Zhou et al., 2020). Sound insulation and absorption materials are commonly utilized for passive noise control, e.g. for comfortable environments of passengers in the automobile industry (Choe, Sung, & Kim, 2018). Polymeric materials have outstanding viscoelastic properties, which make them ideal for damping and noise reduction, particularly lightweight and porous polymeric structures such as polyurethane (PU) foams (Shi et al., 2017; Yıldırım et al., 2018). PU foams are common noise-controlling materials due to their lightweight, damping ability, efficient acoustic absorption and ease of fabrication (Choe et al., 2018; Moghaddam & Naimi-Jamal, 2019; Sung & Kim, 2017). However, the acoustic properties of these polymers should be enhanced to meet the newly revealed requirements. To enhance the sound insulation performance of polymeric materials, novel nanocomposite materials have been widely studied with the addition of carbon nanotubes (Basirjafari, Malekfar, & Esmaielzadeh Khadem, 2012; R Verdejo et al., 2009; Yıldırım et al., 2018), graphene (J. M. Kim, Kim, Kim, Lee, & Kim, 2017) and silica nanoparticles (Asadi Khanouki & Ohadi, 2018; Shi et al., 2017; Yıldırım et al., 2018). Carbon nanofillers such as carbon nanotubes (CNT) and graphene are some of the most encouraging nanomaterials owing to their extraordinary properties. However, improper dispersion of these nanofillers restricted their performance as a result of their restacking tendency and agglomerations (Basirjafari et al., 2012; J. M. Kim et al., 2017; Yıldırım et al., 2018). The study by Yildirim (Yıldırım et al., 2018) et al. showed optimum soundproofing performance with 0.2 wt% incorporations of CNTs in the PU matrix, whereas the acoustic performance diminished at higher CNT loadings. Kim et

al. (J. M. Kim et al., 2017) fabricated PU with graphene to study sound damping properties, in which maximum sound absorption coefficient was reached by incorporation of 0.2 phr graphene with 18.2% improvement relative to pure PU. The interface between nanofillers and polymer matrix can diffract, scatter and reflect the energy of sound waves (Shi et al., 2017), therefore, much more interface is required to enhance acoustic insulation properties of nanocomposites by improving the dispersion rate of nanofillers in the polymer matrix. To solve the dispersion challenge of the carbon nanofillers in a polymer matrix, combining the one-dimensional (1D) carbon nanotubes and two-dimensional (2D) graphene with different dimensions could lead to a synergistic effect with the formation of three-dimensional (3D) architecture, in which mechanical (Amir Navidfar & Trabzon, 2019), thermal (Amir Navidfar & Trabzon, 2021) and viscoelastic properties (Amir Navidfar et al., 2020) of PU nanocomposites improved. However, to the best of our knowledge, the acoustic performance of these hybrid nanofillers with PU has not yet been reported. Kim et al. (M. S. Kim et al., 2013) investigated soundproofing of polypropylene with CNT and exfoliated graphite nanoplatelets (80/10/10 wt% - PP/CNT/GnP) nanocomposites. They reported that sound transmission loss of PP/CNT/GnP enhanced more than 5 dB in comparison with pure PP at low frequency, in which synergistic effect of carbon nanotubes and graphene can be seen.

The acoustic tests were performed according to a Bruuel & Kjaer 4206 acoustic test system comprising an impedance tube, speaker, three microphones and a digital frequency analyzer to measure the sound transmission loss. The understanding the full range of acoustical response in measurements, the small and large tubes of impedance setup were used for the frequency range of 20 Hz–6300 Hz. Samples were cut in small and large sizes with 29mm and 100mm in diameter for acoustical measurements.

6.1.2 Results and discussion

The sound transmission loss (TL) defines as the difference between the incident sound wave and the last sound wave passing through PU samples. The sound TL response of polyurethane with different content of MWCNTs, GNPs and GNPs+MWCNT hybrid in the whole frequency range of 20-6300 Hz is illustrated in Fig. 5(a). PU with GNPs and hybrid GNPs+MWCNTs at 0.25 wt% showed higher acoustic performance, relative to pure PU and PU/MWCNT. The value of average transmission loss (ATL)

of PU and their nanocomposites is calculated to better understanding, in which the value of ATL gradually enhanced from 18 dB (PU) to 21.6 dB (PU/GNP) and 22.6 dB (PU/MWCNT+GNP) in the whole frequency range, approving that GNPs and GNPs+MWCNT promoted sound insulation capability of PU. ATL of PU improved up to about 51% (28.8 dB) at the lower frequencies (<500 Hz) with the addition of MWCNT+GNP hybrids, as Fig 5(b). The sound waves are transmitted through the interface between the PU and nanofillers at low frequencies. The transmission angle of sound waves altered and its transmission path extended further that eventually caused a further consumption of sound through the PU damping [26]. As a result, well-dispersed nanofillers through the polymer matrix and consequently increasing interfaces between them result in higher sound insulation properties. Therefore, PU containing a well-dispersed 3D hybrid MWCNT+GNP showed higher sound insulation performance at lower frequencies.

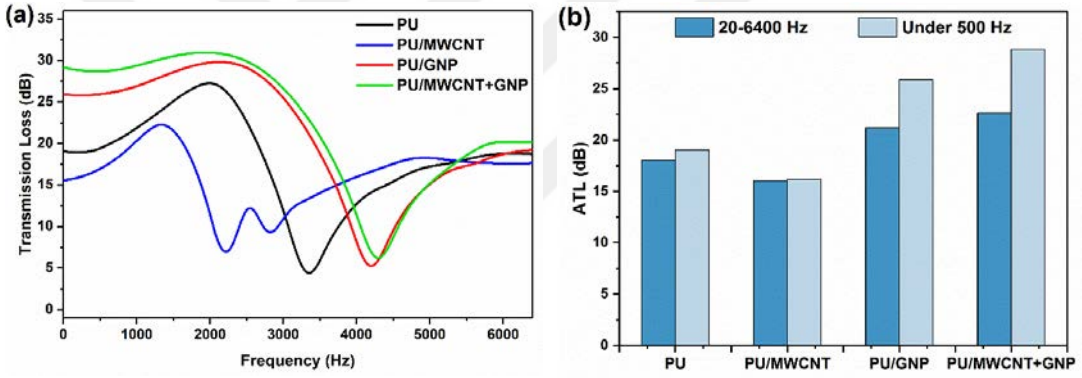

Figure 6.1 : (a) The TL and (b) ATL of PU and their nanocomposites.

6.2 Dielectric properties

6.2.1 Introduction

Functional polymeric nanocomposites with high permittivity are appealing more consideration with the expansion of flexible electronics and large-scale energy storage equipment, due to their simplicity of processing, flexibility, lightweight and low cost, relative to conventional ceramic-based dielectric materials. Carbon nanomaterials such as 1D CNTs and 2D graphene have the excessive potential for recognizing flexible high-k dielectric nanocomposites. The dielectric constant is of distinctive attention to scholars and engineers, which offer awareness of MWCNTs and GNPs appropriateness for electronic applications. The influence of MWCNTs and GNPs on

the dielectric constant of the polymeric nanocomposite is dependent on their response to the polarization process. In addition to electronic and atomic orientation and interfacial polarization (Singha & Thomas, 2008), the conductivity of the nanofillers and the interface adhesion between the nanofillers and polymer matrix controls the electric reaction of the nanocomposites, which initiate the development of micro capacitor and consequently enhance the dielectric constant (Zakaria et al., 2017). Besides, the nanofillers lead to an increase in the polarization of polymers. Homogeneous distribution of carbon nanofillers and inhibition of conductive networks in polymeric nanocomposites are the two main challenges that are still essential to be answered in dielectric materials for power energy storage. Thus, the concentration of nanofillers in the polymer matrix should be close to the percolation threshold. The development of conductive networks brings an increase in leakage current, which reasons high dielectric loss, low breakdown strength and obstructs the enlargement of dielectric nanocomposites (Dang, Zheng, & Zha, 2016). Lu et al. (L. Huang, Lu, Wang, & Wang, 2014) showed a high permittivity of 41 at 10^3 Hz in 0.1 wt% loadings of GNPs in the PVDF matrix. Ruoff et al.(J. Y. Kim et al., 2014) prepared hybrid CNT/GNP nanofillers by the CVD method to be blended in cyanoethyl pullulan (CEP) polymer, where nanocomposites with 0.062 wt% loadings of CNTs/GNPs revealed a permittivity of 32 at 10^2 Hz and a particularly low dielectric loss of 0.051. This hybrid nanofillers system increased the polarization density and specific surface area. Ke et al. (Ke et al., 2019) improved the dielectric properties of TPU with branched CNTs and GNPs with high dielectric constant and low loss tangent. Dielectric measurements were done on specimens of ~1 mm thickness using a broadband dielectric spectroscopy (Novocontrol Technologies) in the frequency range of 1-106 Hz, at 25 ˚C.

6.2.2 Results and discussion

Polymeric nanocomposites reveal a higher dielectric constant than pure polymer matrices. Figures 6.2(a) illustrate the dielectric constant (ε') of PU nanocomposites at 0.25 wt% loading over a frequency from 10 to 10^6 Hz at room temperature. Carbon nanofillers considerably enhanced the dielectric constant over the whole frequency range owing to their high surface areas. The incorporation of hybrid MWCNTs/GNP-1.5 showed a higher dielectric constant, in comparison with the addition of individually MWCNTs and GNP-1.5 at a thickness of 1 mm. This improvement in the dielectric constant of the nanocomposites is attributed to the motion of free charge carriers

because of the development of a continuous conductive pathway of MWCNTs and graphene through the matrix, especially in the hybrid nanofiller system. The polymer-nanofiller interfaces cause variations in dielectric properties, according to the Maxwell–Wagner–Sillars (MWS) effect (J.-K. Yuan et al., 2011). Charges could be accumulated at the interface of PU and nanofillers (two dielectric materials) with dissimilar relaxation time ($\tau=\varepsilon/\sigma$, where σ represent the conductivity). It is shown that carbon nanofillers act as a miniature capacitors and offer a capacitor ability in the PU matrix (Sadasivuni et al., 2014). The dielectric constant of nanocomposites, especially in hybrid MWCNTs/GNP-1.5, is elevated in lower frequencies, which suggests the appearance of charge accumulation at PU/nanofiller interfaces. This phenomenon can be attributed to the uniform dispersion of hybrid MWCNTs/GNP-1.5 in the PU matrix.

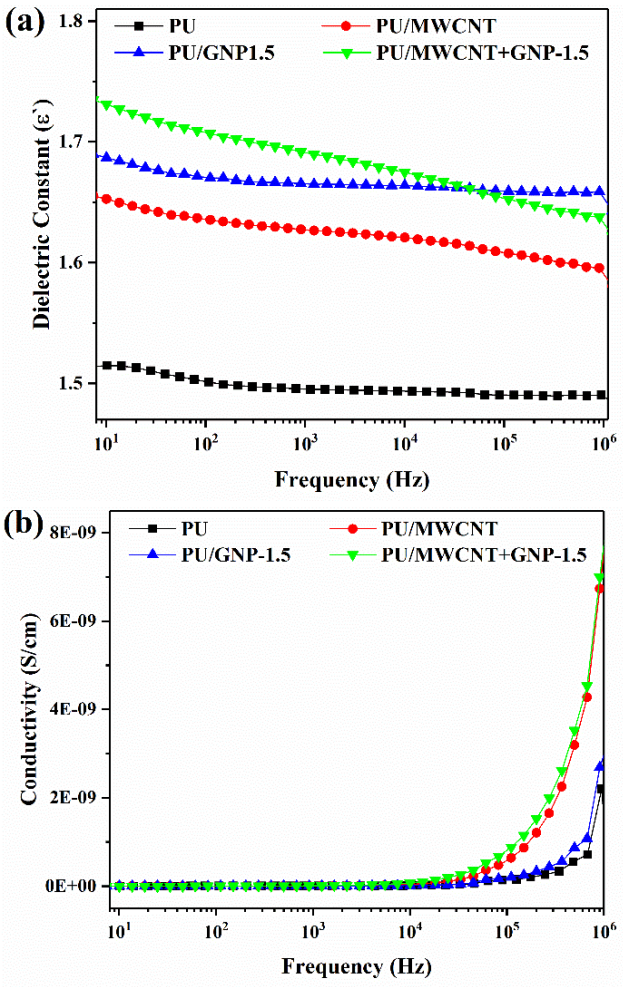

Figure 6.2 : Variation of (a) dielectric permittivity (ε′) and (b) electrical conductivity at 25˚C temperature for PU and its nanocomposites.

Figure 6.2(b) shows the electrical conductivity of PU and its nanocomposite versus the frequency. The conductivity for all nanocomposites is constant at a frequency below

10^4 Hz. However, the PU/MWCNTs and PU/MWCNTs+GNP-1.5 nanocomposites have high electrical conductivity at a higher frequency, relative to pure PU and PU/GNP-1.5 nanocomposite. This suggests that MWCNTs and hybrid MWCNTs/GNP-1.5 partially formed conductive paths in the PU matrix than GNP-1.5, which lead to decreasing the ability of charge storage. Another reason could be a different kind of polarization (Putson, 2018).

Figure 6.3 represents an enhancement in dielectric loss (ε'') and loss tangent ($\delta=\varepsilon''/\varepsilon'$) of PU/MWCNTs and PU/MWCNTs+GNP-1.5 nanocomposites, due to the increase of conductivity, which restricts their energy storage capability. However, GNP-1.5 based nanocomposite provides low dielectric loss and high dielectric constant that is desirable for dielectric materials. This is attributed to the random homogeneous dispersion of GNP-1.5 within the PU matrix, due to its higher percolation threshold as a result of its higher specific surface area ($750 m^2/g$) and lower diameter (1.5 µm).

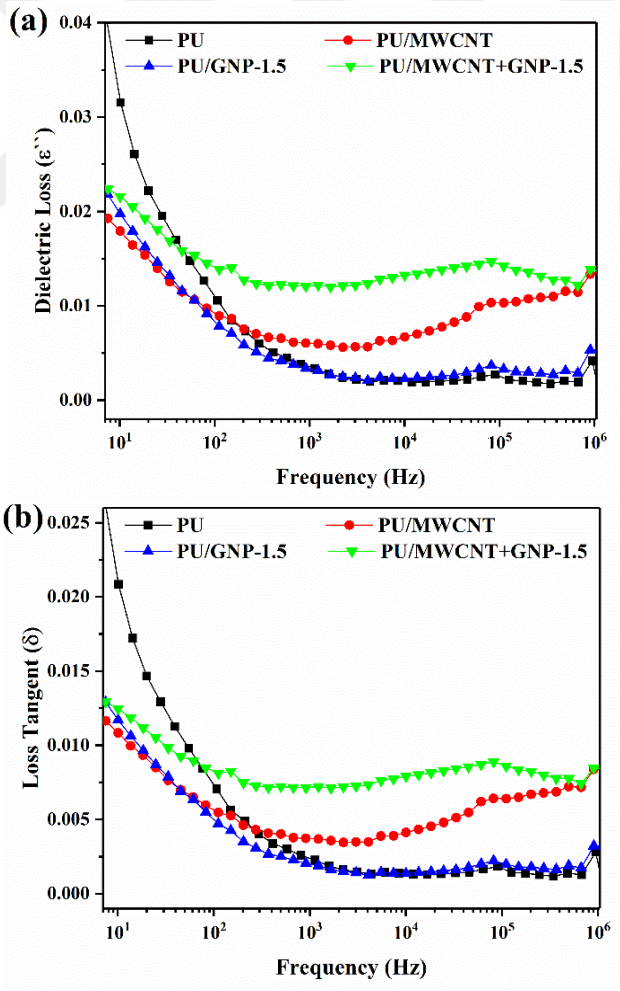

Figure 6.3 : Variation of (a) dielectric loss (ε″) and (b) loss tangent (δ) at 25˚C temperature for PU and its nanocomposites.

7. CONCLUSIONS

7.1 Conclusions

This study has focused on the fabrication and characterization of single and hybrid nanofillers included polyurethane to obtain multifunctional nanocomposites with improved mechanical, thermal, acoustic and dielectric properties.

To determine the thermal stability and mechanical properties of polyurethane reinforced with MWCNTs and/or silica nanoparticles, tensile test, Charpy impact test, hardness, and TGA were performed. For this aim, MWCNTs, Silica-A and Silica-B with varied content up to 1 wt% were added to polyol–isocyanate combinations and then poured into the wooden mold. CNTs were first functionalized with H_2O_2 for making better interfacial adhesion and improve dispersion. After cutting and preparing desired specimens, tests were performed. According to experiments, adding 0.25 wt% of Silica-A, Silica-B, and MWCNT improved the tensile strength of PU about 33, 27, and 15%, respectively, but further nanoparticle adding decreased the strength. Impact test results reveal that maximum strength can be seen in the nanocomposite containing 0.5 wt% MWCNT with approximately 96% improvement in comparison to neat PU. Furthermore, adding 0.75 wt% of Silica-B and 1 wt% of Silica-A improved the impact strength of PU by about 82 and 75%, respectively. Regarding Shore-A hardness, the nanocomposite foam with 0.5 wt% Silica-B has the highest amount.

To fabricate nanocomposites with higher MWCNT content and prevent the appearance of large agglomerations, hybrid nanocomposites were produced, which could lessen large agglomerations. Thereby hybrid nanocomposites can provide a synergistic effect, which can be seen when MWCNTs and silica nanoparticles are simultaneously added to the PU matrix. The hybrid nanocomposite with 0.25 wt% Silica-A and 0.5 wt% MWCNT showed the maximum tensile strength, elastic modulus, and hardness, whereas, in MWCNT/PU nanocomposite, these highest results were obtained in 0.25 wt% MWCNT. In constant overall content of 0.75 wt%, hybrid nanocomposites have higher tensile strength, in comparison to single filler composites. This study revealed

that fabricating a hybrid nanocomposite with different fillers enhanced dispersion of nanoparticles with relatively low cost and consequently the hybrid nanocomposites exhibited synergistic effects, which proved to be more effective than single filler systems. However, after attaining an optimum level, adding further nanoparticles into the polymer matrix noticeably decreased the mechanical properties, due to the appearance of large agglomerations. It is evident from TGA results that the thermal stability of hybrid nanocomposites is higher than that of single filler nanocomposites. In addition, FTIR results demonstrate that there are no major changes in the chemical structure of PU with a dispersion of CNT and silica nanoparticles in the polymer matrix.

Graphene type dependence of three-dimensional GNPs/MWCNTs hybrid nanofillers on mechanical properties improvement of polyurethane nanocomposites was studied using tensile test, impact strength, hardness and micromechanical modeling. Three types of GNPs with various flake sizes and specific surface areas were used to achieve a synergistic effect at 0.25 to 0.75 wt% loadings. MWCNTs and GNP-1.5 (1:1) with a flake size of 1.5 μm and a higher SSA (750 m2/g) exhibited the highest synergistic effect at a low nanofiller content of 0.25 wt%, which the tensile strength was improved about 43%, in comparison with pure PU. Modified Halpin-Tsai modeling with an exponential shape factor was used to fit with the tensile strength results of the single and hybrid nanocomposites. A unit cell containing GNPs and MWCNTs structure was introduced to predict the optimal ratio and content of the nanofillers in hybrid nanocomposites to attaining the synergism, which the modeling results were extremely compatible with the experimental data. The connections between the GNPs and MWCNTs were more possibly formed when the length of carbon nanotubes is higher than the gap between GNPs in the unit cell. The presented model could guide for achieving the synergistic effect between different CNTs and GNPs without many experiments.

The thermal conductivity of PU nanocomposites comprising MWCNTs and three types of graphene was studied by experimental and theoretical approaches. By combining carbon nanotubes and graphene a synergistic thermal conductivity improvement was achieved, which surpasses the performance of individual carbon nanofillers in the PU matrix. The optimization of hybrid nanofillers is essential to

maximize the synergistic effect and the thermal conductivity improvement of the nanocomposites. Synergistic thermal conductivity enhancement using MWCNTs and GNP-S750 with a smaller flake size and higher specific surface area was achieved at low nanofillers contents (0.25 wt%) which is vital for reducing the viscosity and improving the processability of the nanocomposites. In addition, the synergism can be seen at higher nanofiller content (0.75 wt%) for GNP-L150 with a larger flake size. The hybrid nanofillers can effectively enhance the thermal conductivity so that 1D MWCNTs interconnected adjacent 2D graphene to form a more efficient 3D thermally conductive network. As an interesting outcome, the thermal conductivity of MWCNTs/GNP-S750 (1:1) hybrid nanocomposite at 0.25 wt% was approximately equivalent to the thermal conductivity of the individual graphene and MWCNTs at 0.75 wt%. Therefore, it can be concluded that the fabrication of hybrid nanocomposites is a cost-effective method with higher processability through declining required nanofillers content. An analytical study on the thermal conductivity of single and hybrid nanocomposites by incorporating the straightness factor and percolation effect as fitting parameters was presented, in which an outstanding agreement between the modified model predictions and experimental results was achieved. The results showed that the straightness of nanofillers profoundly affected the thermal conductivity of nanocomposites and larger graphene tends to be wavier or less straight in the polymer matrix so that the calculated straightness ratio is reduced by enhancing graphene flake size.

PU foam nanocomposites including MWCNTs and two varieties of graphene were fabricated at low nanofillers loadings and various ratios via a simple, quick and scalable method. TGA, SEM, TEM, Raman spectroscopy and DMA have been performed to evaluate the most substantial enhancement in thermomechanical properties of PU foams. Uniform distribution of the interconnected graphene through CNTs was confirmed using SEM and TEM images. Accordingly, PU foams including solely GNP-S750 or both graphene and MWCNTs had much higher thermal stability relative to pure PU and the samples containing only MWCNTs. The viscoelastic properties of PU nanocomposites were carried out using DMA measurement, in which storage modulus, damping factor (Tan δ) and the glass transition temperature (Tg) were studied. The storage modulus of PU improved with single nanofillers, being higher for PU/GNP-S750 at 0.75 wt% contents with 22% enhancement, whereas the Tg value

diminished at higher concentrations. Results showed that the combination of MWCNTs and graphene in the PU matrix exhibited a synergistic effect regarding storage modulus and *Tg*, which exceeded the influence of each nanofiller. In comparison with pure PU, the storage modulus of hybrid MWCNTs/GNP-S750 (1:1) nanocomposite improved about 86% at a low content of 0.25 wt%, while PU/MWCNTs and PU/GNP-S750 showed a 15% and 19% enhancement at the same loading, respectively. Moreover, the highest storage modulus of PU nanocomposites using single MWCNTs or graphene can be found at 0.75 wt% for GNP-S750 with a 22% improvement. A 3D hybrid network was formed in hybrid nanocomposites, in which MWCNTs interconnected adjacent graphene. When the graphene /MWCNTs hybrid nanocomposites were stretched, the nanofillers distance enhanced, however, the initial nanofillers condition was found again after relaxation, which led to enhancing the storage modulus of PU. The Tg value of PU was also synergically enhanced by about 9.5 ˚C with 0.25 wt% inclusion of well-dispersed 3D MWCNT/GNP-S750 (1:1). The C-factor (reinforcement coefficient), degree of entanglement and cross-link density of fabricated nanocomposites were also examined using the storage modulus value to evaluate the interaction of single and hybrid carbon nanofillers with PU matrix. All of these outcomes revealed that the GNP-S750 with a smaller dimension, a higher SSA and more defects have a higher ability to form a more effective 3D architecture, which further improved the storage modulus and Tg of PU when combined with MWCNTs as hybrid nanofillers. Here, these hybrid graphene /CNTs nanocomposites are favorable for lightweight foam applications in that thermal stability and thermomechanical properties are crucial principles, such as packaging and structural damping materials.

Acoustic and dielectric behavior of PU with single and hybrid inclusion of GNPs and MWCNTs were studied. Acoustic properties of PU at lower frequencies (<500 Hz) enhanced about 51% with the incorporation of GNPs/CNTs at 0.25 wt%. Hybrid GNPs/CNTs showed higher dielectric constant, electrical conductivity and dielectric loss, relative to single CNTs and GNPs included PU. However, the high dielectric loss of hybrid systems restricts their practical applications that need to be solved. To compare diverse nanocomposite systems, the performance index (PI) formula was introduced that is based on mechanical, thermal, acoustic and dielectric results of nanocomposites, in which PU with hybrid GNPs/CNTs showed higher PI compared to

single GNPs and CNTs, approving its higher multifunctionality. The high multifunctionality of the hybrid nanocomposites in comparison with single nanofiller included nanocomposites reveals the superiority of the hybrid approach that is appropriate for a wide range of applications.

The range of nanocomposites and their applicability could be noticeably expanded when multi-functionality can be offered in compliance with requirements. The exploiting hybrid nanofillers offers multiple properties in nanocomposites, which affords potentially relevant findings. In our work, tensile strength, thermal conductivity, acoustic transmission loss and dielectric constant of PU were enhanced by about 43%, 5%, 51% and 13%, respectively (Table 7.1).

Table 7.1 : Summary of properties of PU and its nanocomposites.

	TS (MPa)	TC (W/mK)	ATL (dB)	ATLU* (dB)	ADC** (ε`)	EC (S/cm)	ADL*** (ε``)	PI
PU	0.39	0.02617	18.03	19.05	1.49	8.68 E-11	0.007719722	-
PU/MWCNT	0.47	0.02687	16.07	16.20	1.63	5.66 E-10	0.009975814	0.64
PU/GNP	0.46	0.02681	21.17	25.85	1.67	1.88 E-10	0.007045814	0.79
PU/MWCNT+GNP	0.56	0.02744	22.64	28.8	1.69	6.48 E-10	0.01448	1.50

As a significant result, an overall improvement in the properties of nanocomposites was achieved. Thus, dimensionless amount of Performance Index (PI) is defined, in which desirable properties placed in nominator and undesirable properties are in denominator, as fellow [36]:

$$PI = \frac{TS_r \,.\, TC_r \,.\, ATL_r \,.\, ATLU_r . ADC_r \,.\, Log(EC_r)}{ADL_r} \qquad (7.1)$$

Where Xr refers to relative properties of nanocomposites to pure PU. The *ECr* properties spanned over few orders of magnitude that are used with logarithm. Lower dielectric loss is desirable for dielectric materials; therefore ADLr should be placed in the denominator. The results of PI showed that the hybrid CNT/GNP has the highest PI, followed by the single inclusion of GNPs (Table 7.1). The higher PI value represents a multifunctional nanocomposite, which reveals improved overall properties. Besides, presenting results in the form of a radar chart is another method for determining the overall performance of nanocomposites. A comparison among single CNTs (blue), GNPs (red) and hybrid (green) nanocomposites show that the

hybrid CNT/GNP nanofillers demonstrated better optimal performance in all desired properties excluding average dielectric loss (ADL) results, as Fig. 7.1. As a noteworthy outcome, the addition of hybrid CNTs/GNPs to the polymer matrix even at lower nanofillers loadings can significantly further enhance the overall performance of nanocomposites.

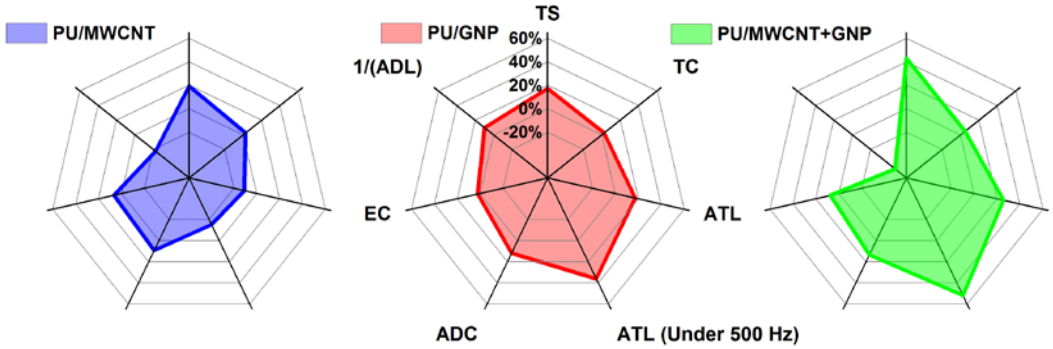

Figure 7.1 : Overall properties of PU/MWCNT (blue), PU/GNP (red) and PU/MWCNT+GNP (green) at the 0.25 wt% presented in a radar graph.

7.2 Recommendations for Future Work

According to the conclusions, it is obvious that more investigation is required to be done to promote the distribution of nanofillers within the polymer matrix. Hence, numerous futures work plans and research aims are suggested as follow;

a) Since the nanofillers dispersion depends on processing conditions, it is worth studying processing conditions such as mixing time that affect the ultimate properties of nanocomposites. Additional methods such as probe ultrasonication could further improve the dispersion rate.

b) It is advantageous for the industry in the future to fabricate nanocomposites without the use of any chemicals or solvents, however, simple modifications of nanofillers should be investigated.

c) To find the synergistic effect of various nanofillers leading to enhancement in properties, GNPs and CNTs could be used with other nanofillers such as hexagonal boron nitride (h-BN), cellulose nanocrystals (CNC), clay, zinc oxide, titanium dioxide, nano diamond and Mxene.

d) As an example of hybrid nanofillers, quantum dots (a few nanometres in size) can be used in nanocomposites to further enhance the interfacial adhesion of

nanofillers within the polymer matrix. Therefore higher dispersion rates and improved properties of nanocomposites could be achieved. For instance, extra work was done in collaboration with another student to explore the synergistic effect of carbon quantum dots with CNT/GNP hybrid in the PU matrix. The tensile and modulus of PU nanocomposites with CNTs, GNPs, QDs and their hybrids were improved up to about 54% and 71% at 0.25 wt%, respectively. Therefore, further studies should be promoted to improve interfacial adhesion and dispersion of nanofillers within the polymer matrix.

The outcomes of this work regarding fabrication and characterization of hybrid nanocomposites have been filed for a patent with application number “2019/00222”. In this thesis, PU nanocomposites containing hybrid nanofillers were fabricated via a simple, quick and scalable method. In addition, the mentioned hybrid nanofiller structures can be used with other polymers besides polyurethane matrix and their desired properties can be improved. Therefore, well-organized hybrid nanocomposite fabrications with multifunctional aspects has great potential for commercialization and industiral applications shortly.

In general, novel materials are discovered and characterized experimentally, however, experiments take a long time and are generally complicated and costly. Researchers could use computational methods to powerfully explore the composition and properties of materials, where experimental data are needed for confirming models. In fact, time and cost savings can be made by relating appropriate simulations and experiments. The presence of various factors in a single work requires extensive effort and is generally difficult to realize. However, by using well-trained machine learning (ML) models, one can simply attain results with any combination of factors within a fraction of a second. Machine learning has been enormously utilized in several fields, but its application in engineering science remains in infancy. In the future, practical Machine Learning-based models can be developed to predict the properties of polymeric nanocomposites.

REFERENCES

Abbasi, S. (2009). *Rheology, Properties and Microstructure Development of Polymer/Carbon Nanotube Composites in Microinjection Molding Process*. École Polytechnique de Montréal,

Aghadavoudi, F., Golestanian, H., & Zarasvand, K. A. (2018). Elastic behaviour of hybrid cross-linked epoxy-based nanocomposite reinforced with GNP and CNT: experimental and multiscale modelling. *Polymer Bulletin*, 1-20.

Akinwande, D., Brennan, C. J., Bunch, J. S., Egberts, P., Felts, J. R., Gao, H., . . . Li, Y. (2017). A review on mechanics and mechanical properties of 2D materials—Graphene and beyond. *Extreme Mechanics Letters, 13*, 42-77.

Amirkhosravi, M., Yue, L., & Manas-Zloczower, I. (2020). Dusting Thermoplastic Polyurethane Granules with Carbon Nanotubes toward Highly Stretchable Conductive Elastomer Composites. *ACS Applied Polymer Materials, 2*(9), 4037-4044.

Antunes, M., & Velasco, J. I. (2014). Multifunctional polymer foams with carbon nanoparticles. *Progress in Polymer Science, 39*(3), 486-509.

Araby, S., Zaman, I., Meng, Q., Kawashima, N., Michelmore, A., Kuan, H.-C., . . . Zhang, L. (2013). Melt compounding with graphene to develop functional, high-performance elastomers. *Nanotechnology, 24*(16), 165601.

Arif, M., Alhashmi, H., Varadarajan, K., Koo, J. H., Hart, A., & Kumar, S. (2020). Multifunctional performance of carbon nanotubes and graphene nanoplatelets reinforced PEEK composites enabled via FFF additive manufacturing. *Composites Part B: Engineering, 184*, 107625.

Asadi Khanouki, M., & Ohadi, A. (2018). Improved acoustic damping in polyurethane foams by the inclusion of silicon dioxide nanoparticles. *Advances in Polymer Technology, 37*(8), 2799-2810.

Athanasopoulos, N., Baltopoulos, A., Matzakou, M., Vavouliotis, A., & Kostopoulos, V. (2012). Electrical conductivity of polyurethane/MWCNT nanocomposite foams. *Polymer Composites, 33*(8), 1302-1312.

Badakhsh, A., Lee, Y.-M., Rhee, K. Y., Park, C. W., An, K.-H., & Kim, B.-J. (2019). Improvement of thermal, electrical and mechanical properties of composites using a synergistic network of length controlled-CNTs and graphene nanoplatelets. *Composites Part B: Engineering, 175*, 107075.

Bagotia, N., Choudhary, V., & Sharma, D. (2018). A review on the mechanical, electrical and EMI shielding properties of carbon nanotubes and graphene reinforced polycarbonate nanocomposites. *Polymers for Advanced Technologies, 29*(6), 1547-1567.

Bagotia, N., Choudhary, V., & Sharma, D. (2019). Synergistic effect of graphene/multiwalled carbon nanotube hybrid fillers on mechanical, electrical and EMI shielding properties of polycarbonate/ethylene methyl acrylate nanocomposites. *Composites Part B: Engineering, 159*, 378-388.

Bagotia, N., & Sharma, D. (2019). Systematic study of dynamic mechanical and thermal properties of multiwalled carbon nanotube reinforced polycarbonate/ethylene methyl acrylate nanocomposites. *Polymer Testing, 73*, 425-432.

Baltopoulos, A., Athanasopoulos, N., Fotiou, I., Vavouliotis, A., & Kostopoulos, V. (2013). Sensing strain and damage in polyurethane-MWCNT nano-composite foams using electrical measurements. *Express Polym Lett, 7*(1), 40-54.

Bandarian, M., Shojaei, A., & Rashidi, A. M. (2011). Thermal, mechanical and acoustic damping properties of flexible open-cell polyurethane/multi-walled carbon nanotube foams: effect of surface functionality of nanotubes. *Polymer International, 60*(3), 475-482.

Basirjafari, S., Malekfar, R., & Esmaielzadeh Khadem, S. (2012). Low loading of carbon nanotubes to enhance acoustical properties of poly (ether) urethane foams. *Journal of Applied Physics, 112*(10), 104312.

Benzait, Z., & Trabzon, L. (2018). A review of recent research on materials used in polymer–matrix composites for body armor application. *Journal of Composite Materials, 52*(23), 3241-3263.

Berber, S., Kwon, Y.-K., & Tománek, D. (2000). Unusually high thermal conductivity of carbon nanotubes. *Physical Review Letters, 84*(20), 4613.

Bisht, A., Dasgupta, K., & Lahiri, D. (2018). Effect of graphene and CNT reinforcement on mechanical and thermomechanical behavior of epoxy—A comparative study. *Journal of applied polymer science, 135*(14), 46101.

Boukhvalov, D., & Katsnelson, M. (2009). Chemical functionalization of graphene. *Journal of Physics: Condensed Matter, 21*(34), 344205.

Burgaz, E., & Kendirlioglu, C. (2019). Thermomechanical behavior and thermal stability of polyurethane rigid nanocomposite foams containing binary nanoparticle mixtures. *Polymer Testing, 77*, 105930.

Charitos, I., Georgousis, G., Klonos, P. A., Kyritsis, A., Mouzakis, D., Raptis, Y., . . . Kontou, E. (2021). The synergistic effect on the thermomechanical and electrical properties of carbonaceous hybrid polymer nanocomposites. *Polymer Testing*, 107102.

Chatterjee, S., Nafezarefi, F., Tai, N., Schlagenhauf, L., Nüesch, F., & Chu, B. (2012). Size and synergy effects of nanofiller hybrids including graphene nanoplatelets and carbon nanotubes in mechanical properties of epoxy composites. *Carbon, 50*(15), 5380-5386.

Chen, D., & Chen, G. (2013). In situ synthesis of thermoplastic polyurethane/graphene nanoplatelets conductive composite by ball milling. *Journal of Reinforced Plastics and Composites, 32*(5), 300-307.

Chen, G., Zhou, S., Gu, G., & Wu, L. (2007). Modification of colloidal silica on the mechanical properties of acrylic based polyurethane/silica composites. *Colloids and Surfaces A: Physicochemical and Engineering Aspects, 296*(1-3), 29-36.

Chen, L., Sun, Y.-Y., Lin, J., Du, X.-Z., Wei, G.-S., He, S.-J., & Nazarenko, S. (2015). Modeling and analysis of synergistic effect in thermal conductivity enhancement of polymer composites with hybrid filler. *International Journal of Heat and Mass Transfer, 81*, 457-464.

Chen, Y., Zhou, S., Yang, H., & Wu, L. (2005). Structure and properties of polyurethane/nanosilica composites. *Journal of applied polymer science, 95*(5), 1032-1039.

Cheni, S.-W., Guo, B.-L., & Wu, W.-S. (2012). Influence of the variation of carbon nanotubes on the morphology of carbon nanotubes–SiO2 hybrid materials. *Nanoscience Methods, 1*(1), 78-85.

Choe, H., Sung, G., & Kim, J. H. (2018). Chemical treatment of wood fibers to enhance the sound absorption coefficient of flexible polyurethane composite foams. *Composites Science and Technology, 156*, 19-27.

Chong, H., Hinder, S., & Taylor, A. (2016). Graphene nanoplatelet-modified epoxy: effect of aspect ratio and surface functionality on mechanical properties and toughening mechanisms. *Journal of materials science, 51*(19), 8764-8790.

Chu, K., Jia, C.-c., & Li, W.-s. (2012). Effective thermal conductivity of graphene-based composites. *Applied physics letters, 101*(12), 121916.

Chu, K., Li, W.-s., & Dong, H. (2013). Role of graphene waviness on the thermal conductivity of graphene composites. *Applied Physics A, 111*(1), 221-225.

Chu, K., Li, W.-s., Jia, C.-c., & Tang, F.-l. (2012). Thermal conductivity of composites with hybrid carbon nanotubes and graphene nanoplatelets. *Applied physics letters, 101*(21), 211903.

Chu, K., Li, W.-s., & Tang, F.-l. (2013). Flatness-dependent thermal conductivity of graphene-based composites. *Physics Letters A, 377*(12), 910-914.

Ciecierska, E., Jurczyk-Kowalska, M., Bazarnik, P., Gloc, M., Kulesza, M., Kowalski, M., . . . Lewandowska, M. (2016). Flammability, mechanical properties and structure of rigid polyurethane foams with different types of carbon reinforcing materials. *Composite Structures, 140*, 67-76.

Coleman, J. N., Khan, U., Blau, W. J., & Gun'ko, Y. K. (2006). Small but strong: A review of the mechanical properties of carbon nanotube–polymer composites. *Carbon, 44*(9), 1624-1652. doi:http://dx.doi.org/10.1016/j.carbon.2006.02.038

Czichos, H., Saito, T., & Smith, L. (2006). *Springer handbook of materials measurement methods* (Vol. 978): Springer.

Dai, H., Wong, E. W., & Lieber, C. M. (1996). Probing electrical transport in nanomaterials: conductivity of individual carbon nanotubes. *science, 272*(5261), 523-526.

Dang, Z. M., Zheng, M. S., & Zha, J. W. (2016). 1D/2D carbon nanomaterial-polymer dielectric composites with high permittivity for power energy storage applications. *Small, 12*(13), 1688-1701.

Dasari, A., Yu, Z.-Z., & Mai, Y.-W. (2009). Electrically conductive and super-tough polyamide-based nanocomposites. *Polymer, 50*(16), 4112-4121.

Deng, F., Zheng, Q.-S., Wang, L.-F., & Nan, C.-W. (2007). Effects of anisotropy, aspect ratio, and nonstraightness of carbon nanotubes on thermal conductivity of carbon nanotube composites. *Applied physics letters, 90*(2), 021914.

Ding, P., Su, S., Song, N., Tang, S., Liu, Y., & Shi, L. (2014). Highly thermal conductive composites with polyamide-6 covalently-grafted graphene by an in situ polymerization and thermal reduction process. *Carbon, 66*, 576-584.

Du, F., Fischer, J. E., & Winey, K. I. (2003). Coagulation method for preparing single-walled carbon nanotube/poly (methyl methacrylate) composites and their modulus, electrical conductivity, and thermal stability. *Journal of Polymer Science Part B: Polymer Physics, 41*(24), 3333-3338.

Ebbesen, T., Lezec, H., Hiura, H., Bennett, J., Ghaemi, H., & Thio, T. (1996). Electrical conductivity of individual carbon nanotubes. *Nature, 382*(6586), 54-56.

Eda, G., Fanchini, G., & Chhowalla, M. (2008). Large-area ultrathin films of reduced graphene oxide as a transparent and flexible electronic material. *Nature nanotechnology, 3*(5), 270-274.

Elashmawi, I., Alatawi, N. S., & Elsayed, N. H. (2017). Preparation and characterization of polymer nanocomposites based on PVDF/PVC doped with graphene nanoparticles. *Results in physics, 7*, 636-640.

Engels, H. W., Pirkl, H. G., Albers, R., Albach, R. W., Krause, J., Hoffmann, A., . . . Dormish, J. (2013). Polyurethanes: versatile materials and sustainable problem solvers for today's challenges. *Angewandte Chemie International Edition, 52*(36), 9422-9441.

Espadas-Escalante, J., Avilés, F., Gonzalez-Chi, P., & Oliva, A. (2017). Thermal conductivity and flammability of multiwall carbon nanotube/polyurethane foam composites. *Journal of Cellular Plastics, 53*(2), 215-230.

Eungkee Lee, R., Afsari Ghazi, A., Azdast, T., Hasanzadeh, R., & Mamaghani Shishavan, S. (2018). Tensile and hardness properties of polycarbonate nanocomposites in the presence of styrene maleic anhydride as compatibilizer. *Advances in Polymer Technology, 37*(6), 1737-1743.

Fan, Z., Yan, J., Ning, G., Wei, T., Zhi, L., & Wei, F. (2013). Porous graphene networks as high performance anode materials for lithium ion batteries. *Carbon, 60*, 558-561.

Faraji, S., Yardim, M. F., Can, D. S., & Sarac, A. S. (2017). Characterization of polyacrylonitrile, poly (acrylonitrile-co-vinyl acetate), and poly (acrylonitrile-co-itaconic acid) based activated carbon nanofibers. *Journal of applied polymer science, 134*(2).

Ferreira, F. V., Cividanes, L. D. S., Brito, F. S., de Menezes, B. R. C., Franceschi, W., Simonetti, E. A. N., & Thim, G. P. (2016). Functionalization of graphene and applications. In *Functionalizing graphene and carbon nanotubes* (pp. 1-29): Springer.

Gaisford, S., Kett, V., & Haines, P. (2019). *Principles of thermal analysis and calorimetry*: Royal society of chemistry.

Gao, X., Zhu, Y., Zhao, X., Wang, Z., An, D., Ma, Y., . . . Zhou, B. (2011). Synthesis and characterization of polyurethane/SiO 2 nanocomposites. *Applied Surface Science, 257*(10), 4719-4724.

Gao, Y., Picot, O. T., Bilotti, E., & Peijs, T. (2017). Influence of filler size on the properties of poly (lactic acid)(PLA)/graphene nanoplatelet (GNP) nanocomposites. *European Polymer Journal, 86*, 117-131.

Gaska, K., Kádár, R., Rybak, A., Siwek, A., & Gubanski, S. (2017). Gas barrier, thermal, mechanical and rheological properties of highly aligned graphene-LDPE nanocomposites. *Polymers, 9*(7), 294.

Geim, A. K. (2009). Graphene: status and prospects. *science, 324*(5934), 1530-1534.

Ghavidel, A. K., Azdast, T., Shabgard, M., Navidfar, A., & Sadighikia, S. (2015). Improving electrical conductivity of poly methyl methacrylate by utilization of carbon nanotube and CO2 laser. *Journal of applied polymer science, 132*(42).

Ghavidel, A. K., Azdast, T., Shabgard, M. R., Navidfar, A., & Shishavan, S. M. (2015). Effect of carbon nanotubes on laser cutting of multi-walled carbon nanotubes/poly methyl methacrylate nanocomposites. *Optics & Laser Technology, 67*, 119-124.

Guan, J., Xing, C., Wang, Y., Li, Y., & Li, J. (2017). Poly (vinylidene fluoride) dielectric composites with both ionic nanoclusters and well dispersed graphene oxide. *Composites Science and Technology, 138*, 98-105.

Guo, Y., Ruan, K., Shi, X., Yang, X., & Gu, J. (2020). Factors affecting thermal conductivities of the polymers and polymer composites: A review. *Composites Science and Technology*, 108134.

Habibpour, S., Um, J. G., Jun, Y.-s., Bhargava, P., Park, C. B., & Yu, A. Structural Impact of Graphene Nanoribbon on Mechanical Properties and Anti-corrosion Performance of Polyurethane Nanocomposites. *Chemical Engineering Journal, 405*, 126858.

Hamidinejad, S. M., Chu, R. K., Zhao, B., Park, C. B., & Filleter, T. (2018). Enhanced Thermal Conductivity of Graphene Nanoplatelet–Polymer Nanocomposites Fabricated via Supercritical Fluid-Assisted in Situ Exfoliation. *ACS applied materials & interfaces, 10*(1), 1225-1236.

Hasanzadeh, R., Azdast, T., & Doniavi, A. (2020). Thermal Conductivity of Low-Density Polyethylene Foams Part II: Deep Investigation using Response Surface Methodology. *Journal of Thermal Science, 29*(1), 159-168.

He, G., Zhou, X., Liu, J., Zhang, J., Pan, L., & Liu, S. (2018). Synergetic enhancement of thermal conductivity for highly explosive-filled polymer composites through hybrid carbon nanomaterials. *Polymer Composites, 39*(S3), E1452-E1462.

Higgins, B. A., & Brittain, W. J. (2005). Polycarbonate carbon nanofiber composites. *European Polymer Journal, 41*(5), 889-893.

Hone, J., Whitney, M., Piskoti, C., & Zettl, A. (1999). Thermal conductivity of single-walled carbon nanotubes. *Physical Review B, 59*(4), R2514.

Hoseinabadi, M., Naderi, M., Najafi, M., Motahari, S., & Shokri, M. (2017). A study of rigid polyurethane foams: The effect of synthesized polyols and nanoporous graphene. *Journal of applied polymer science, 134*(26).

Hu, K., Kulkarni, D. D., Choi, I., & Tsukruk, V. V. (2014). Graphene-polymer nanocomposites for structural and functional applications. *Progress in Polymer Science, 39*(11), 1934-1972.

Huang, C., Qian, X., & Yang, R. (2018). Thermal conductivity of polymers and polymer nanocomposites. *Materials Science and Engineering: R: Reports, 132*, 1-22.

Huang, J., Gao, M., Pan, T., Zhang, Y., & Lin, Y. (2014). Effective thermal conductivity of epoxy matrix filled with poly (ethyleneimine) functionalized carbon nanotubes. *Composites Science and Technology, 95*, 16-20.

Huang, L., Lu, C., Wang, F., & Wang, L. (2014). Preparation of PVDF/graphene ferroelectric composite films by in situ reduction with hydrobromic acids and their properties. *RSC advances, 4*(85), 45220-45229.

Iijima, S. (2002). Carbon nanotubes: past, present, and future. *Physica B: Condensed Matter, 323*(1-4), 1-5.

Jancar, J., Douglas, J., Starr, F. W., Kumar, S., Cassagnau, P., Lesser, A., . . . Buehler, M. (2010). Current issues in research on structure–property relationships in polymer nanocomposites. *Polymer, 51*(15), 3321-3343.

Jen, Y.-M., & Huang, J.-C. (2019). Synergistic Effect on the Thermomechanical and Electrical Properties of Epoxy Composites with the Enhancement of Carbon Nanotubes and Graphene Nano Platelets. *Materials, 12*(2), 255.

Ji, X., Xu, Y., Zhang, W., Cui, L., & Liu, J. (2016). Review of functionalization, structure and properties of graphene/polymer composite fibers. *Composites Part A: Applied Science and Manufacturing, 87*, 29-45.

Johnson, D. W., Dobson, B. P., & Coleman, K. S. (2015). A manufacturing perspective on graphene dispersions. *Current Opinion in Colloid & Interface Science, 20*(5-6), 367-382.

Jyoti, J., Babal, A. S., Sharma, S., Dhakate, S., & Singh, B. P. (2018). Significant improvement in static and dynamic mechanical properties of graphene oxide–carbon nanotube acrylonitrile butadiene styrene hybrid composites. *Journal of materials science, 53*(4), 2520-2536.

Jyoti, J., Singh, B. P., Arya, A. K., & Dhakate, S. (2016). Dynamic mechanical properties of multiwall carbon nanotube reinforced ABS composites and their correlation with entanglement density, adhesion, reinforcement and C factor. *RSC advances, 6*(5), 3997-4006.

Kang, T. J., Shin, S. J., Jung, K., & Park, J. K. (2006). Mechanical, thermal and ablative properties of interply continuous/spun hybrid carbon composites. *Carbon, 44*(5), 833-839.

Karim, N., Afroj, S., Tan, S., He, P., Fernando, A., Carr, C., & Novoselov, K. S. (2017). Scalable production of graphene-based wearable e-textiles. *ACS nano, 11*(12), 12266-12275.

Karimzad Ghavidel, A., Azdast, T., Shabgard, M. R., Navidfar, A., & Mamaghani Shishavan, S. (2015). Effect of carbon nanotubes on laser cutting of multi-walled carbon nanotubes/poly methyl methacrylate nanocomposites. *Optics & Laser Technology, 67*(0), 119-124. doi:http://dx.doi.org/10.1016/j.optlastec.2014.10.003

Karimzad Ghavidel, A., Navidfar, A., Shabgard, M., & Azdast, T. (2016). Role of CO2 laser cutting conditions on anisotropic properties of nanocomposite contain carbon nanotubes. *Journal of Laser Applications, 28*(3), 032006.

Kausar, A. (2017). Polyurethane Composite Foams in High Performance Applications: A Review. *Polymer-Plastics Technology and Engineering*(just-accepted).

Kausar, A. (2018). Polyurethane composite foams in high-performance applications: A review. *Polymer-Plastics Technology and Engineering, 57*(4), 346-369.

Kausar, A., Anwar, Z., & Muhammad, B. (2016). Recent developments in epoxy/graphite, epoxy/graphene, and epoxy/graphene nanoplatelet composites: a comparative review. *Polymer-Plastics Technology and Engineering, 55*(11), 1192-1210.

Ke, K., McMaster, M., Christopherson, W., Singer, K. D., & Manas-Zloczower, I. (2019). Effects of branched carbon nanotubes and graphene nanoplatelets on dielectric properties of thermoplastic polyurethane at different temperatures. *Composites Part B: Engineering, 166*, 673-680.

Kim, H., Abdala, A. A., & Macosko, C. W. (2010). Graphene/polymer nanocomposites. *Macromolecules, 43*(16), 6515-6530.

Kim, H. S., Bae, H. S., Yu, J., & Kim, S. Y. (2016). Thermal conductivity of polymer composites with the geometrical characteristics of graphene nanoplatelets. *Scientific reports, 6*(1), 1-9.

Kim, J.-M., Kim, J.-H., Ahn, J.-H., Kim, J.-D., Park, S., Park, K. H., & Lee, J.-M. (2018). Synthesis of nanoparticle-enhanced polyurethane foams and evaluation of mechanical characteristics. *Composites Part B: Engineering, 136*, 28-38.

Kim, J. M., Kim, D. H., Kim, J., Lee, J. W., & Kim, W. N. (2017). Effect of graphene on the sound damping properties of flexible polyurethane foams. *Macromolecular Research, 25*(2), 190-196.

Kim, J. Y., Kim, T., Suk, J. W., Chou, H., Jang, J. H., Lee, J. H., . . . Ruoff, R. S. (2014). Enhanced Dielectric Performance in Polymer Composite Films with Carbon Nanotube-Reduced Graphene Oxide Hybrid Filler. *Small, 10*(16), 3405-3411.

Kim, M. S., Yan, J., Joo, K. H., Pandey, J. K., Kang, Y. J., & Ahn, S. H. (2013). Synergistic effects of carbon nanotubes and exfoliated graphite nanoplatelets for electromagnetic interference shielding and soundproofing. *Journal of applied polymer science, 130*(6), 3947-3951.

Klempner, D., & Frisch, K. C. (1991). *Handbook of polymeric foams and foam technology* (Vol. 404): Hanser New York.

Kong, H. (2013). Hybrids of carbon nanotubes and graphene/graphene oxide. *Current Opinion in Solid State and Materials Science, 17*(1), 31-37.

Kumar, A., Sharma, K., & Dixit, A. R. (2019). A review of the mechanical and thermal properties of graphene and its hybrid polymer nanocomposites for structural applications. *Journal of materials science, 54*(8), 5992-6026.

Kumar, A., Sharma, K., & Dixit, A. R. (2020a). Carbon nanotube-and graphene-reinforced multiphase polymeric composites: review on their properties and applications. *Journal of materials science*, 1-43.

Kumar, A., Sharma, K., & Dixit, A. R. (2020b). A review on the mechanical properties of polymer composites reinforced by carbon nanotubes and graphene. *Carbon Letters*, 1-17.

Kumar, S., Sun, L., Caceres, S., Li, B., Wood, W., Perugini, A., . . . Zhong, W. (2010). Dynamic synergy of graphitic nanoplatelets and multi-walled carbon nanotubes in polyetherimide nanocomposites. *Nanotechnology, 21*(10), 105702.

Kyrylyuk, A. V., Hermant, M. C., Schilling, T., Klumperman, B., Koning, C. E., & van der Schoot, P. (2011). Controlling electrical percolation in multicomponent carbon nanotube dispersions. *Nat Nano, 6*(6), 364-369. doi:http://www.nature.com/nnano/journal/v6/n6/abs/nnano.2011.40.html#supplementary-information

Lawal, A. T. (2019). Graphene-based nano composites and their applications. A review. *Biosensors and Bioelectronics, 141*, 111384.

Layek, R. K., & Nandi, A. K. (2013). A review on synthesis and properties of polymer functionalized graphene. *Polymer, 54*(19), 5087-5103.

Lee, C., Wei, X., Kysar, J. W., & Hone, J. (2008). Measurement of the elastic properties and intrinsic strength of monolayer graphene. *science, 321*(5887), 385-388.

Lee, J., Kim, G. H., & Ha, C. S. (2012). Sound absorption properties of polyurethane/nano-silica nanocomposite foams. *Journal of applied polymer science, 123*(4), 2384-2390.

Lee, T., Min, S. H., Gu, M., Jung, Y. K., Lee, W., Lee, J. U., . . . Kim, B.-S. (2015). Layer-by-layer assembly for graphene-based multilayer nanocomposites: synthesis and applications. *Chemistry of Materials, 27*(11), 3785-3796.

Li, B., & Zhong, W.-H. (2011). Review on polymer/graphite nanoplatelet nanocomposites. *Journal of materials science, 46*(17), 5595-5614.

Li, M., Deng, T., Zheng, B., Zhang, Y., Liao, Y., & Zhou, H. (2019). Effect of defects on the mechanical and thermal properties of graphene. *Nanomaterials, 9*(3), 347.

Li, W., Dichiara, A., & Bai, J. (2013). Carbon nanotube–graphene nanoplatelet hybrids as high-performance multifunctional reinforcements in epoxy composites. *Composites Science and Technology, 74*, 221-227.

Liao, K.-H., Park, Y. T., Abdala, A., & Macosko, C. (2013). Aqueous reduced graphene/thermoplastic polyurethane nanocomposites. *Polymer, 54*(17), 4555-4559.

Liu, H., Gao, J., Huang, W., Dai, K., Zheng, G., Liu, C., . . . Guo, Z. (2016). Electrically conductive strain sensing polyurethane nanocomposites with synergistic carbon nanotubes and graphene bifillers. *Nanoscale, 8*(26), 12977-12989.

Liu, M., Papageorgiou, D. G., Li, S., Lin, K., Kinloch, I. A., & Young, R. J. (2018). Micromechanics of reinforcement of a graphene-based thermoplastic elastomer nanocomposite. *Composites Part A: Applied Science and Manufacturing, 110*, 84-92.

Liu, W.-W., Chai, S.-P., Mohamed, A. R., & Hashim, U. (2014). Synthesis and characterization of graphene and carbon nanotubes: A review on the past and recent developments. *Journal of Industrial and Engineering Chemistry, 20*(4), 1171-1185.

Lourie, O., & Wagner, H. (1998). Evaluation of Young's modulus of carbon nanotubes by micro-Raman spectroscopy. *Journal of Materials Research, 13*(9), 2418-2422.

Lu, H., Zhang, J., Luo, J., Gong, W., Li, C., Li, Q., . . . Yao, Y. (2017). Enhanced thermal conductivity of free-standing 3D hierarchical carbon nanotube-graphene hybrid paper. *Composites Part A: Applied Science and Manufacturing, 102*, 1-8.

Lu, J. P. (1997). Elastic properties of carbon nanotubes and nanoropes. *Physical Review Letters, 79*(7), 1297.

Ma, L., Wang, G., & Dai, J. (2017). Preparation of a functional reduced graphene oxide and carbon nanotube hybrid and its reinforcement effects on the properties of polyimide composites. *Journal of applied polymer science, 134*(11).

Mahmoodi, M., Arjmand, M., Sundararaj, U., & Park, S. (2012). The electrical conductivity and electromagnetic interference shielding of injection molded multi-walled carbon nanotube/polystyrene composites. *Carbon, 50*(4), 1455-1464.

Mahmoud, W. E. (2011). Morphology and physical properties of poly (ethylene oxide) loaded graphene nanocomposites prepared by two different techniques. *European Polymer Journal, 47*(8), 1534-1540.

Mansour, G., & Tzetzis, D. (2013). Nanomechanical characterization of hybrid multiwall carbon nanotube and fumed silica epoxy nanocomposites. *Polymer-Plastics Technology and Engineering, 52*(10), 1054-1062.

McClory, C., McNally, T., Brennan, G. P., & Erskine, J. (2007). Thermosetting polyurethane multiwalled carbon nanotube composites. *Journal of applied polymer science, 105*(3), 1003-1011.

Menard, K. P., & Menard, N. R. (2020). *Dynamic mechanical analysis*: CRC press.

Min, C., Liu, D., Shen, C., Zhang, Q., Song, H., Li, S., . . . Zhang, K. (2018). Unique synergistic effects of graphene oxide and carbon nanotube hybrids on the tribological properties of polyimide nanocomposites. *Tribology International, 117*, 217-224.

min Kim, H., Lee, S., Song, Y. S., & Lee, D. (2019). Synergistic improvement of electrical and thermal conductivities of carbon-based nanocomposites and its prediction by Mori-Tanaka scheme with interfacial resistances. *Composite Structures, 211*, 56-62.

Mittal, G., Dhand, V., Rhee, K. Y., Park, S.-J., & Lee, W. R. (2015). A review on carbon nanotubes and graphene as fillers in reinforced polymer nanocomposites. *Journal of Industrial and Engineering Chemistry, 21*, 11-25.

Moghaddam, S. T., & Naimi-Jamal, M. R. (2019). Reinforced magnetic polyurethane rigid (PUR) foam nanocomposites and investigation of thermal, mechanical, and sound absorption properties. *Journal of Thermoplastic Composite Materials, 32*(9), 1224-1241.

Mohamadi, S., & Sharifi-Sanjani, N. (2016). Crystallization of PVDF in graphene-filled electrospun PVDF/PMMA nanofibers processed at three different conditions. *Fibers and Polymers, 17*(4), 582-592.

Montazeri, A., Javadpour, J., Khavandi, A., Tcharkhtchi, A., & Mohajeri, A. (2010). Mechanical properties of multi-walled carbon nanotube/epoxy composites. *Materials & Design, 31*(9), 4202-4208.

Monthioux, M., Smith, B., Burteaux, B., Claye, A., Fischer, J., & Luzzi, D. (2001). Sensitivity of single-wall carbon nanotubes to chemical processing: an electron microscopy investigation. *Carbon, 39*(8), 1251-1272.

Moosaei, R., Sharif, M., & Ramezannezhad, A. (2017). Enhancement of tensile, electrical and thermal properties of epoxy nanocomposites through chemical hybridization of polypyrrole and graphene oxide. *Polymer Testing, 60*, 173-186.

Moriche, R., Prolongo, S., Sánchez, M., Jiménez-Suárez, A., Sayagués, M., & Ureña, A. (2015). Morphological changes on graphene nanoplatelets induced during dispersion into an epoxy resin by different methods. *Composites Part B: Engineering, 72*, 199-205.

Mubarak, N., Abdullah, E., Jayakumar, N., & Sahu, J. (2014). An overview on methods for the production of carbon nanotubes. *Journal of Industrial and Engineering Chemistry, 20*(4), 1186-1197.

Nan, C.-W., Liu, G., Lin, Y., & Li, M. (2004). Interface effect on thermal conductivity of carbon nanotube composites. *Applied physics letters, 85*(16), 3549-3551.

Naumis, G. G., Barraza-Lopez, S., Oliva-Leyva, M., & Terrones, H. (2017). Electronic and optical properties of strained graphene and other strained 2D materials: a review. *Reports on Progress in Physics, 80*(9), 096501.

Navidfar, A. (2014). Experimental study of mechanical properties of nano-composites containing carbon nanotubes produced by injection molding. *MD Thesis, Ourmieh University, Ourmieh*.

Navidfar, A., Azdast, T., & Karimzad Ghavidel, A. (2016a). Influence of processing condition and carbon nanotube on mechanical properties of injection molded multi-walled carbon nanotube/poly (methyl methacrylate) nanocomposites. *Journal of applied polymer science, 133*(31), 43738.

Navidfar, A., Azdast, T., & Karimzad Ghavidel, A. (2016b). Influence of processing condition and carbon nanotube on mechanical properties of injection molded multi-walled carbon nanotube/poly (methyl methacrylate) nanocomposites. *Journal of Applied Polymer Science, 133*(31).

Navidfar, A., Azdast, T., Karimzad Ghavidel, A., Sadighikia, S., & Mamaghani Shishevan, S. (2014). *Investigation of Rockwell hardness and Charpy impact test of injection molded multi-walled carbon nanotubes/poly methyl methacrylate nanocomposites.* Paper presented at the 5th International Congress on Nanoscience & Nanotechnology (ICNN2014), Tehran, Iran.

Navidfar, A., Baytak, T., Bulut, O., & Trabzon, L. (2020). Synergically enhanced viscoelastic behavior of binary nanocarbon based polyurethane hybrid nanocomposite foams. *arXiv preprint arXiv:2006.13363*.

Navidfar, A., Sancak, A., Yildirim, K. B., & Trabzon, L. (2018). A Study on Polyurethane Hybrid Nanocomposite Foams Reinforced with Multiwalled Carbon Nanotubes and Silica Nanoparticles. *Polymer-Plastics Technology and Engineering, 57*(14), 1463-1473.

Navidfar, A., & Trabzon, L. (2019). Graphene type dependence of carbon nanotubes/graphene nanoplatelets polyurethane hybrid nanocomposites: Micromechanical modeling and mechanical properties. *Composites Part B: Engineering, 176*, 107337.

Navidfar, A., & Trabzon, L. (2020). Analytical modeling and experimentally optimizing synergistic effect on thermal conductivity enhancement of polyurethane nanocomposites with hybrid carbon nanofillers. *Polymer Composites*.

Navidfar, A., & Trabzon, L. (2021). Analytical modeling and experimentally optimizing synergistic effect on thermal conductivity enhancement of polyurethane nanocomposites with hybrid carbon nanofillers. *Polymer Composites, 42*(2), 944-954.

Ning, G., Li, T., Yan, J., Xu, C., Wei, T., & Fan, Z. (2013). Three-dimensional hybrid materials of fish scale-like polyaniline nanosheet arrays on graphene oxide and carbon nanotube for high-performance ultracapacitors. *Carbon, 54*, 241-248.

Pandit, S., Gaska, K., Mokkapati, V. R., Celauro, E., Derouiche, A., Forsberg, S., . . . Mijakovic, I. (2020). Precontrolled Alignment of Graphite Nanoplatelets in Polymeric Composites Prevents Bacterial Attachment. *Small, 16*(5), 1904756.

Papageorgiou, D. G., Kinloch, I. A., & Young, R. J. (2017). Mechanical properties of graphene and graphene-based nanocomposites. *Progress in materials science, 90*, 75-127.

Pokharel, P., Pant, B., Pokhrel, K., Pant, H. R., Lim, J.-g., Kim, H.-Y., & Choi, S. (2015). Effects of functional groups on the graphene sheet for improving the thermomechanical properties of polyurethane nanocomposites. *Composites Part B: Engineering, 78*, 192-201.

Ponnamma, D., Sadasivuni, K. K., Strankowski, M., Guo, Q., & Thomas, S. (2013). Synergistic effect of multi walled carbon nanotubes and reduced graphene oxides in natural rubber for sensing application. *Soft Matter, 9*(43), 10343-10353.

Pradhan, B., & Srivastava, S. K. (2014). Synergistic effect of three-dimensional multi-walled carbon nanotube–graphene nanofiller in enhancing the mechanical and thermal properties of high-performance silicone rubber. *Polymer International, 63*(7), 1219-1228.

Prasad, K. E., Das, B., Maitra, U., Ramamurty, U., & Rao, C. (2009). Extraordinary synergy in the mechanical properties of polymer matrix composites reinforced with 2 nanocarbons. *Proceedings of the National Academy of Sciences, 106*(32), 13186-13189.

Prolongo, S. G., Jiménez-Suárez, A., Moriche, R., & Urena, A. (2014). Graphene nanoplatelets thickness and lateral size influence on the morphology and behavior of epoxy composites. *European Polymer Journal, 53*, 292-301.

Putson, C. (2018). *Enhanced Dielectric and Electrical Properties in Polyurethane Composites with Graphene Nanosheets.* Paper presented at the Materials Science Forum.

Qin, X., Yan, W., Guo, X., & Gao, T. (2018). Effects of area, aspect ratio and orientation of rectangular nanohole on the tensile strength of defective graphene–a molecular dynamics study. *RSC advances, 8*(31), 17034-17043.

Raccichini, R., Varzi, A., Passerini, S., & Scrosati, B. (2015). The role of graphene for electrochemical energy storage. *Nature materials, 14*(3), 271-279.

Rafiee, M. A., Rafiee, J., Wang, Z., Song, H., Yu, Z.-Z., & Koratkar, N. (2009). Enhanced mechanical properties of nanocomposites at low graphene content. *ACS nano, 3*(12), 3884-3890.

Rahmanian, S., Suraya, A., Roshanravan, B., Othman, R., Nasser, A., Zahari, R., & Zainudin, E. (2015). The influence of multiscale fillers on the rheological and mechanical properties of carbon-nanotube–silica-reinforced epoxy composite. *Materials & Design, 88*, 227-235.

Rasana, N., Jayanarayanan, K., Deeraj, B., & Joseph, K. (2019). The thermal degradation and dynamic mechanical properties modeling of MWCNT/glass fiber multiscale filler reinforced polypropylene composites. *Composites Science and Technology, 169*, 249-259.

Rashahmadi, S., Hasanzadeh, R., & Mosalman, S. (2017). Improving the mechanical properties of poly methyl methacrylate nanocomposites for dentistry applications reinforced with different nanoparticles. *Polymer-Plastics Technology and Engineering, 56*(16), 1730-1740.

Reich, S., Thomsen, C., & Maultzsch, J. (2008). *Carbon nanotubes: basic concepts and physical properties*: John Wiley & Sons.

Roy, S., Srivastava, S. K., Pionteck, J., & Mittal, V. (2015). Mechanically and Thermally Enhanced Multiwalled Carbon Nanotube–Graphene Hybrid filled Thermoplastic Polyurethane Nanocomposites. *Macromolecular Materials and Engineering, 300*(3), 346-357.

Sadasivuni, K. K., Ponnamma, D., Kumar, B., Strankowski, M., Cardinaels, R., Moldenaers, P., . . . Grohens, Y. (2014). Dielectric properties of modified graphene oxide filled polyurethane nanocomposites and its correlation with rheology. *Composites Science and Technology, 104*, 18-25.

Sapkota, J., Shirole, A., Foster, E. J., Garcia, J. C. M., Lattuada, M., & Weder, C. (2017). Polymer nanocomposites with nanorods having different length distributions. *Polymer, 110*, 284-291.

Scaffaro, R., & Maio, A. (2019). Integrated ternary bionanocomposites with superior mechanical performance via the synergistic role of graphene and plasma treated carbon nanotubes. *Composites Part B: Engineering, 168*, 550-559.

Schadler, L. (2007). Model interfaces. *Nature materials, 6*(4), 257-258.

Sen, R., Zhao, B., Perea, D., Itkis, M. E., Hu, H., Love, J., . . . Haddon, R. C. (2004). Preparation of single-walled carbon nanotube reinforced polystyrene and polyurethane nanofibers and membranes by electrospinning. *Nano letters, 4*(3), 459-464.

Shamsi, R., Mir Mohamad Sadeghi, G., & Asghari, G. H. (2018). Dynamic mechanical analysis of polyurethanes and carbon nanotube based composites obtained from PET waste. *Polymer Composites, 39*(S2), E754-E764.

Shang, J., Chen, Y., Zhou, Y., Liu, L., Wang, G., Li, X., . . . Miao, H. (2015). Effect of folded and crumpled morphologies of graphene oxide platelets on the mechanical performances of polymer nanocomposites. *Polymer, 68*, 131-139.

Shen, B., Zhai, W., Tao, M., Lu, D., & Zheng, W. (2013). Chemical functionalization of graphene oxide toward the tailoring of the interface in polymer composites. *Composites Science and Technology*, *77*, 87-94.

Shi, X., Wu, J., Wang, X., Zhou, X., Xie, X., & Xue, Z. (2017). Novel sound insulation materials based on epoxy/hollow silica nanotubes composites. *Composites Part B: Engineering*, *131*, 125-133.

Shin, M. K., Lee, B., Kim, S. H., Lee, J. A., Spinks, G. M., Gambhir, S., . . . Kim, S. J. (2012). Synergistic toughening of composite fibres by self-alignment of reduced graphene oxide and carbon nanotubes. *Nature communications*, *3*, 650.

Simmons, T. J., Hashim, D., Vajtai, R., & Ajayan, P. M. (2007). Large area-aligned arrays from direct deposition of single-wall carbon nanotube inks. *Journal of the American Chemical Society*, *129*(33), 10088-10089.

Singh, V., Joung, D., Zhai, L., Das, S., Khondaker, S. I., & Seal, S. (2011). Graphene based materials: past, present and future. *Progress in materials science*, *56*(8), 1178-1271.

Singha, S., & Thomas, M. J. (2008). Dielectric properties of epoxy nanocomposites. *IEEE transactions on Dielectrics and Electrical Insulation*, *15*(1), 12-23.

Song, K., Zhang, Y., Meng, J., Green, E. C., Tajaddod, N., Li, H., & Minus, M. L. (2013). Structural polymer-based carbon nanotube composite fibers: understanding the processing–structure–performance relationship. *Materials*, *6*(6), 2543-2577.

Song, P. a., Liu, L., Fu, S., Yu, Y., Jin, C., Wu, Q., . . . Li, Q. (2013). Striking multiple synergies created by combining reduced graphene oxides and carbon nanotubes for polymer nanocomposites. *Nanotechnology*, *24*(12), 125704.

Srivastava, V. K. (2012). Modeling and mechanical performance of carbon nanotube/epoxy resin composites. *Materials & Design*, *39*, 432-436.

Stand, A. (1987). Test Method for Thermal Conductivity of Solid by Means of the Guarded Comparative Longitudinal Heat-Flow Technique. *ASTM E1225*.

Steuerman, D. W., Star, A., Narizzano, R., Choi, H., Ries, R. S., Nicolini, C., . . . Heath, J. R. (2002). Interactions between conjugated polymers and single-walled carbon nanotubes. *The Journal of Physical Chemistry B*, *106*(12), 3124-3130.

Sun, X., Huang, C., Wang, L., Liang, L., Cheng, Y., Fei, W., & Li, Y. (2020). Recent progress in graphene/polymer nanocomposites. *Advanced Materials*, 2001105.

Sun, Y. J., Ma, F., & Xu, K. (2013). *Size dependent mechanical properties of graphene nanoribbons: molecular dynamics simulation.* Paper presented at the Materials Science Forum.

Sung, G., & Kim, J. H. (2017). Influence of filler surface characteristics on morphological, physical, acoustic properties of polyurethane composite foams filled with inorganic fillers. *Composites Science and Technology, 146*, 147-154.

Szeluga, U., Kumanek, B., & Trzebicka, B. (2015). Synergy in hybrid polymer/nanocarbon composites. A review. *Composites Part A: Applied Science and Manufacturing, 73*, 204-231.

Tang, L.-C., Wan, Y.-J., Yan, D., Pei, Y.-B., Zhao, L., Li, Y.-B., . . . Lai, G.-Q. (2013). The effect of graphene dispersion on the mechanical properties of graphene/epoxy composites. *Carbon, 60*, 16-27.

Terrones, M., Botello-Méndez, A. R., Campos-Delgado, J., López-Urías, F., Vega-Cantú, Y. I., Rodríguez-Macías, F. J., . . . Charlier, J.-C. (2010). Graphene and graphite nanoribbons: Morphology, properties, synthesis, defects and applications. *Nano today, 5*(4), 351-372.

Tessema, A., Zhao, D., Moll, J., Xu, S., Yang, R., Li, C., . . . Kidane, A. (2017). Effect of filler loading, geometry, dispersion and temperature on thermal conductivity of polymer nanocomposites. *Polymer Testing, 57*, 101-106.

Tian, W., Li, W., Yu, W., & Liu, X. (2017). A review on lattice defects in graphene: types, generation, effects and regulation. *Micromachines, 8*(5), 163.

Trovati, G., Sanches, E. A., Neto, S. C., Mascarenhas, Y. P., & Chierice, G. O. (2010). Characterization of polyurethane resins by FTIR, TGA, and XRD. *Journal of applied polymer science, 115*(1), 263-268.

Uyor, U. O., Popoola, A. P., Popoola, O., & Aigbodion, V. S. (2018). Energy storage and loss capacity of graphene-reinforced poly (vinylidene fluoride) nanocomposites from electrical and dielectric properties perspective: A review. *Advances in Polymer Technology, 37*(8), 2838-2858.

Valles, C., Abdelkader, A. M., Young, R. J., & Kinloch, I. A. (2015). The effect of flake diameter on the reinforcement of few-layer graphene–PMMA composites. *Composites Science and Technology, 111*, 17-22.

Verdejo, R., Bernal, M. M., Romasanta, L. J., & Lopez-Manchado, M. A. (2011). Graphene filled polymer nanocomposites. *Journal of Materials Chemistry, 21*(10), 3301-3310.

Verdejo, R., Stämpfli, R., Alvarez-Lainez, M., Mourad, S., Rodriguez-Perez, M., Brühwiler, P., & Shaffer, M. (2009). Enhanced acoustic damping in flexible polyurethane foams filled with carbon nanotubes. *Composites Science and Technology, 69*(10), 1564-1569.

Verma, M., Chauhan, S. S., Dhawan, S., & Choudhary, V. (2017). Graphene nanoplatelets/carbon nanotubes/polyurethane composites as efficient shield against electromagnetic polluting radiations. *Composites Part B: Engineering, 120*, 118-127.

Wang, E., Dong, Y., Islam, M. Z., Yu, L., Liu, F., Chen, S., . . . Xu, Z. (2019). Effect of graphene oxide-carbon nanotube hybrid filler on the mechanical property and thermal response speed of shape memory epoxy composites. *Composites Science and Technology, 169*, 209-216.

Wang, F., Drzal, L. T., Qin, Y., & Huang, Z. (2015). Mechanical properties and thermal conductivity of graphene nanoplatelet/epoxy composites. *Journal of materials science, 50*(3), 1082-1093.

Wang, J., Jin, X., Wu, H., & Guo, S. (2017). Polyimide reinforced with hybrid graphene oxide@ carbon nanotube: toward high strength, toughness, electrical conductivity. *Carbon, 123*, 502-513.

Wang, Z. (2018). *The Effect of Particle Size and Functionalisation on Electro-thermo-mechanical Properties of Graphene-enhanced Epoxy and Carbon Fibre Epoxy Nano-Composites.* The University of Manchester (United Kingdom),

Wang, Z., & Li, X. (2017). Mechanical properties and flame retardancy of rigid polyurethane foams containing a SiO2 nanospheres/graphene oxide hybrid and dimethyl methylphosphonate. *Polymer-Plastics Technology and Engineering*(just-accepted).

Wu, X.-F., Zhao, Y.-K., Zhao, Z.-H., Sun, Y., Zhang, H., Yu, M.-T., & Jia, F.-F. (2017). Crystallization Behaviors of Graphene Oxide–Carbon Nanotubes Hybrids/Polyamide 66 Composites. *Polymer-Plastics Technology and Engineering, 56*(5), 556-562.

Xia, L., Wu, H., Guo, S., Sun, X., & Liang, W. (2016). Enhanced sound insulation and mechanical properties of LDPE/mica composites through multilayered distribution and orientation of the mica. *Composites Part A: Applied Science and Manufacturing, 81*, 225-233.

Xiao, Y.-j., Wang, W.-y., Chen, X.-j., Lin, T., Zhang, Y.-t., Yang, J.-h., . . . Zhou, Z.-w. (2016). Hybrid network structure and thermal conductive properties in poly (vinylidene fluoride) composites based on carbon nanotubes and graphene nanoplatelets. *Composites Part A: Applied Science and Manufacturing, 90*, 614-625.

Xiong, J., Zheng, Z., Qin, X., Li, M., Li, H., & Wang, X. (2006). The thermal and mechanical properties of a polyurethane/multi-walled carbon nanotube composite. *Carbon, 44*(13), 2701-2707.

Xu, Z., Tang, X., Gu, A., & Fang, Z. (2007). Novel preparation and mechanical properties of rigid polyurethane foam/organoclay nanocomposites. *Journal of applied polymer science, 106*(1), 439-447.

Yakobson, B. I., Brabec, C., & Bernholc, J. (1996). Nanomechanics of carbon tubes: instabilities beyond linear response. *Physical Review Letters, 76*(14), 2511.

Yan, D., Xu, L., Chen, C., Tang, J., Ji, X., & Li, Z. (2012). Enhanced mechanical and thermal properties of rigid polyurethane foam composites containing graphene nanosheets and carbon nanotubes. *Polymer International, 61*(7), 1107-1114.

Yang, C., Hao, S.-J., Dai, S.-L., & Zhang, X.-Y. (2017). Nanocomposites of poly (vinylidene fluoride)-Controllable hydroxylated/carboxylated graphene with enhanced dielectric performance for large energy density capacitor. *Carbon, 117*, 301-312.

Yang, G.-h., Bao, D.-d., Liu, H., Zhang, D.-q., Wang, N., & Li, H.-t. (2017). Functionalization of graphene and applications of the derivatives. *Journal of Inorganic and Organometallic Polymers and Materials, 27*(5), 1129-1141.

Yang, K., & Gu, M. (2010). Enhanced thermal conductivity of epoxy nanocomposites filled with hybrid filler system of triethylenetetramine-functionalized multi-walled carbon nanotube/silane-modified nano-sized silicon carbide. *Composites Part A: Applied Science and Manufacturing, 41*(2), 215-221.

Yang, S.-Y., Lin, W.-N., Huang, Y.-L., Tien, H.-W., Wang, J.-Y., Ma, C.-C. M., . . . Wang, Y.-S. (2011). Synergetic effects of graphene platelets and carbon nanotubes on the mechanical and thermal properties of epoxy composites. *Carbon, 49*(3), 793-803.

Yang, S.-Y., Ma, C.-C. M., Teng, C.-C., Huang, Y.-W., Liao, S.-H., Huang, Y.-L., . . . Chiou, K.-C. (2010). Effect of functionalized carbon nanotubes on the thermal conductivity of epoxy composites. Carbon, 48(3), 592-603.

Yang, X., Fan, S., Li, Y., Guo, Y., Li, Y., Ruan, K., . . . Gu, J. (2020). Synchronously improved electromagnetic interference shielding and thermal conductivity for epoxy nanocomposites by constructing 3D copper nanowires/thermally annealed graphene aerogel framework. Composites Part A: Applied Science and Manufacturing, 128, 105670.

Yeh, M.-K., Tai, N.-H., & Liu, J.-H. (2006). Mechanical behavior of phenolic-based composites reinforced with multi-walled carbon nanotubes. Carbon, 44(1), 1-9.

Yıldırım, B., Sancak, A., Navidfar, A., Trabzon, L., & Orfali, W. (2018). Acoustic properties of polyurethane compositions enhanced with multi-walled carbon nanotubes and silica nanoparticles. *Materialwissenschaft und Werkstofftechnik, 49*(8), 978-985.

Yousefi, N., Gudarzi, M. M., Zheng, Q., Lin, X., Shen, X., Jia, J., . . . Kim, J.-K. (2013). Highly aligned, ultralarge-size reduced graphene oxide/polyurethane nanocomposites: mechanical properties and moisture permeability. *Composites Part A: Applied Science and Manufacturing*, *49*, 42-50.

Yu, A., Ramesh, P., Sun, X., Bekyarova, E., Itkis, M. E., & Haddon, R. C. (2008). Enhanced thermal conductivity in a hybrid graphite nanoplatelet–carbon nanotube filler for epoxy composites. *Advanced Materials, 20*(24), 4740-4744.

Yu, J., Choi, H. K., Kim, H. S., & Kim, S. Y. (2016). Synergistic effect of hybrid graphene nanoplatelet and multi-walled carbon nanotube fillers on the thermal conductivity of polymer composites and theoretical modeling of the synergistic effect. *Composites Part A: Applied Science and Manufacturing*, *88*, 79-85.

Yu, M.-F., Files, B. S., Arepalli, S., & Ruoff, R. S. (2000). Tensile loading of ropes of single wall carbon nanotubes and their mechanical properties. *Physical Review Letters, 84*(24), 5552.

Yuan, D., Pedrazzoli, D., Pircheraghi, G., & Manas-Zloczower, I. (2017). Melt compounding of thermoplastic polyurethanes incorporating 1D and 2D carbon nanofillers. *Polymer-Plastics Technology and Engineering, 56*(7), 732-743.

Yuan, J.-K., Yao, S.-H., Dang, Z.-M., Sylvestre, A., Genestoux, M., & Bai1, J. (2011). Giant dielectric permittivity nanocomposites: realizing true potential of pristine carbon nanotubes in polyvinylidene fluoride matrix through an enhanced interfacial interaction. *The Journal of Physical Chemistry C, 115*(13), 5515-5521.

Zakaria, M. R., Kudus, M. H. A., Akil, H. M., & Thirmizir, M. Z. M. (2017). Comparative study of graphene nanoparticle and multiwall carbon nanotube filled epoxy nanocomposites based on mechanical, thermal and dielectric properties. *Composites Part B: Engineering, 119*, 57-66.

Zandiatashbar, A., Lee, G.-H., An, S. J., Lee, S., Mathew, N., Terrones, M., . . . Koratkar, N. (2014). Effect of defects on the intrinsic strength and stiffness of graphene. *Nature communications, 5*(1), 1-9.

Zarasvand, K. A., & Golestanian, H. (2017). Investigating the effects of number and distribution of GNP layers on graphene reinforced polymer properties: Physical, numerical and micromechanical methods. *Composites Science and Technology, 139*, 117-126.

Zeng, X., Yang, D., Liu, H., Zhou, N., Wang, Y., Zhou, W., . . . Kataura, H. (2018). Detecting and Tuning the Interactions between Surfactants and Carbon Nanotubes for Their High-Efficiency Structure Separation. *Advanced Materials Interfaces, 5*(2), 1700727.

Zhang, D., Chi, B., Li, B., Gao, Z., Du, Y., Guo, J., & Wei, J. (2016). Fabrication of highly conductive graphene flexible circuits by 3D printing. *Synthetic Metals, 217*, 79-86.

Zhang, H., Fang, W.-Z., Li, Y.-M., & Tao, W.-Q. (2017). Experimental study of the thermal conductivity of polyurethane foams. *Applied Thermal Engineering, 115*, 528-538.

Zhang, H., Zhang, G., Tang, M., Zhou, L., Li, J., Fan, X., . . . Qin, J. (2018). Synergistic effect of carbon nanotube and graphene nanoplates on the mechanical, electrical and electromagnetic interference shielding properties of polymer composites and polymer composite foams. *Chemical Engineering Journal, 353*, 381-393.

Zhang, L., Yilmaz, E. D., Schjødt-Thomsen, J., Rauhe, J. C., & Pyrz, R. (2011). MWNT reinforced polyurethane foam: Processing, characterization and modelling of mechanical properties. *Composites Science and Technology, 71*(6), 877-884.

Zhang, Y. Y., & Gu, Y. (2013). Mechanical properties of graphene: Effects of layer number, temperature and isotope. *Computational Materials Science, 71*, 197-200.

Zhou, D., Xiong, Y., Yuan, H., Shen, Q., Luo, G., & Guo, W. (2020). Enhanced sound insulation properties of microporous PMMA foams by constructing novel multilayered and directional cell structure (MDCS). *Journal of applied polymer science, 137*(35), 49020.

CURRICULUM VITAE

Name Surname **:** Amir Navidfar

EDUCATION :

- **B.Sc. :** 2012, Tabriz Azad University, Mechanical Engineering (Manufacturing)
- **M.Sc. :** 2015, Urmia University, Mechanical Engineering (Manufacturing)

PROFESSIONAL EXPERIENCE AND REWARDS:

- 2019 Bronze Medal Winner of 4th Istanbul International Invention Fair (ISIF 19), TEKNOFEST Istanbul.
- Research Assistant: The Scientific and Technological Research Council of Turkey (TUBİTAK 1001), Project No: 115R002 (June 2016 - March 2017).
- Research Assistant: (TUBİTAK 1003), Project No: 218M528 (April 2019 – July 2021)

PUBLICATIONS, PRESENTATIONS AND PATENTS ON THE THESIS:

Papers

- **A.Navidfar**, L.Trabzon, "*Analytical modeling and experimentally optimizing synergistic effect on thermal conductivity enhancement of polyurethane nanocomposites with hybrid carbon nanofiller*", Polymer Composites, 2021, 42(2), 944-954.
- **A.Navidfar,** L.Trabzon, "*Graphene type dependence of carbon nanotubes/graphene nanoplatelets polyurethane hybrid nanocomposites: Micromechanical modeling and mechanical properties*", Composites Part B: Engineering, 2019: 107337.
- **A.Navidfar**, A.Sancak, K.B.Yildirim, L.Trabzon, "*A study on polyurethane hybrid nanocomposite foam reinforced with multi-walled carbon nanotubes and silica nanoparticles*", Polymer-Plastic Technology and Engineering, 2018, 57(14), 1463.
- **A.Navidfar**, L.Trabzon, "*Fabrication and characterization of polyurethane hybrid nanocomposites: mechanical, thermal, acoustic and dielectric properties*" Emerging Materials, 2021, Just Accepted.
- **A.Navidfar,** L.Trabzon, "*Synergically enhanced viscoelastic behavior of binary nanocarbon based polyurethane hybrid nanocomposite foams*", Under Review.

Conferences

- **A.Navidfar**, L.Trabzon, "*Synergistic mechanical properties improvement of carbon nanotubes/graphene reinforced polyurethane hybrid nanocomposite*s", Spring Meeting of the European Materials Research Society (E-MRS), 2019, Nice, France. (Oral Presentaion)

- **A.Navidfar**, L.Trabzon, "*Synergistic effect of multi walled carbon nanotubes and silica nanoparticles on polyurethane nanocomposites*", NANOTR-14, 2018, Çeşme, İzmir, Turkey. (Oral Presentation)
- **A.Navidfar**, L.Trabzon, "*Effect of graphene nanoplatelets and multi-walled carbon nanotubes on tensile properties of rigid polyurethane*" 6th World Congress on Nanotechnology and Materials Science, 2018, Valencia, Spain. (Oral Presentation)
- **A.Navidfar**, A.Sancak, K.B.Yildirim, L.Trabzon, "*Influence of multi walled carbon nanotubes and silica nanoparticles on tensile properties of polyurethane*", Applied Nanotechnology and Nanoscience International Conference (ANNIC 2016), Barcelona, Spain. (Oral Presentation)

Patent

- **A.Navidfar**, L.Trabzon, "*Hybrid Nanofiller Reinforced Polyurethane Nanocomposites and Fabrication Methods*", Turk Patent, Application No: 2019/00222

OTHER PUBLICATIONS, PRESENTATIONS AND PATENTS:

- **A.Navidfar**, T. Azdast, A. K. Ghavidel, "*Influence of processing condition and carbon nanotube on mechanical properties of injection molded multi-walled carbon nanotube/polymethyl methacrylate nanocomposites*" Journal of Applied Polymer Science, 2016, 133 (31).
- K. B. Yildirim, A. Sancak, **A.Navidfar**, L. Trabzon, W. Orfali, "*Acoustic properties of polyurethane compositions enhanced with multi-walled carbon nanotubes and silica nanoparticles*" Journal of Material Science and Engineering Technology, 2018, 49, 978.
- A. K Ghavidel, **A.Navidfar**, M.R. Shabgard, T. Azdast, "*Role of CO2 laser cutting conditions on anisotropic properties of nanocomposite contain carbon nanotubes*", Journal of Laser Applications, 2016, 28, 032006.
- A.K Ghavidel, T. Azdast, M. R. Shabgard, **A.Navidfar**, S. Sadighikia, "*Improving electrical conductivity of polymethyl methacrylate by utilization of carbon nanotube and CO2 laser*", Journal of Applied Polymer Science, 2015, 132, 42671.
- A.K Ghavidel, T. Azdast, M. R. Shabgard, **A.Navidfar**, S. Mamaghani Shishavan "*Effect of carbon nanotubes on laser cutting of multi-walled carbon nanotubes/polymethyl methacrylate nanocomposites*", Optics & Laser Technology, 2015, 67, 119.
- M. I. Peker, **A. Navidfar**, E. Budak, C. Unlu, L. Trabzon, "*Synergistic effect of* graphene *in 3D network of carbon based quantum dots on mechanical properties of polyurethane hybrid nanocomposite foams*" 8th Annual Graphene and Beyond: From Atoms to Applications Workshop, 2021.
- **A. Navidfar**, A. Karimzad Ghavidel, T. Azdast, "*Investigation of Rockwell hardness and Charpy impact test of injection molded multi- walled carbon nanotubes/poly methyl methacrylate nanocomposites*", 5th International Congress on Nanoscience & Nanotechnology (ICNN 2014), October 2014, Tehran, Iran.